MASTER IN CHEMISTRY RESEARCH FOCUS

Multistep synthesis of a 2-Fluoro-galactofuranoside as a mechanistic probe of a novel glycosidase from mycobacterium tuberculosis

Rigotti, Thibaut

Award date:
2019

Awarding institution:
University of Namur

Université de Namur

Faculté des Sciences

MULTISTEP SYNTHESIS OF A 2-FLUORO-GALACTOFURANOSIDE AS A MECHANISTIC PROBE OF A NOVEL GLYCOSIDASE FROM *MYCOBACTERIUM TUBERCULOSIS*

Mémoire présenté pour l'obtention

du grade académique de Master Chimie «Chimie du Vivant et des Nanomatériaux» : Finalité Spécialisée

Thibaut RIGOTTI

Janvier 2019

UNIVERSITE DE NAMUR
Faculté des Sciences
Secrétariat du Département de Chimie
Rue de Bruxelles 61 – 5000 NAMUR
Téléphone : +32(0)81 72.54.44 – Téléfax : +32(0)81 72.54.40
E-mail : enseignement.chimie@unamur.be - www.unamur.be/sciences

Synthèse multi-étapes d'un 2-fluoro-galactofuranoside en tant que sonde mécanistique d'une nouvelle glycosidase de *Mycobacterium tuberculosis*

RIGOTTI Thibaut

Résumé

Les glycoside hydrolases (glycosidases) sont une classe d'enzymes capables de cliver les liens glycosidiques entre les sous-unités de monosaccharides principalement dans les polysaccharides, les glycolipides ou les glycoprotéines. Récemment, les recherches de l'équipe du Dr. Yann Guérardel à l'Université de Lille ont mené à la découverte d'une nouvelle glycosidase de *Mycobacterium tuberculosis (Mtb).* Cette enzyme, qui hydrolyse le galactane présent dans la paroi cellulaire de *Mtb*, pourrait expliquer la capacité de ces bactéries à remodeler leur paroi. Afin de permettre une caractérisation complète de cette nouvelle glycosidase (constantes cinétiques, mécanisme, site actif et acides aminés catalytiques), une sonde synthétique **5** a été conçue sur base de son mécanisme procédant par rétention de la configuration anomérique. Grâce à son atome de fluor placé à proximité de la position anomérique, la molécule **5** sera utilisée pour piéger l'acide aminé nucléophile de l'enzyme. La voie synthétique utilisée pour obtenir cette molécule est représentée ci-dessous.

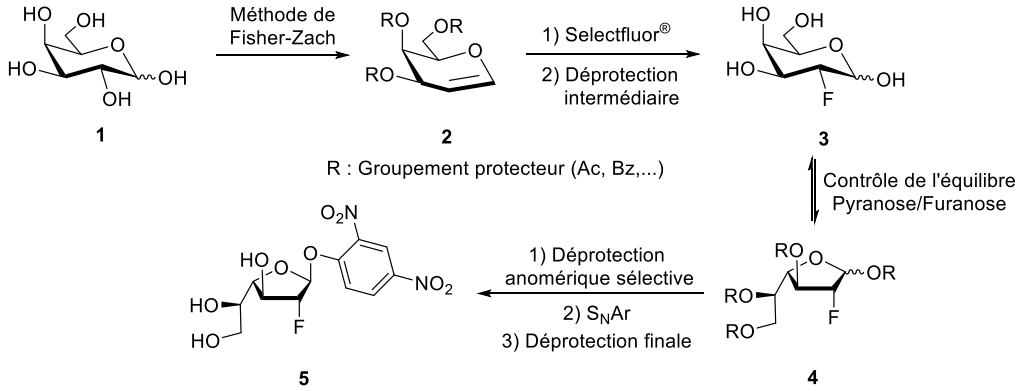

Mémoire de master en Sciences Chimiques à Finalité spécialisée

Janvier 2019

Promoteur: Prof. Stéphane Vincent

Remerciements

En tout premier lieu, je tiens à remercier sincèrement le professeur Stéphane Vincent qui m'a accueilli dans son laboratoire et au sein de son équipe. Ses conseils avisés et son suivi durant toute la période de mon mémoire m'ont permis de mener à bien mon projet de recherche. J'ai notamment fort apprécié son dévouement et sa disponibilité pour ses mémorants malgré son emploi du temps fort chargé.

Je suis également très reconnaissant envers mon encadrant de mémoire, Loïc Chêne, avec qui j'ai pu partager beaucoup de bons moments. Il aura toujours été là pour me soutenir et m'aider en toutes circonstances, ce qui m'a vraiment poussé à atteindre à chaque fois de nouveaux objectifs. J'ai pu découvrir en lui un véritable ami bienveillant.

Je remercie bien entendu les membres du CBO qui ont tous à un moment ou l'autre pu m'apporter de l'aide. Je remercie particulièrement Sydney Villaume, qui mérite amplement son récent titre de docteur ; Julien Delbrouck et Christophe Frédéric, qui m'ont particulièrement aidé pour ce qui est de la chimie des sucres ; Valentin Bochatay, qui partage aisément son souci du détail ; Marine Lacritick et Léa Chartier, qui ont apporté bonne humeur et convivialité au CBO.

Je me dois de remercier de tout cœur mon meilleur ami de parcours universitaire qui est Arnaud Beaufays. Mon aventure au CBO n'aurait jamais pu être aussi agréable sans sa présence. Il aura été présent dès le premier jour pour écouter mes problèmes et m'aider à les relativiser. C'est un super ami à l'origine de nombreuses anecdotes que je ne suis pas prêt d'oublier.

Enfin, je remercie ma famille proche et ma petite amie qui m'ont soutenu lors des moments les plus difficiles et qui ont su se montrer intéressés par ma recherche au laboratoire.

Abbreviations and symbols

Å	Ångström
AG	Arabinogalactan
AIDS	Acquired immunodeficiency syndrome
Ara*f*	Arabinofuranosyl
Asp	Aspartic acid
δ	Chemical shift
DABCO	1,4-diazabicyclo[2.2.2]octane
DCM	Dichloromethane
DI_{50}	50 % infection dose
DMAP	*N*,*N*-dimethyl-4-aminopyridine
DMAPA	3-(dimethylamino)-1-propylamine
DMF	*N*,*N*-dimethylformamide
DNA	Deoxyribonucleic acid
DNP	Dinitrophenol
Eq.	Equivalent
ESI	Electron Spray ionization
FDNB	1-fluoro-2,4-dinitrobenzene
Gal*f*	Galactofuranosyl
GalN	Galactosamine
GH	Glycoside hydrolase
GlcNAc	*N*-acetylglucosamine
Glu	Glutamic acid
Gram-	Gram negative
Gram+	Gram positive
HIV	Human immunodeficiency virus
HRMS	High resolution mass spectroscopy
J	Coupling constant
LAM	Lipoarabinomannan
LM	Lipomannan
LPS	Lipopolysaccharide
mAGP	Mycolyl-arabinogalactan-peptidoglycan complex
MDR	Multi-drug resistant
Mtb	*Mycobacterium tuberculosis*
Mur	Muramic acid
MurNAc	*N*-acetyl-muramic acid
MurNGly	*N*-glycolyl-muramic acid
NAD	Nicotinamide adenine dinucleotide
NFSI	*N*-fluorobenzenesulfonimide
NMR	Nuclear magnetic resonance
NOE	Nuclear Overhauser effect
PG	Peptidoglycan
PIM	Phosphatidyl-*myo*inositol
ppm	parts-per-million
r.t.	Room temperature
R_f	Retention factor
Rha*p*	Rhamnopyranosyl
S_N1 / S_N2	Nucleophilic substitution of $1^{st}/2^{nd}$ order
S_NAr	Nucleophilic aromatic substitution
TB	Tuberculosis
THF	Tetrahydrofuran
TLC	Thin layer chromatography
TMS	Trimethylsilyl
XDR	Extensively drug resistant

Table of contents

I. Introduction

I.1 *Mycobacterium tuberculosis*, a major human pathogen

Tuberculosis (TB) is an infectious disease caused by the pathogenic organism *Mycobacterium tuberculosis* (*Mtb*).[1] It is estimated that 1.7 billion people (23 % of the world population) is currently infected by this pathogen in a latent phase.[2] In 2017, this disease caused 1.6 million casualties and it is then categorized as one of the deadliest infectious diseases among HIV/AIDS and malaria. The specific TB antibiotics that were discovered five decades ago and that are still used to cure tuberculosis are becoming less and less effective over time because of the appearance of new resistant strains. Accordingly, rifampicin and isoniazid, which are first-line drugs for the treatment of TB, are ineffective against multi-drug resistant TB (MDR-TB). Among cases of MDR-TB, 8.5 % of them are estimated to be extensively drug-resistant TB (XDR-TB). Those infections are caused by bacteria that are MDR but also resistant to any fluoroquinolone and at least one of the second-line injectable drugs such as amikacin, capreomycin or kanamycin.[3] Furthermore TB strains that are resistant to every known TB drugs have been characterized, which places tuberculosis as a major issue for public health. It also means that the search for new essential targets of *Mtb* is a current major topic as there is an urgent need for controlling the proliferation of TB.

I.2 Tuberculosis infection cycle

Mtb is transmitted through the air thanks to tiny water droplets containing bacteria (Figure 1). Those are produced when an infected person cough or spit. The DI_{50} (the minimum number of pathogenic species inhaled to infect 50 % of a population) is estimated to be less than 10 for the human.[4] When a healthy person breathes in the bacilli in suspension **[A]**, *Mtb* travels through the lungs to reach its final location which is the pulmonary alveoli. First, the innate immune response takes place with the recruitment of immune cells such as neutrophils, inflammatory monocytes or interstitial macrophages.[5] The purpose of those cells is to eliminate *Mtb* but they quickly become infected by the growing population of mycobacteria **[B]**. The adverse effect of this infection is that the recruitment of more phagocytic cells to the site of the infection benefits the pathogen as they provide additional niches for the bacterial population expansion. The ultimate step of the innate immune response is the formation of an early granuloma **[C]**. In some patients, this granuloma is sufficient to give rise to the eradication of the infection **[D]**, while in others, this situation leads to a primary tuberculosis.[6]

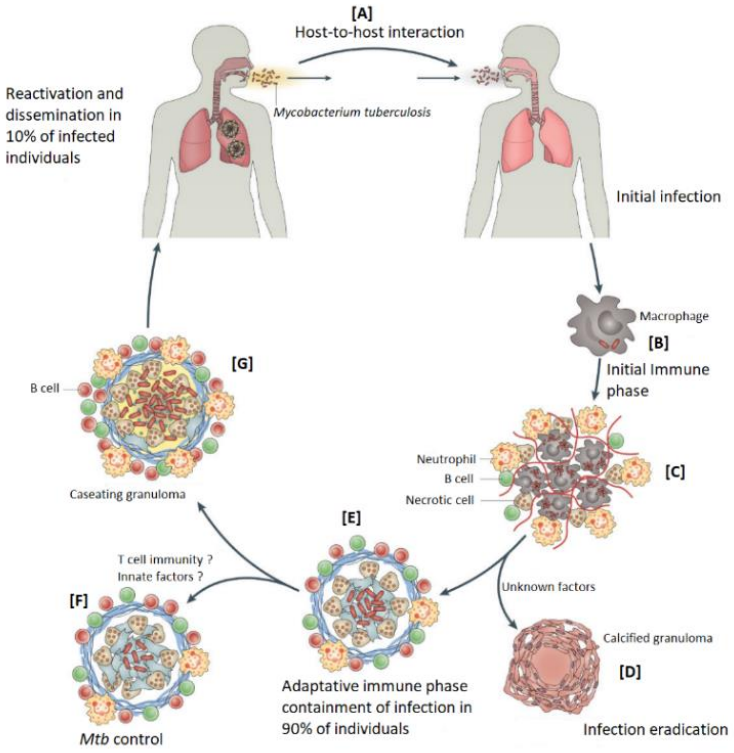

Figure 1. Infection cycle of Mtb. Figure taken from C. Nunes-Alves et al.[6]

After some time, an adaptive immune response takes place **[E]**. It consists in the recruitment of many leucocytes such as dendritic cells, T-cells, B-cells, *etc*. Those cells can activate the formation of a more advanced granuloma that will allow an interruption of the proliferation of bacteria **[F]**. The infection will stay in a latent phase and only a small percentage of individuals will develop an active tuberculosis afterwards. In those sensitive patients (mainly in immunosuppressed people), mycobacteria will multiply themselves inside the macrophage **[G]**. Upon coughing, the granuloma will break and the bacilli will be expectorated in the air. A new infectious cycle can start again. The particularity of *Mtb* is its ability to survive in macrophages which are a hostile environment. Its cell wall structure is believed to be the main reason for this unusual characteristic.[7]

I.3 The cell wall of *Mycobacterium tuberculosis*

I.3.1 Overview

Conventionally, bacteria are divided into two major groups according to the composition of their cell wall: Gram-positive (Gram+) and Gram-negative (Gram-) (Figure 2).[8] While the Gram+ bacteria possess a thick layer of peptidoglycans present on the surface of the bacterial

cell wall, Gram- bacteria do not have such accessible layer of peptidoglycans. Indeed, their cell wall structure is very different and is actually composed of a supplementary membrane above the plasma membrane. A thin layer of peptidoglycan is thus found in between the two lipidic bilayers (a location named "periplasm"). The external membrane is decorated by a layer of lipopolysaccharides (LPS) which are not found in Gram+ bacteria. The differentiation between the two types of bacteria was originally based on their sensitivity to the Gram staining test. It consisted in using a special dye that was able to color the Gram+ bacteria by interacting with the peptidoglycan on the surface of their cell wall. As the peptidoglycans in Gram- bacteria are entrapped in between the two lipidic bilayers of the cell wall, they cannot be reached by the dye and the Gram- bacteria are left uncolored.

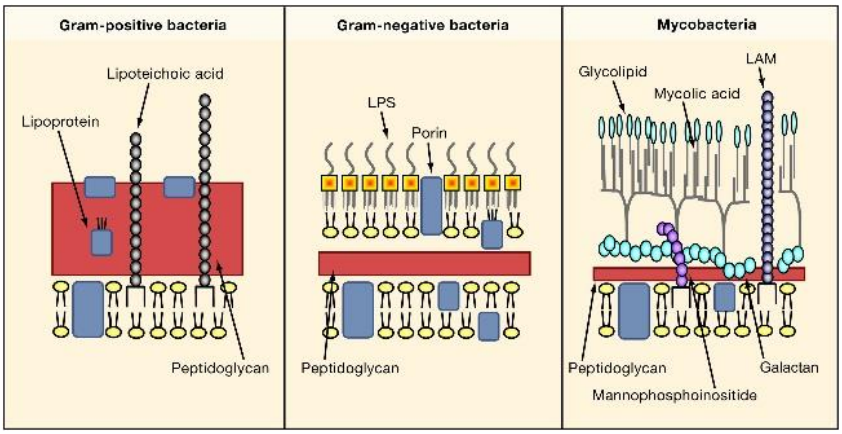

Figure 2. Comparison of cell wall structures between Gram-positive bacteria, Gram-negative bacteria and mycobacteria. Illustration taken from S. Akira et al.[8]

While mycobacteria could be classified as Gram+ bacteria, their cell wall structure significantly differs from the cell wall composition of traditional Gram+ bacteria. The main difference is the higher proportion of lipids in the cell wall of mycobacteria. Those lipids may represent up to 40 % of the cell dry mass while it is only 5 % in other Gram+ bacteria.[9] They render the cell wall very impermeable (up to 10-100 times more impermeable than the cell wall of *Pseudomonas aeruginosa* which is already known to be quite impermeable).[9] This feature explains the difficulty for the host (or even the usual antibiotics) to interact and eliminate mycobacteria.

The mycobacterial envelope is composed of three main components (Figure 3):

- A plasma membrane found just like in any other cells.
- An elaborated mycolyl-arabinogalactan-peptidoglycan (mAGP) complex. Mycolic acids are bound covalently to the arabinogalactan to form the mycomembrane with other glycolipids and lypoglycans.
- An outer layer called "capsule" found only in the pathogenic strains.

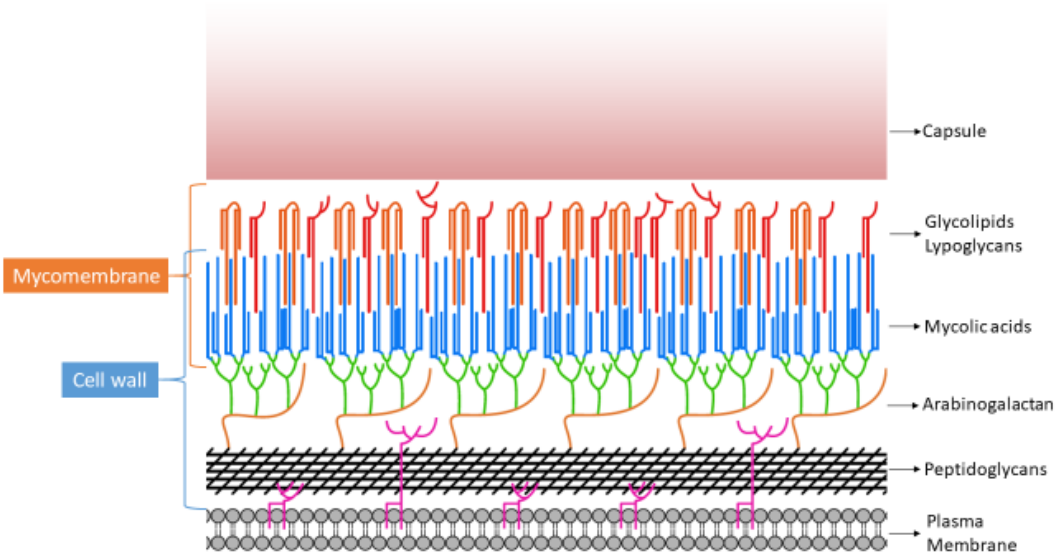

Figure 3. Cell wall structure of Mtb. Illustration taken from L. Shen.[10]

The heart of this cell wall envelope is the mAGP complex which is composed of three layers bound covalently: mycolic acids, the arabinogalactan and the peptidoglycan.

Peptidoglycans (PG) are made of long chains of alternating *N*-acetylglucosamine (GlcNAc) and muramic acid (Mur) linked in a β(1→4) fashion (Figure 4 and Scheme 1).[11] The muramic acid residues in *Mtb* are a mixture of both the *N*-acetyl-muramic acid (MurNAc) and the *N*-glycolyl-muramic acid (MurNGly). The latter is obtained by oxidation of MurNAc and it has only been observed in *Mtb* and *Mycobacterium smegmatis*. This modification would allow additional hydrogen bonding interactions between glycan chains and thus give a stronger rigidity to the PG. The glycan chains are cross-linked by tetrapeptide (L-alanilyl-D-isoglutaminyl-*meso*-diaminopimelyl-D-alanine) side chains to form a mesh-like arrangement that confers rigidity to the cell.

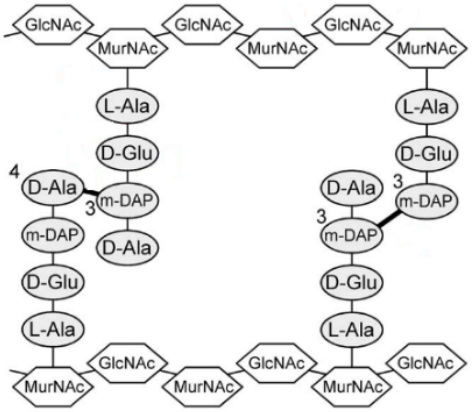

Figure 4. Schematic structure of the PG. Illustration taken from K.M. Payne et al.[12]

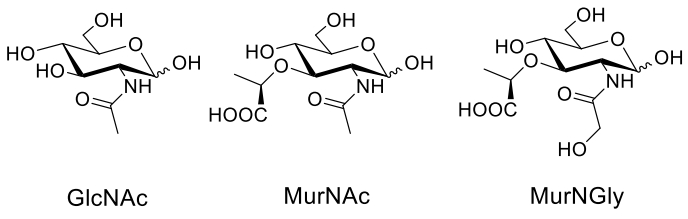

Scheme 1. Chemical structures of the glycosides found in the PG.

Mycolic acids are very long fatty acids (up to 90 carbons) that are α-branched and β-hydroxylated (Figure 5).[9] They are esterified to two thirds of the non-reducing end of the last arabinofuranose residue of the arabinogalactan. They help to bind other fatty molecules like lipids, glycolipids and lipoproteins that are composing the outer membrane of the envelope. Those molecules (such as phosphatidyl-*myo*inositol (PIM), lipomannan (LM) and lipoarabinomannan (LAM)) have the ability to activate the immune system.[13]

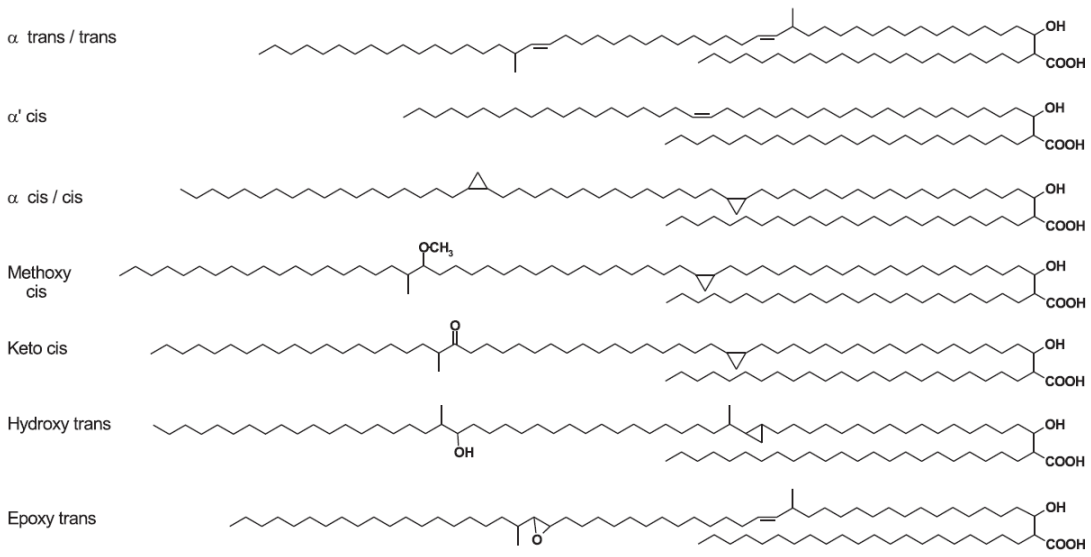

Figure 5. Structure of the mycolic acids found in Mtb. Illustration taken from M. Daffé.[9]

The arabinogalactan (AG) is the crucial part of the mAGP complex as it is the linker between the last two components. It is a heteropolysaccharide that contains two different chains of polysaccharides : the galactan and the arabinan (Figure 6 and Scheme 2).[11] The first one is made of approximately 30 alternating β(1→5) and β(1→6)-linked D-galactofuranosyl (D-Gal*f*) residues. It is covalently bound to approximately 10 % of the Mur residues of the PG by a phosphodiester linker. This linker unit is also composed of a disaccharide made of L-rhamnopyranosyl (L-Rha*p*) (1→3)-linked to a GlcNAc.

Three chains of arabinan are linked to the galactan via a bound to the C-5 hydroxyl of β(1→6)-linked Gal*f* units (on the 8th, 10th and 12th Gal*f* residues).[11] The arabinan itself is a polysaccharide made of 23 D-arabinofuranosyl (D-Ara*f*) units with α(1→5) and α(1→3) bonds. There is a possibility of branching at the C-3 of α(1→5)-linked D-Ara*f* units. The arabinan is terminated with a β(1→2) D-Ara*f* residue. Then, it can be further decorated with succinyl and galactosamine (GalN) residues at the C-2 of α(3→5) linked D-Ara*f* units.

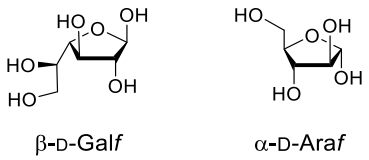

Scheme 2. Chemical structure of β-D-Galf and α-D-Araf.

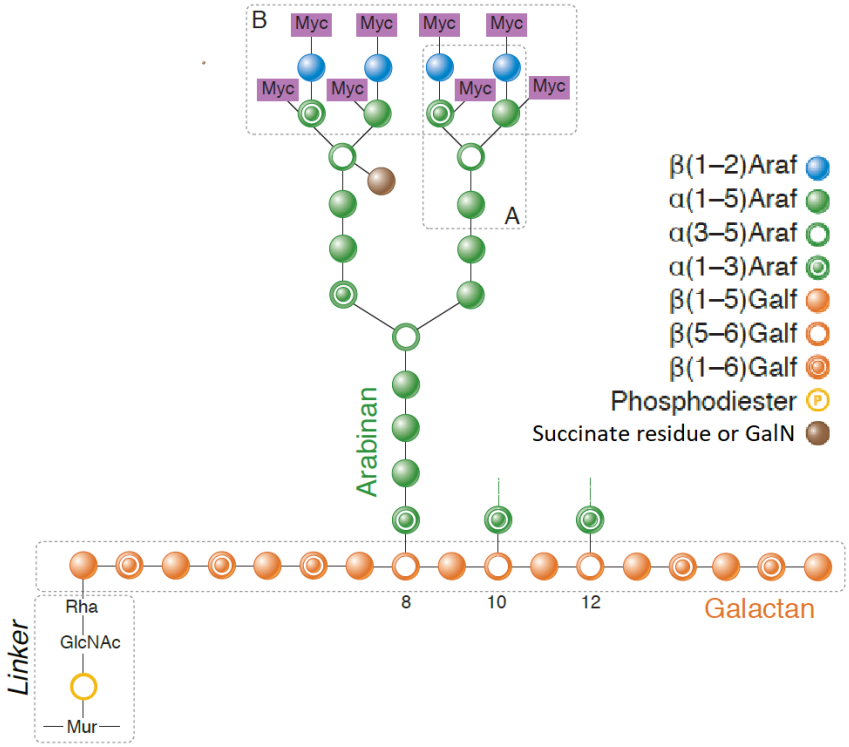

Figure 6. Structure of the arabinogalactan oligomers. Illustration taken from L. Shen.[10]

It is important to note that the overall structure of the mAGP complex is actually dynamic. Indeed, since the infection cycle of *Mtb* goes through many different environments, it induces many modifications of the mAGP complex for a better survival of *Mtb* in every situation. This aspect will be discussed in the following section.

I.3.2 Cell wall remodeling

The cell wall remodeling of *Mtb* is a major aspect of the immuno-evasion of the pathogen. By doing subtle variation to its envelope, *Mtb* can adapt itself better to the changing host environment during the different stages of the infection.[14]

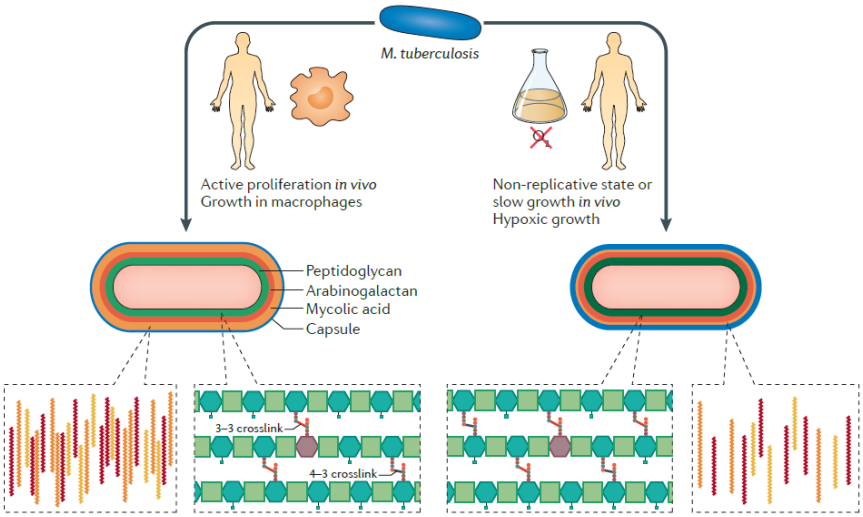

Figure 7. Structural differences of Mtb cell wall components between a fast in vivo and a slow in vitro growth. Illustration taken from K.J. Kieser et al.[14]

The three main components of the mAGP complex (AG, PG and mycolic acids) can undergo various modifications. It has been shown that the composition of mycolic acids are different between mycobacteria growing *in vivo* and *in vitro* (Figure 7).[14] The mycolic acids, along with the cell wall lipids, are much more present in the cells growing *in vivo*. Indeed, the thicker is the cell wall, the easier it is for *Mtb* to restrict the transit of toxic molecules. In that fashion, the lipids bound to the mycolic acids help trap toxic by-products from the catabolism of cholesterol during the growth in macrophages.[14] Mycolic acids also have two additional functions: they participate in the immuno-evasion of the pathogen and have the ability to absorb toxic oxidative radicals. In a slow growth state (*in vitro* conditions), the abundance of immunostimulatory mycolic acids is reduced to potentially avoid recognition by the immune system.[14]

The peptidoglycan also needs to undergo modifications to withstand the harmful conditions in the macrophages. The most important characteristic of the PG, *in vivo*, is the maintenance of

the 3-3 peptidic cross-links between the glycan chains as they promote chronic infection and antibiotic resistance. When *Mtb* has a slow growth such as in *in vitro* conditions, the number of peptidic cross-links is increased to obtain a better cell wall rigidity.[14]

Finally, with regards to the arabinogalactan, the number of those polysaccharide chains increases during an *in vivo* growth.[15] This observation is quite logical as it is the support for the mycolic acids that are more importantly found in the same conditions.

Those modifications of the cell wall component and the ability of the bacteria to switch between different rates of growth implies the need for catabolic enzymes. Those enzymes are able to break down big molecules found in the cell wall into smaller pieces. It is especially the case for the breakdown of polysaccharides (a major component of the mAGP complex) performed by glycosidases.

I.4 Glycoside hydrolases

Glycoside hydrolases (GH) (also named glycosidases) are a group of enzymes that are capable of catalyzing the cleavage of glycosidic bonds (Scheme 3). The reaction itself consists in the hydrolysis of the anomeric acetal and the release of the previous acceptor which can either be a glycoside (such as in polysaccharide) or an aglycon (such as in glycoproteins or glycolipids).

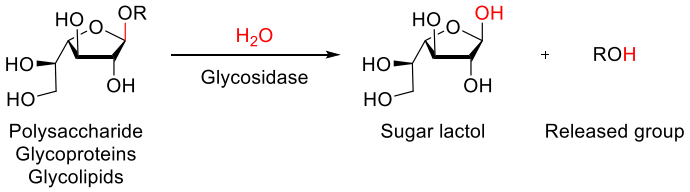

Scheme 3. Reaction catalyzed by glycoside hydrolases. The acceptor of the glycoside is a water molecule.

They are usually highly specific to their substrate and this specificity is associated to four criteria.

- Carbohydrate monomer specificity: GHs are highly selective towards the sugar unit whose anomeric acetal is hydrolyzed into a lactol. This specificity is linked to the three main characteristics of every monosaccharide which are the series (L or D), the relative configuration (galactose, glucose, arabinose, *etc*.) and also the cycle size (pyranose or furanose). The group attached to the anomeric center of the substrate brings much less selectivity to the enzymatic process.

- Anomeric specificity (α or β bond cleavage): The anomeric configuration is the configuration of the C-1 stereocenter of the glycosidic substrate. It can either be α or β. An α-GH cannot hydrolyze a β-glycoside and *vice-versa*.
- Bond cleavage location: Two classes of GHs are defined as a function of the hydrolyzed bond location: if the cleavage occurs at the terminal sugar unit of the polysaccharide chain, the enzyme is named *exo*, if it is "inside" the chain, it is named *endo*.
- Reaction stereochemistry: All GHs use one of the two possible mechanisms that result in either the retention or the inversion of the anomeric configuration of the released monosaccharide.

The reaction stereochemistry is an important characteristic of a glycosidase as it is directly linked to its mechanism. The understanding of this mechanism helps to identify which amino acids are essential in the enzyme active site. Mechanisms for these enzymes were first proposed by D. Koshland[16] in 1953 but it was only confirmed later by S. Withers[17] thanks to structures of GHs with inhibitors or substrate analogs bound in their active site.

The glycoside hydrolases that act by inversion of configuration uses a one-step process. Only two catalytic amino acids are needed for the acetal hydrolysis and they are used in a general acid/base catalysis fashion.[17] As illustrated in Scheme 4, the acidic amino acid activates first the leaving group by protonation to allow the basic amino acid to catalyze the attack from a water molecule to the free face of the anomeric position. The final molecule has an opposite anomeric configuration than the substrate. Although the mechanism depicted in Scheme 4 suggests a pure S_N2 mechanism, there is still a debate for a competition between S_N1 and S_N2 mechanisms.

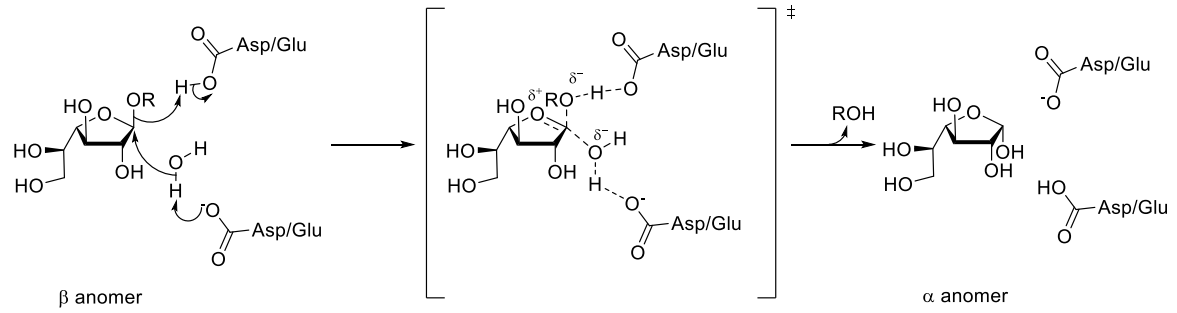

Scheme 4. Inversion of configuration mechanism for the cleavage of a glycosidic bond catalyzed by an inverting glycoside hydrolase.

The enzymes that act by retention of configuration use a two-step process. The binding site also requires only two catalytic amino acids but in contrast with the previous mechanism, one of

them acts as a catalytic nucleophile. First, the acidic amino acid activates the leaving group by protonation to allow the other amino acid to perform a nucleophilic attack on the free side of the anomeric carbon (Scheme 5). This situation leads to the formation of an intermediate where the enzyme is covalently bound to the substrate. In a second step, the deprotonated acidic amino acid activates the nucleophilic substitution from the bound amino acid to a water molecule. As a consequence of this double inversion sequence, the final product possesses the same anomeric configuration as the starting substrate. In both mechanisms, all the reactions go through a cationic oxycarbenium-like transition state.

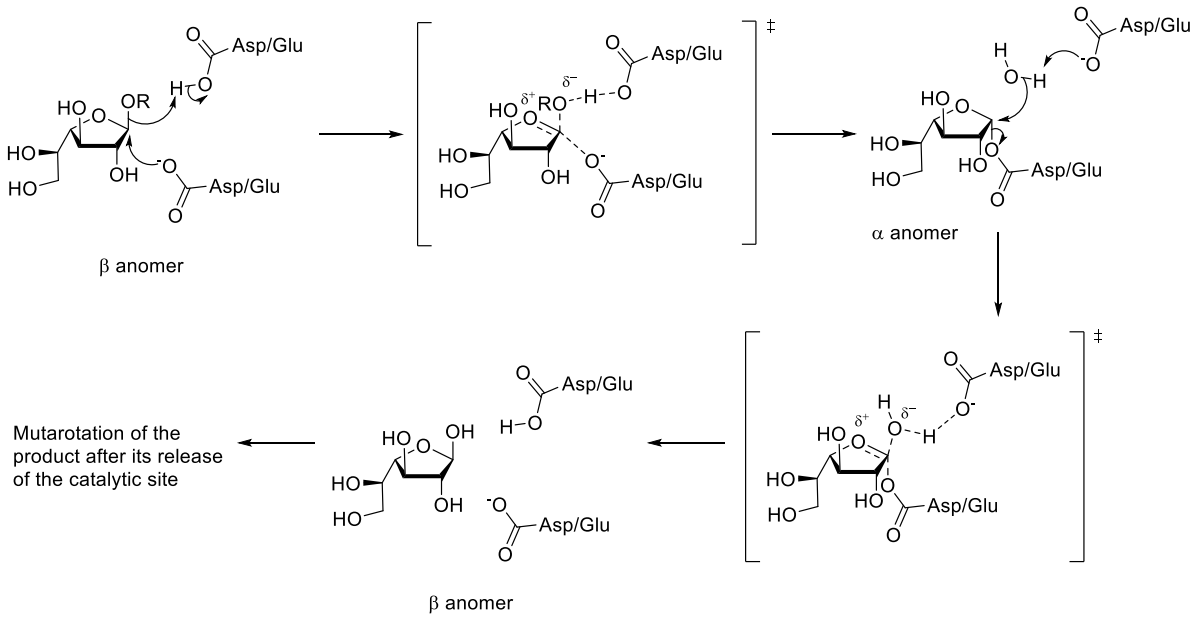

Scheme 5. Double inversion of configuration mechanism for the cleavage of a glycosidic bond catalyzed by a retaining glycoside hydrolase.

It is noteworthy to mention that even if inverting and retaining glycosidases have similar active site structures, the distance between the two catalytic amino acids is not the same. Crystallographic structures show that this distance is in averages 5 Å for retaining GHs while it is 6-11 Å for inverting GHs.[17] This proximity between the catalytic amino acids in retaining glycosidases is coherent with the fact that the enzyme actually binds covalently to the substrate between the two inversion steps. Noteworthy, not all the retaining glycosidases use an aspartic or a glutamic acid as the nucleophilic amino acid. For example, in the case of sialidases, a tyrosine acts as the nucleophile and is assisted by a neighboring basic amino acid.[18] It is even possible for a retaining GH not to include a nucleophilic amino acid when the substrate possesses an *N*-acetyl or an *N*-glycolyl group at the C-2.[19] The oxygen of those groups acts as an intramolecular nucleophile during the first inversion step. Lastly, there are retaining GHs that use an NAD cofactor and go through a very different mechanism than traditional retaining

GHs.[20] This mechanism consists in the oxidation of the hydroxyl at the C-3, followed by the elimination of the anomeric group and finally the conjugate addition of a water molecule and the reduction of the C-3 carbon.

I.5 A novel glycosidase from *Mycobacterium tuberculosis*

The team of Dr. Yann Guérardel in the Glycobiology unit at the University of Lille (in collaboration with the team of Pr. Laurent Kremer) addressed the question of *Mtb* membrane remodeling.[10] They were more specifically interested in the arabinan part of the cell wall and they looked for a catabolic enzyme targeting this specific part. To reach such objective, they searched into the DNA of *Mtb* to find coding sequences that were similar to already known L-arabinanases from other species. This research allowed them to isolate three interesting coding genes: Rv0186, Rv0237 and Rv3096. After overexpression of those genes in *E. coli* bacteria and purification of the corresponding proteins, the researchers have conducted enzymatic assays and they have found that only Rv3096 was showing an activity towards the AG. To their surprise, they were able to determine that it was not an arabinanase but it was in fact targeting the galactan part of the AG! This demonstration was possible thanks to enzymatic assays with synthetic substrates bearing an anomeric paranitrophenyl group (Scheme 6 and Figure 8). Their conclusion to those experiments was that Rv3096 was a gene coding for a β-D-galactofuranosidase that acts by retention of the anomeric configuration (unpublished results).

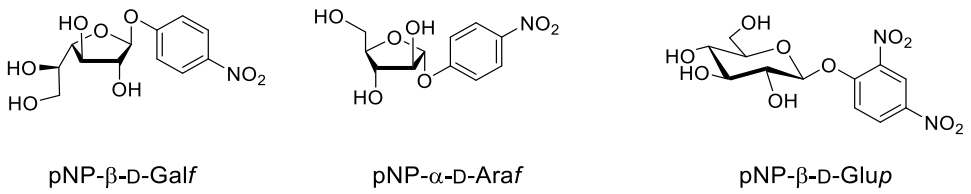

Scheme 6. Examples of a synthetic substrate used to determine substrate specificity of Rv3096.

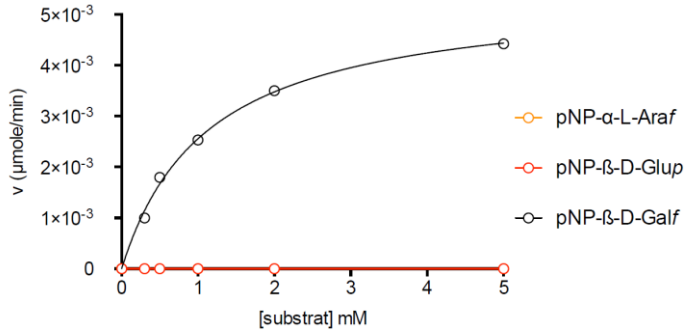

Figure 8. Activity of Rv3096 towards three synthetic substrates: pNP-β-D-Galf, pNP-β-D-Glup et pNP-α-L-Araf. Figure taken from L. Shen.[10]

II. Objective

Even if the team of Dr. Yann Guérardel has partially characterized this new glycosidase from *Mtb*, some important features remain to be studied. The first objective is to determine, experimentally, which residue (Asp or Glu) is the catalytic nucleophile. Based on sequence analogies and directed mutagenesis, Glu^{295} and Glu^{197} are likely candidates but an absolute proof has not yet been provided.[10] Moreover, it would be of great importance to provide a tri-dimensional structure of a covalent complex between the enzyme and its substrate. This structure would allow mapping and visualizing the active site and help identify the amino acids involved in the catalytic process. Such structure would also provide the conformational state of both the enzyme and the substrate at the heart of the catalytic process: just in between the two inversion steps.

However, this enzyme cannot be co-crystallized with its natural substrate as the reaction is so fast it would be difficult to crystallize the enzyme while it is processing the reaction. A solution to circumvent this problem would be to incubate the enzyme during the crystallization process with a close synthetic analog of the substrate that would be slower than the natural substrate. This molecule would need to stabilize the enzyme-substrate complex so that it slows down the hydrolysis step and thus the release of the product from the active site. This scenario seems possible with molecule **1β** derived from D-galactose as it possesses two major features illustrated in Scheme 7.

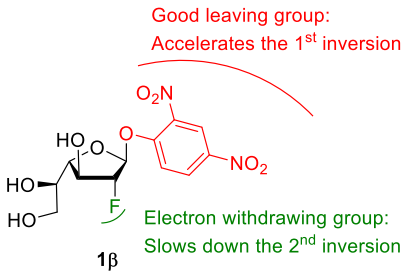

Scheme 7. Structure of a potent mechanistic probe of Mtb novel β-D-galactofuranosidase.

First, it has a very good leaving group (2,4-dinitrophenol) at the anomeric position. It means that the anomeric C-O bond cleavage and the binding of the probe to the enzyme during the first step of the enzymatic mechanism will be fast (Scheme 8). Secondly, it possesses a fluorine atom at the C-2 instead of a hydroxyl group. As the electronegativity of fluorine is much more superior to oxygen, the fluorine will destabilize the cationic oxycarbenium-like transition states. In particular, it will dramatically slow down the second inversion and thus restrict the ability of the enzyme to separate from its substrate. Moreover, the replacement of a hydroxyl group by a fluorine atom will result in the disruption of important hydrogen bonding interactions that have

been shown to stabilize the transition state for some GHs.[21] Even though the fluorine also destabilizes the first transition state by the same principle, the formation of the intermediate will still happen since 2,4-dinitrophenol is a very good leaving group. As fluorine has a smaller size compared to a hydroxyl group, the replacement of a secondary alcohol at C-2 of molecule **1β** by a fluorine atom should not affect, sterically, the binding process to the enzyme.

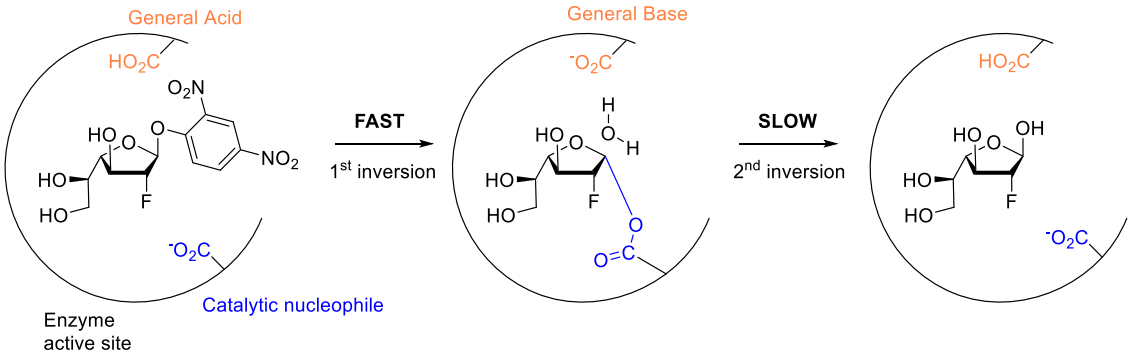

*Scheme 8. Predicted inhibition mechanism of retaining glycosidases by molecule **1β**.*

This molecule would not only give the possibility to obtain a 3D structure of the key covalent intermediate but it will help to confirm the retention of configuration nature of this mechanism thanks to kinetic assays. Indeed, this molecule should act as a time-dependent inactivator of the novel GH which would demonstrate, kinetically, that this enzyme proceeds through covalent catalysis. According to the litterature[17,22], this principle has already been demonstrated and tested on many glycosidases. However, no reports have been made on the synthesis of molecule **1β**. This master thesis is thus aimed at developing a synthetic pathway for this molecule. The enzymatic assays and the co-crystallization experiments will be performed in the laboratory of our collaborators in the University of Lille.

In the following "Results and discussion" section, we will first discuss the possible synthetic strategies for the preparation of molecule **1β** based on its specific structural features. Then, we will describe our experimental efforts toward the synthesis of **1β** and thus elaborate some concluding remarks.

III. Results and discussion

III.1 Synthetic pathway

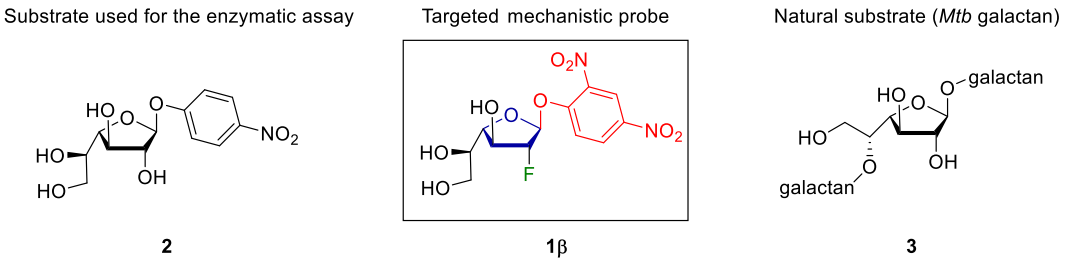

Scheme 9. Structures of the substrate used for the enzymatic assay, the targeted mechanistic probe and the enzyme natural substrate. There are three main characteristics of the targeted mechanistic probe: a five membered ring (blue), a fluorine atom at C-2 (green) and a good leaving group at C-1 (red).

As shown in Scheme 9, the molecular probe has the following features:

1) An overall structure similar to the enzyme natural substrate. There are in total five stereogenic centers that have to be firmly set as the enzyme is highly specific to its natural substrate (D-galactofuranose) and thus the molecular probe must have the hydroxyl groups oriented in the same way. One of the stereogenic centers is the anomeric carbon. It can either be α or β and this enzyme is only active towards the latter. On top of this, the ring size must be controlled. The enzyme will not bind the more commonly found pyranoside (six-membered ring) structure of D-galactose. The formation of the furanoside structure (five-membered ring) will be an important aspect of the synthesis.

2) A fluorine atom at the C-2. This atom will be at the heart of the inactivation of the enzyme. It will need to be placed on the bottom α face of the ring to mimic the original position of the hydroxyl group present at the C-2.

3) A good leaving group positioned at the anomeric position such as 2,4-dinitrophenol. This group will need to be placed with the β configuration as it is the normal configuration of the bond between sugar subunits in the natural polysaccharide on which the enzyme acts.

With those features in mind, the synthetic pathway illustrated in Scheme 10 can be envisioned.

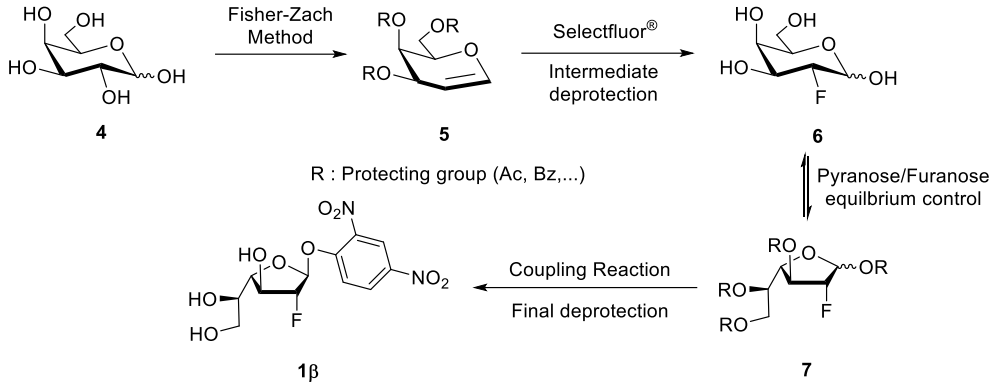

Scheme 10. The synthetic pathway envisioned for the synthesis of the mechanistic probe of Rv3096.

The starting material of the synthesis is the cheap and commercially available D-galactose (**4**) which is mostly in its pyranose form at room temperature.[23] This molecule has the advantage of having right away the desired configurations of the stereogenic center at the C-3, C-4 and C-5.

The first step will be the synthesis of a useful intermediate allowing a fluorination reaction. This intermediate **5** is called D-galactal and its enol ether function is nucleophilic enough to react with electrophilic fluorination reagents such as Selectfluor®.[24] This will allow the addition of an electrophilic fluorine atom regioselectively at C-2 and with an excellent stereoselectivity, as required.

After deprotection, molecule **6** will be obtained. As this molecule is mainly present in its pyranoside form, it will need to be converted in its less stable furanoside structure **7** thanks to a control or a shift of the equilibrium between the two species.

The key coupling reaction can be achieved either as a direct glycosylation of a nitrophenol derivative which will require a preliminary anomeric activation or through a S_NAr reaction after a selective anomeric deprotection. The stereoselectivity of this coupling step will have to be examined and controlled as the desired anomer must be β.

Finally, the target molecule **1β** can be obtained after a final careful deprotection of the remaining protecting groups without hydrolyzing the sensitive anomeric dinitrophenolate.

III.2 Synthesis of D-galactal

Carbohydrates possessing a double bond between C-1 and C-2 are named *endo*-glycals. They are used for many purposes such as glycosylating agents in the synthesis of 2-deoxy sugars, as versatile chiral building blocks or even in the synthesis of glycoproteins.[25] Among the various existing techniques to prepare them, the easiest one is probably the Fisher-Zach method. It consists in the reductive elimination of a protected 1-halogenoglycoside **9** which itself is easily prepared from the corresponding per ester **8**. This elimination is realized thanks to zinc powder in an aqueous acetic acid solution. The zinc reacts with the organohalide to form an organozinc intermediate which rapidly undergoes elimination. The mechanism of this reaction is thought to involve a two-electron reduction process on the anomeric carbon, which is followed by the elimination of the C-2 acetate group.[25]

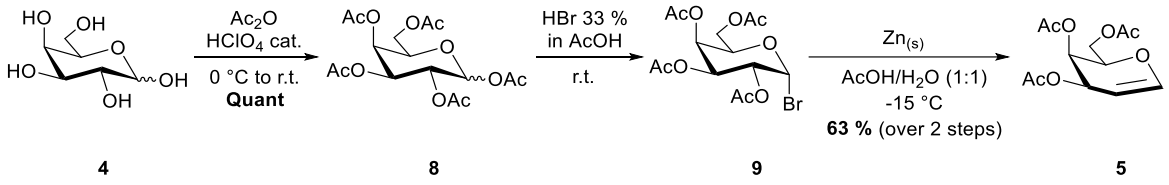

*Scheme 11. Preparation of D-galactal **5** thanks to the Fisher-Zach method.*

This widely employed sequence was thus performed starting with the peracetylation of D-galactose **4** in acetic anhydride with perchloric acid as a catalyst (Scheme 11).[26] The use of acetic anhydride as the solvent allows keeping the reaction mixture water free. The temperature must be controlled to avoid excess heat to be generated due to the exothermic nature of this reaction. This reaction had two important justifications. The first one is that an acetate group is a better leaving group than a hydroxyl group, which will be helpful for the elimination step. Secondly, it makes the substrate more lipophilic and thus more soluble in solvent of low to moderate polarity such as CH_2Cl_2 or EtOAc. As an important consequence, this characteristic renders workup with aqueous solutions possible.

Then, **8** was treated with HBr in acetic acid to obtain **9**. No work-up is realized on this sensitive intermediate as the treatment of the crude mixture with cold water can partially degrade the molecule. Instead, the crude was only concentrated *in vacuo* with precautions being taken (such as a NaOH trap) to avoid the release of corrosive vapors. Finally, molecule **5** was obtained by adding zinc dust in suspension to a solution of reagent cooled to -15 °C. Purification by silica gel chromatography allowed the obtention of a colorless syrup with 63 % yield over two steps.

It has been discussed in the literature[25] that the heterogeneous reaction conditions can explain the difficulty to reproduce results from other authors for such elimination. The quality of the zinc powder can be mentioned as a factor influencing the yield though it is not, in this case, as critical as in other organometallic transformations. Solutions exist to diminish the lack of reproducibility problems. Those include pre-washing the zinc dust with diluted HCl or using platinum and copper salts to promote the reaction at the surface of the zinc particles. There is also the possibility of formation of minor side products resulting, for instance, from the solvolytic displacement of the anomeric bromide by acetic acid and water.

In an attempt to increase the yield obtained with the traditional method, reaction conditions more recently described in the literature were tested for the reductive elimination step.[27] In this method, the crude bromide **9** is treated with $Zn_{(s)}/NH_4Cl_{(s)}$ in acetonitrile at 60 °C for 1 hour (Scheme 12). The ammonium chloride acts as a source of protons similarly to acetic acid in the previous conditions. The final yield obtained with this method was only 25 % over two steps. As it is much lower than in the first method, it has been decided to use the original conditions instead.

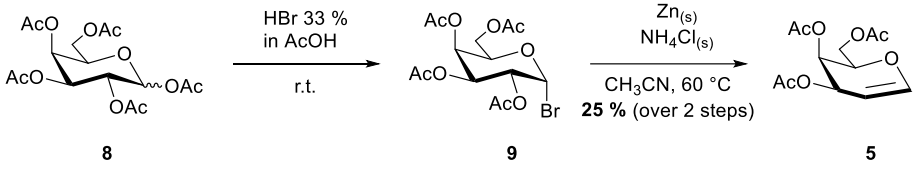

*Scheme 12. Alternative conditions used for the formation of D-galactal **5**.*

III.3 Fluorination with Selectfluor®

Protected D-galactal **5** being nucleophilic at C-2, an addition of an electrophilic fluorine atom on the double bond can then be envisioned. Historically, the first source of electrophilic fluorine used on glycals was molecular fluorine F_2 which is highly toxic and very difficult to handle.[24] Later on, electrophilic fluorination reagents such as CF_3OF, $FClO_3$ and XeF_2 were explored and tested with glycals but the results were not fully satisfactory. A major breakthrough in the field of electrophilic fluorination of glycals arose from the discovery of the exceptional properties of Selectfluor® **10** (1-chloromethyl-4-fluorodiazoniabicylo[2,2,2] bis(tetrafluorobotate)) (Scheme 13). This reagent has the advantages of being mild, safe, and stable besides being an effective source of electrophilic fluorine. Indeed, the fluorine atom in this molecule is bound to a positively charged nitrogen which renders it highly electrophilic. With glycals, Selectfluor®

gives much better results than two other very popular electrophilic fluorination reagents: NFSI (*N*-Fluorobenzenesulfonimide) **11** and N-Fluoropyridinium **12**.

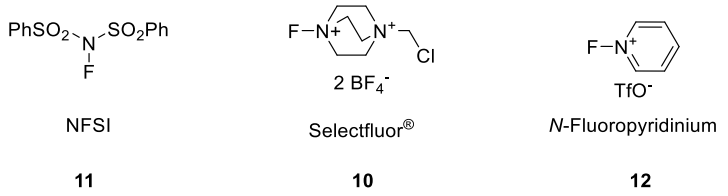

Scheme 13. Structure of commercially available selectfluor®, NFSI and N-Fluoropyridinium.

The electronic distribution of the enol ether function of D-galactal implies that the C-2 is the most nucleophilic position which means that the addition of the fluorine will be regioselective. As depicted in Scheme 14, the first step of the reaction mechanism is the formation, in a *syn* manner, of a 2-fluoro-1-trisalkylammonium intermediate **14.**[28] The stereoselectivity of this first step is dictated by the steric hindrance of the top face of D-galactal that is mainly due to the substituent at the C-4. It means that the fluorine exclusively reacts from the bottom α face. The second step is the attack of a nucleophile **15** that substitutes the ammonium on the anomeric position. There is a strong debate about the nature of this substitution. It is believed that it is not a pure S_N2 process. A mechanistic study[28] has shown that increasing the bulk size of the incoming nucleophile in that kind of reaction does change the α/β ratio in favor of the product with the less steric clash. This result suggests a S_N1-like process, despite the presence of the fluorine atom.

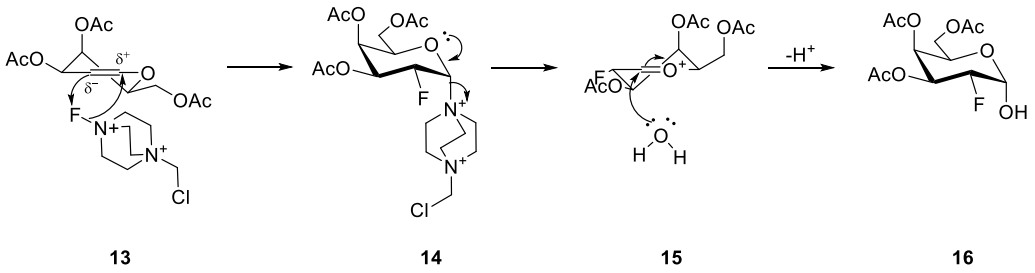

*Scheme 14. Mechanism of the fluorination of D-galactal **5** with Selectfluor® **10**.*

This reaction is realized at room temperature in a mixture of water and nitromethane (Scheme 15).[29] Nitromethane is chosen as the solvent because it can dissolve the charged Selectfluor salt and it remains inert during the reaction. After consumption of the starting material (monitored by TLC, usually 5 hours), the reaction is heated to reflux for 1 hour so that all the 2-fluoro-1-trisalkylammonium **14** intermediate is hydrolyzed. Glycoside **16** is obtained after purification by silica-gel chromatography with a 68 % yield.

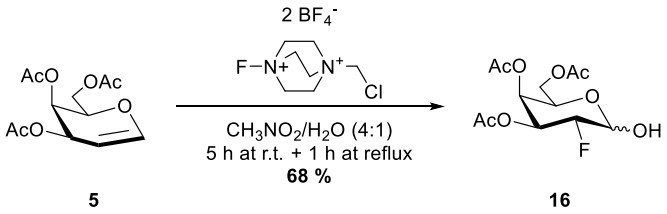

*Scheme 15. Fluorination of D-galactal with selectfluor bis-tetrafluoroborate **10**.*

It is known in the literature[22] that the counterion of Selectfluor® can have an effect on the formation of side products and subsequently on the yield. Selectfluor® is commercially available as a bis-tetrafluoroborate salt. This counter anion is actually a source of nucleophilic fluorine and thus can allow the formation of a 1,2-difluorosaccharide as a side product. Based on that hypothesis, the use of a triflate counterion, which is much less nucleophilic and more soluble in nitromethane, may increase the yield in the desired product. For example, the reported yields for the fluorination of diacetylfucal with benzyl alcohol as the nucleophile varied from 26 % to 72 % when Selectfluor bis-triflate **17** was used instead of commercial Selectfluor® **10**. However, the impact of the counterion effect also depends a lot on the nature of the substrate and on the nucleophilic species that adds to the anomeric center. To test if the same effect could be observed on D-galactal, Selectfluor bis-triflate **17** has been synthesized from commercially available Selectfluor bis-tetrafluoroborate **10** with a 91 % yield (Scheme 16).

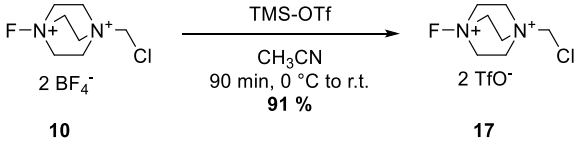

Scheme 16. Synthesis of Selectfluor® bis-triflate from commercially available Selectfluor®.

Then, the fluorination of D-galactal was performed with that particular salt to see the effect on the obtained yield after purification (Scheme 17). Unfortunately, the yield (42 %) was actually lower than with the commercial Selectfluor®. It can be explained by the fact that the reactions were not performed on the same scale. Indeed, minor losses by experimental errors can have a higher impact on the yield with reactions done on small scale. Still, as the yield with standard Selectfluor® is satisfactory to fulfill our objectives, it has been decided to carry on the fluorination step with commercially available Selectfluor®.

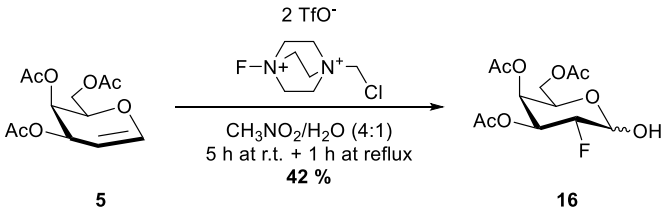

*Scheme 17. Fluorination of D-galactal with selectfluor bis-triflate **17**.*

Once the fluorination step was optimized, the acetyl groups could then be deprotected. For that matter, the Zemplén deacetylation procedure has been followed (Scheme 18).[30] It consists in using a catalytic amount of sodium methoxide in methanol to deprotect quickly all the acetyl groups. After complete consumption of the starting material (monitored by TLC, usually 20 minutes), the final crude mixture is passed through a short column of Dowex 50WX8. This resin is an ion-exchange resin with sulfonic acid functional groups that will allow the removal of sodium salts from the desired product. Then the solution is concentrated *in vacuo* to obtain **6** as a slight yellowish syrup (99 % yield) that eventually solidifies into a white solid after a day at rest.

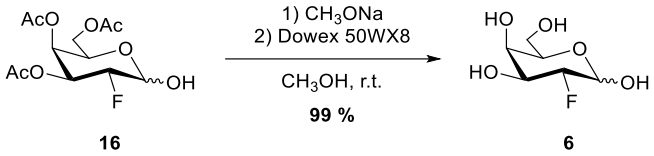

Scheme 18. Deprotection of the acetyl functions with MeONa to obtain 2-deoxy-2-fluoro-D-galactopyranose.

III.4 Conversion from pyranose to furanose

The predominant isomer of D-galactose at 30 °C is its pyranoside form (94 %) and its furanoside form accounts only for 6 %.[23] In general, pyranosides are thermodynamically favored over their furanoside counterparts. This is mainly due to the minimization of the steric interactions between the hydroxyl groups in six-membered ring.[31] As the desired form of the target molecule is the furanoside, molecule **6** needs to be converted with the highest possible yield to the 5-membered ring. A few approaches (Scheme 19) to achieve this objective exist such as the one-step anomeric *O*-alkylation of galactose[32], per-*O*-benzoylation of galactose in hot pyridine[33] or the one-step *tert*-butyldimethylsilylation of galactose in DMF.[34]

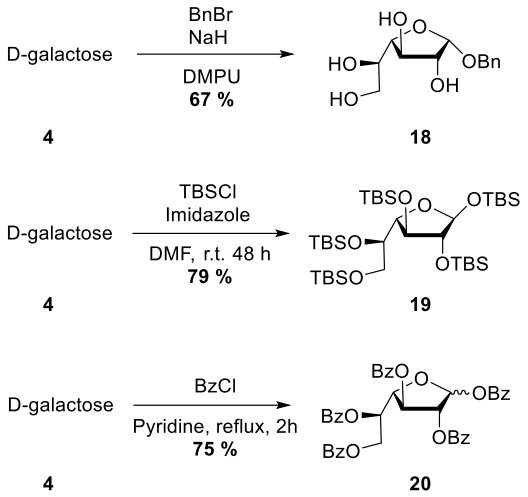

Scheme 19. Described reactions of galactose conversion to its furanose form found in the literature.

However, one technique related to 2-deoxy-2-fluoro-D-galactose **6** is described in the literature: it consists in the per-*O*-acetylation in pyridine at reflux by Q. Zhang and H.-W. Liu to get **7** with a 28 % yield (Scheme 20).[35] We thus decided to assess first whether this reaction was reproducible in our hands. In this reaction, the totally unprotected carbohydrate **6** is first heated at 110 °C for 2 hours in pyridine and acetic anhydride is then added dropwise to the solution which is left for 90 minutes under stirring. After cooling down to room temperature, a mixture of both pyranoside and furanoside products is obtained and the separation can be performed by silica-gel column chromatography. In practice, the final yield of furanoside product obtained is 25 %.

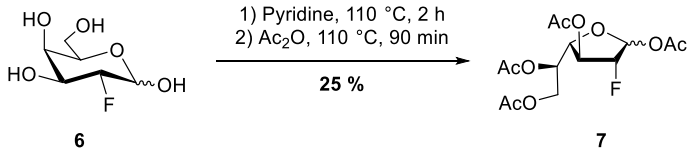

*Scheme 20. Pyranoside into furanoside conversion of molecule **6**.*

There are two possible hypotheses that can explain this conversion (Scheme 21). The first one is based on thermodynamics and would suppose that the equilibrium constant of the furanoside/pyranoside interconversion ($K_{p\text{-}f}$) is more favorable at 110 °C than at room temperature. Once this equilibrium is established at high temperature, it is frozen by the acetylation of the anomeric lactol with acetic anhydride. This protection will prevent the furanoside ring to re-open and to re-cyclize into the 6-membered ring when the glycoside cools back to room temperature.

The second explanation is based on kinetics and would imply that the anomeric acetylation rate constant of the furanoside (k_f) is faster than the one of the pyranoside (k_p) at higher temperature. It means that, based on the Curtin-Hammett principle, the product that forms the fastest will be the most present in the reaction mixture.

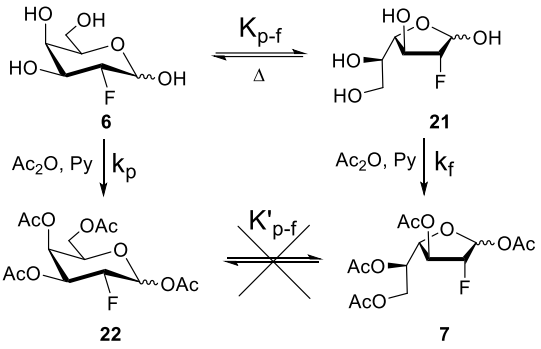

*Scheme 21. General scheme of formation of fluorogalactosides **7** and **22**.*

As the obtained yield with those conditions is quite low, a set of reaction times has been tested to evaluate their impacts on the conversion to furanoside product **7** (Table 1). The percentages of α,β-furanoside and α,β-pyranoside in the crude have been determined by ^{19}F NMR. As each molecule possesses only one fluorine atom, the integration of each peak indicates the proportion of each molecule relative to the others. To identify which peaks correspond to the pyranosides (α and β), a reference has been synthesized from molecule **16** (Scheme 22). In this experiment, a furanoside cannot be formed as the hydroxyl group at C-4 is already protected in **16**.

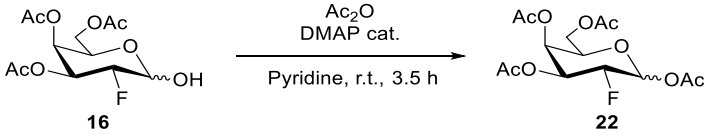

*Scheme 22. Acetylation reaction of molecule **16** to obtain a NMR reference.*

The results gathered in Table 1 suggest that the equilibrium between the pyranoside and the furanoside is achieved within 1 hour and does not lead to any change within a 4-hours time scale. The conversion is total in all cases.

Equilibration time	α/β-furanoses (%)	α/β-pyranoses (%)	Unknown molecules (%)
1 h	23.0	58.2	18.9
2 h	24.7	57.5	17.8
4 h	23.0	59.3	17.7

*Table 1. Calculated NMR yields for different equilibration times in hot pyridine of the pyranoside to furanoside conversion. Reaction conditions: 1) Pyridine (reflux), **6** (0.38 mmol.L^{-1}), equilibration time 2) Dropwise addition of Ac_2O (16.7 eq.), pyridine (reflux), 1h30 3) Addition of DMAP, 0.5 eq, 1h (r.t.).*

To investigate the effect of the acylating agent on latter transformations, the same reaction was performed with benzoyl chloride instead of acetic anhydride (Scheme 23).[33] NMR of the crude showed indeed the formation of the furanoside product with approximately the same proportion of furanoside to pyranoside products than with acetyl protecting groups. However, it was impossible to separate these two molecules by silica gel chromatography. As shown in the next section, this pyranoside/furanoside mixture was still used for further reactions since it allowed us to compare the effect of the protecting esters on the reactivity and thus the stability of these glycosides.

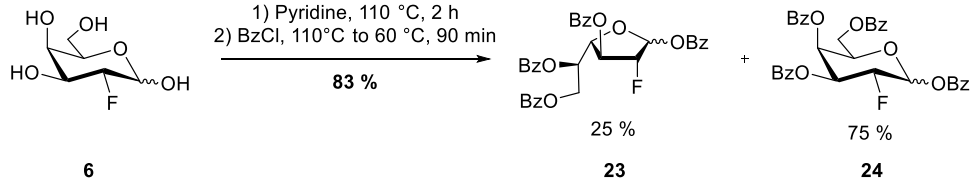

*Scheme 23. Benzoylation reaction of molecule **6** at 110 °C in pyridine.*

III.5 Glycosylation reaction of a nitrophenol derivative

The last major structure modification that has to be done to obtain the target molecule is to couple glycoside **7** with a good leaving such as 4-nitrophenol or 2,4-dinitrophenol. Two distinct approaches have been explored and are described in the following sections.

III.5.1 Direct substitution of the anomeric group.

The method consists in a direct substitution of the anomeric acetate by a nucleophile under Lewis acid activation (Scheme 24). The chosen nucleophile is 4-nitrophenol as it has a good leaving group characteristic and its deprotonated form (4-nitrophenolate) has the particular characteristic of absorbing light in the visible spectrum. This feature facilitates enzymatic assays with GHs by using a simple UV-visible spectrometer and measuring the absorbance at 410 nm.[36]

The first reaction tested is the $SnCl_4$ catalyzed substitution of the anomeric acetate by 4-nitrophenol. This reaction was selected because it is described in the literature for the non-fluorinated D-galactofuranose.[37] It consists in first adding the Lewis acid in a solution of the glycoside to activate it and in a second time, adding the nucleophile to allow the substitution.

This reaction is realized at room temperature for 3 hours, followed by an aqueous work-up and a final purification by column chromatography. Many trials of this reaction have been

performed by modifying some parameters such as the number of equivalents of reagents or the nature of the protecting group on the glycoside (Table 2). Unfortunately, none of them have allowed the formation of the target molecule **25**.

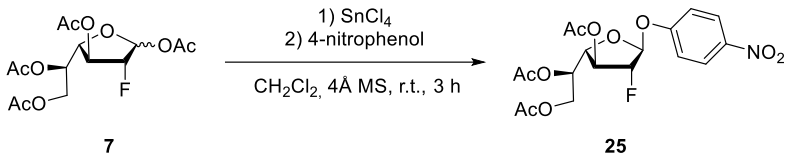

Scheme 24. Lewis acid catalyzed substitution of the anomeric acetate group by 4-nitrophenol.

Entry	Protecting groups	Eq. $SnCl_4$	Eq. 4-nitrophenol	Conversion (%)	Yield (%)
1	Acetyl	1.4	1.2	54	0
2	Acetyl	2.8	2.2	39	0
3	Benzoyl	1.4 + 0.5	1.2	37	0

Table 2. Conversions observed for the $SnCl_4$ catalyzed coupling reaction with 4-nitrophenol (Scheme 24). The conversions have been evaluated by ^{19}F NMR.

In every case, the ^{19}F NMR spectrum of the crude shows partial consumption of the starting material (α and β furanosides) and apparition of one major product. The isolation of this product was possible by column chromatography and it was postulated first that it was the lactol by-product **26** that would be obtained by hydrolysis of the desired molecule during the aqueous work-up (Scheme 25). This hypothesis was supported by the fact that the ^{1}H NMR spectrum of that by-product was clearly (Figure 9) showing seven protons and three acetyl groups.

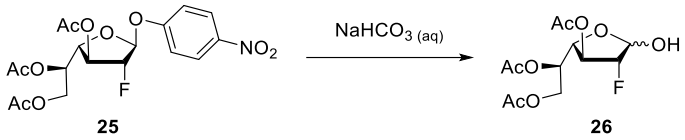

*Scheme 25. Hypothesized formation of the lactol by-product **26** after aqueous work up of glycoside **25**.*

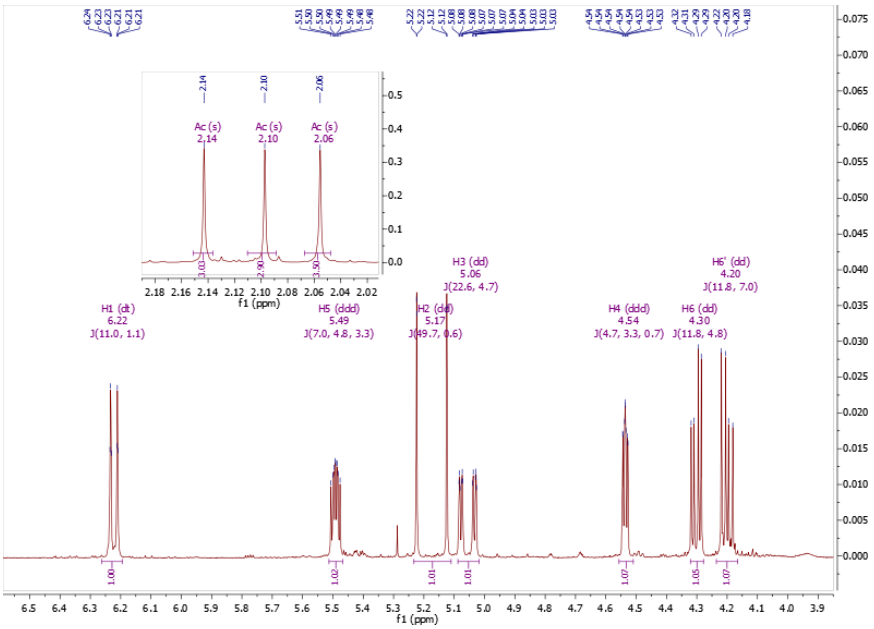

*Figure 9. ^{1}H NMR spectrum of molecule **27** (main product of the $SnCl_4$ coupling reaction).*

However, there were some oddities about this assumption:

1) The supposed "lactol" was eluting at a higher R_f than the starting material although it is supposed to be more polar.
2) Only one anomer of the lactol could be observed by NMR. It seems quite unusual as there is an equilibrium between α and β lactols which should allow for the formation of both of them even if one is minor.
3) The NMR spectra of the reaction mixture before and after aqueous work-up are the same. Yet, the reaction is water-free before work-up. It thus raises the question of how the lactol could have been formed without water?

Based on those facts, another hypothesis was formulated and was later confirmed by high resolution mass spectroscopy. The by-product was actually the anomeric chloride **27** formed by reaction of the glycoside **7** with $SnCl_4$ (Scheme 26).

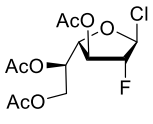

27

Scheme 26. Confirmed by-product structure obtained by the coupling reaction with $SnCl_4$.

This molecule is indeed less polar and its formation can be explained even without the presence of water. The apparition of molecule **27** can be rationalized by the destabilization of the oxycarbenium intermediate because of the fluorine atom at C-2. With the non-fluorinated D-

galactofuranose, the formation of the target molecule **31** is realized by anchimeric assistance of the nearest acetyl group at C-2 (Scheme 27).[38] This explains how 4-nitrophenol has the ability to bind to the anomeric position even if it is a poor nucleophile. This mechanism cannot be applied to the fluorinated D-galactofuranose as there is not a C-2 acetyl group. Furthermore, the putative oxycarbenium intermediate is highly destabilized by the fluorine. As the chloride is the best nucleophile in the reaction mixture and the anomeric acetyl group can still be activated by $SnCl_4$, there is a direct substitution of the acetate group by the chloride. Then the intermediate **27** prevents the reaction from going further because 4-nitrophenol is not nucleophilic enough to substitute the chloride directly under those conditions.

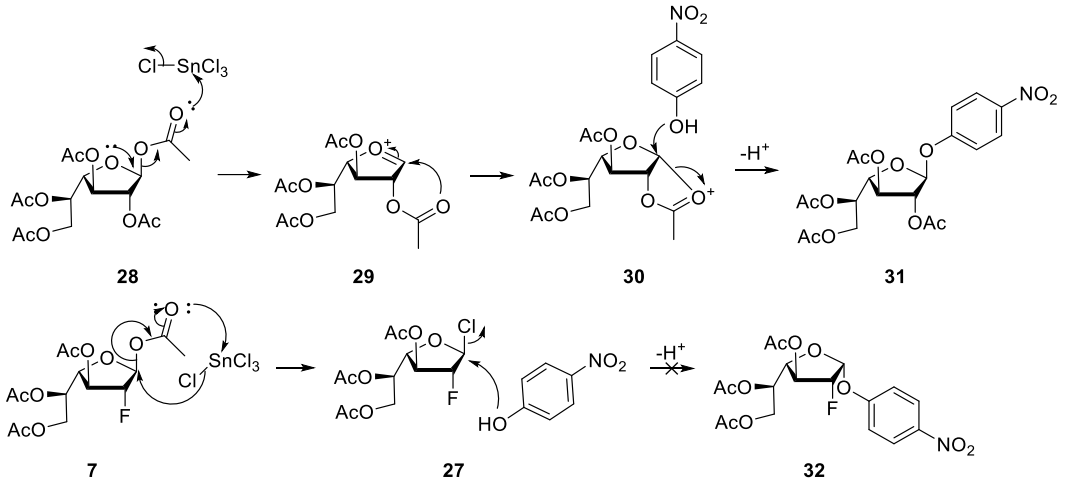

Scheme 27. Mechanism of $SnCl_4$ catalyzed coupling reaction with 4-nitrophenol with fluorinated and non-fluorinated D-galactofuranose.

Another way of activating the anomeric position needed to be envisioned. Q. Zhang and H.-W. Liu[35] were the first one working on molecule **7** and their objective was to couple it with a uridine diphosphate group so that they could conduct mechanistic studies on the UDP-Galactopyranose Mutase enzyme from *Mtb*. In their synthesis, they substituted the anomeric acetate group of **7** by a phosphate group using TMSBr and Et_3N. This method has been tried for our purposes with the only modification being that the nucleophilic species is 4-nitrophenol instead of a phosphate molecule (Scheme 28). Unfortunately, the reaction was not successful as the conversion was really low (6 %) according to the ^{19}F NMR spectrum.

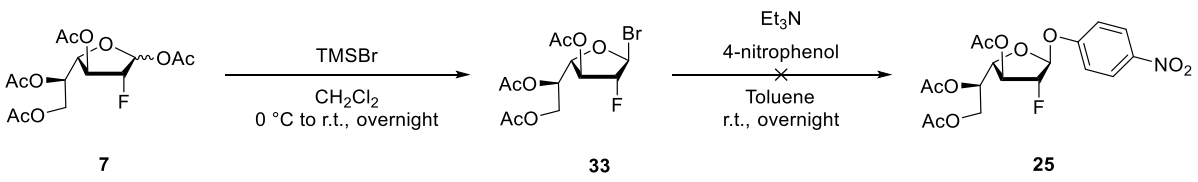

*Scheme 28. Synthetic scheme of **25** through the intermediate bromide **33**.*

As a direct substitution did not seem to work well, it has been decided to explore a different synthetic route.

III.5.2 Selective anomeric deprotection and S_NAr

An important class of reactions in aromatic chemistry is the nucleophilic aromatic substitution (S_NAr). This kind of reaction relies on the displacement of a leaving group bound on an aromatic ring by a nucleophile. For this reaction to happen, the aromatic ring has to bear an electron-withdrawing group ortho or para to the position of the leaving group.

For our purpose, the S_NAr reaction can be used to couple 4-nitrophenol with the glycoside as the presence of a nitro function on the structure of the leaving group fulfills one of the conditions required for a successful S_NAr reaction. It is even conceivable to install a 2,4-dinitrophenol derivative on the glycoside as this molecule is more activated towards S_NAr thanks to the presence of two electron withdrawing groups. Moreover, dinitrophenol (pKa = 4.07)[39] is even a better leaving group than 4-nitrophenol (pKa = 7.15)[39] which is a strong advantage in view of the use of this molecule as a reactive inhibitor of a glycosidase. Indeed, the better is the leaving group on the anomeric center, the easier is the first step of the enzymatic mechanism and thus the formation of the covalent enzyme-substrate complex.

The idea would be to first selectively deprotect the anomeric acetyl function of molecule **7** to form a lactol and in a second time, perform a reaction between the free hydroxyl group and 1-fluoro-2,4-dinitrobenzene. Those reactions will be described in the following sections.

III.5.2.1 Selective anomeric deprotection

In carbohydrate chemistry, the selective deprotection of anomeric acetates is classically performed thanks to hydrazine acetate. This reaction has even been described in the literature on the penta-*O*-acetyl-D-galactofuranose in DMF.[40] The selective deprotection of the anomeric ester in presence of several primary and secondary acetate has been ascribed to the better leaving group ability of a lactol over alcohols.

However, the use of hydrazine as a reagent has some drawbacks as it has a bad shelf stability and toxicity. In addition, DMF is a hazardous solvent which may complicate workup due to its polarity and high boiling point. Recently, a novel method of selective anomeric acetyl deprotection has been developed. It consists in using 3-(dimethylamino)-1-propylamine (DMAPA) and THF as the solvent (Scheme 29).[41] DMAPA **34** features a primary amine that

can act as a nucleophile for the deprotection of the acetyl function and a tertiary amine acting as a base. This allows an easy elimination of the amide formed after deacetylation by a simple acidic work-up which can dramatically facilitate silica gel chromatography.

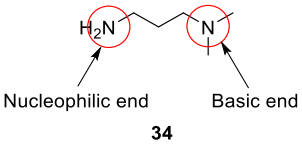

Scheme 29. Structure of 3-(dimethylamino)-1-propylamine (DMAPA).

These two different conditions (hydrazine and DMAPA) have been tested for this purpose and the results are summarized in Table 3.

Entry	Deprotecting agent	Eq.	Reaction time	Conversion (%)	Products composition (%)	
					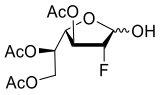 **26**	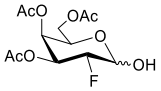 **16**
1	DMAPA	5	2 h	88	0	100
2	DMAPA	1.15	4 h	52	57	33
3	Hydrazine acetate	1.2	2 h	43	62	27

Table 3. Conversion and distribution of products from reaction crude of the anomeric deprotection (Scheme 30). Percentages were calculated from the ^{19}F NMR.

We first used the conditions including DMAPA described by Andersen et al. (Table 3, entry 1).[41] The conversion was quite high but the main product was found to be the pyranoside lactol **16** (Scheme 30). This result was quite unexpected because it meant that not only the anomeric position had been deprotected but also the acetyl at C-5. Moreover, the ^{1}H NMR of the crude showed that the pyranoside lactol **16** had its C-4 re-acetylated. These transformations are difficult to rationalize as the amide **35** formed with DMAPA by the anomeric deprotection is a poor acylating agent. To prevent the formation of pyranoside **16**, we modified the original method by reducing the number of equivalents of DMAPA to 1.15 (entry 2). It indeed allowed the formation of the lactol furanoside but also of a non-negligible amount of pyranoside at the same time.

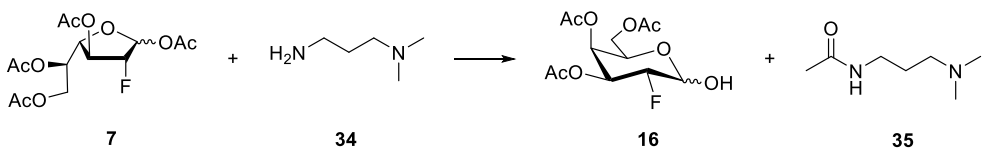

*Scheme 30. Selective anomeric deprotection of furanoside **7** with DMAPA **34**.*

A reasonable way to explain the formation of molecule **16** would be an intramolecular transfer of an acetyl group from C-5 to C-4 (Scheme 31). In that case, the pyranoside lactol acts as a thermodynamic sink and shifts the equilibria towards its formation.

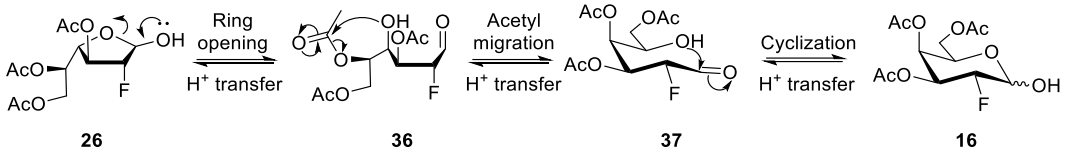

Scheme 31. Possible mechanism of the conversion of furanoside into pyranoside through a C-5 acetyl migration.

The final attempt of direct selective anomeric deprotection was made using hydrazine acetate (Scheme 32). But as shown in the entry 3 of Table 3, the conversion was low and there was still formation of the pyranoside lactol **16**. All those trials show that deprotecting selectively the anomeric acetyl group requires finding a compromise between conversion and furanose/pyranose ratio. Instead of optimizing further this nucleophilic regioselective deacetylation reaction, we decided to explore a different pathway.

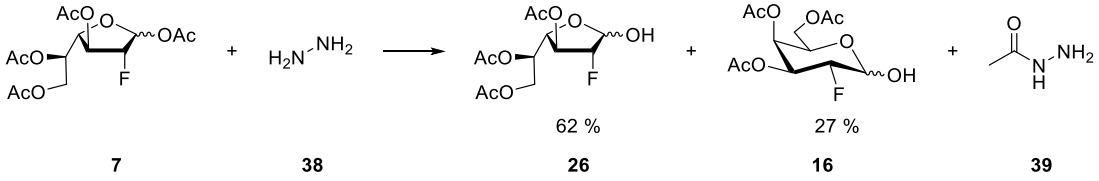

*Scheme 32. Selective anomeric deprotection of furanoside **7** with hydrazine.*

In reference to the synthesis of D-galactal in section III.2, it was discovered that the 1-bromo intermediate **9** was relatively unstable and could be hydrolyzed in the presence of water. This gave us the idea to follow such a sequence. Indeed, if it is possible to substitute the anomeric acetate group by a bromide, then this reactive intermediate could be transformed into lactol **26** (Scheme 33). The bromination reaction is usually performed under strongly acidic conditions which would be different from the problematic basic conditions described above.

The bromination was performed with a large excess of HBr in DCM (Scheme 33). After 12 hours at room temperature, the conversion was total and the only major product observed by NMR was the expected β-1-bromo glycoside **33**. Since bromide **33** was unreactive in wet toluene, we turned our attention to different hydrolytic conditions. An aqueous work-up with saturated $NaHCO_3$ of a solution of molecule **33** in DCM was performed but no reaction was observed either. In fact, by destabilizing the oxycarbenium intermediate, the fluorine atom at C-2 greatly stabilizes bromide **33**.

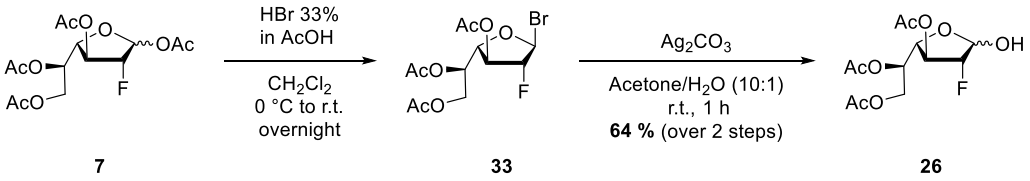

*Scheme 33. Synthetic route used to obtain the furanoside lactol **26**.*

Conditions were found eventually in the literature for hydrolyzing tri-*O*-acetyl-2-deoxy-2-fluoro-α-D-mannopyrannose.[42] Those conditions include the use of silver carbonate in a solution of Acetone/Water. The silver cation plays an important role as it forms an insoluble salt with bromide which prevents it from rebinding to the glycoside. The carbonate is a mild base allowing some hydroxide ions to be generated in the mixture and those will react with the oxycarbenium anomeric center. After purification by column chromatography, molecule **26** was obtained with a 64 % yield over two steps. The ratio of α to β is 1:9 as determined by ^{19}F NMR. However, this ratio should not be considered as definitive for the further S_NAr reaction as the equilibrium between the two anomers can lead to different distribution of diastereoisomers.

III.5.2.2 Nucleophilic aromatic substitution on the lactol

Once the lactol **26** is obtained, it was possible to envision a reaction between the free hydroxyl group and an aromatic derivative in a nucleophilic aromatic substitution fashion. This reaction is performed with 1-fluoro-2,4-dinitrobenzene (FDNB) and 1,4-diazabicyclo[2.2.2]octane (DABCO) which acts as a base. This reaction has been initially described in DMF for 1.5 hours at room temperature with other lactols.[43] However, the same reaction has also been described in acetonitrile which is a huge advantage considering the lower boiling point of this solvent. This allows then an easier elimination of the solvent at the end of the reaction.[44]

This reaction is most often described as a two-step mechanism[45] in which the first step consists in the nucleophilic attack of the oxygen from the hydroxyl group to the C-1 of FDNB (Scheme 34). In the second step, there is elimination of the fluorine atom and recovering of the aromaticity of the benzene ring. The by-product of the reaction is a salt of protonated DABCO and fluoride. Recent results in the literature suggested that such a reaction could follow a concerted mechanism.[46]

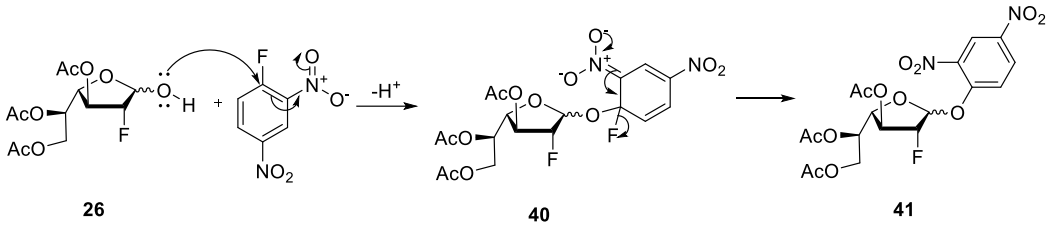

*Scheme 34. Possible mechanism of a S_NAr applied for the coupling of 2,4-dinitrophenol with glycoside **26**.*

This reaction has been performed at room temperature for 2.5 hours (Scheme 35). After purification, glycoside **41** was obtained with a combined 57 % yield and an α/β ratio of isolated anomers of 2:3. The separation of each diastereoisomer by silica gel chromatography was facilitated by the large difference in polarity between both molecules. Indeed, with an eluent made of EtOAc and cyclohexane in a 1:1 ratio, the α anomer has a R_f of 0.30 while the β anomer has a R_f of 0.72.

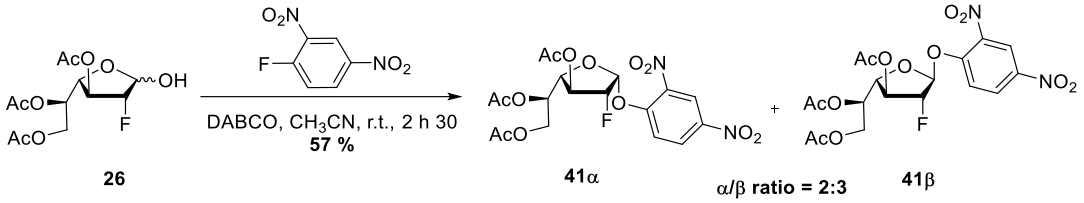

*Scheme 35. Reaction scheme of the S_NAr reaction with lactol **26** and FDNB.*

Once those two molecules were isolated, it was necessary to demonstrate the α/β absolute configurations of the two anomers. First assumptions could be made based on the NMR coupling constants. Indeed, it is well known that based on the 3D conformations for pyranosides, the ^{1}H-^{1}H coupling constants can differ between trans-diaxial protons and axial-equatorial protons.[47] Equatorial-axial coupling constants are usually found between 1 Hz and 4 Hz while equatorial to equatorial coupling constants range between 0 Hz to 2 Hz. If we consider that furanoside molecules are mainly present in an envelope conformation, the measured coupling constants between H-1 and H-2 might possibly be characteristic of the anomeric configuration (Scheme 36).[31] In the β anomer there is a pseudo-equatorial to pseudo-equatorial relationship between H-1 and H-2 which correlates with the 0 Hz observed coupling constant while in the α anomer, this relation is pseudo-axial to pseudo-equatorial and the measured coupling constant equals 4.3 Hz. The same kind of relationship between dihedral angles has also been observed with the coupling constants between H-1 and the fluorine. This coupling constant equals 9.4 Hz in the β anomer where the fluorine is in pseudo-axial position while it is 0 Hz for the α anomer where the fluorine is in pseudo-equatorial position.

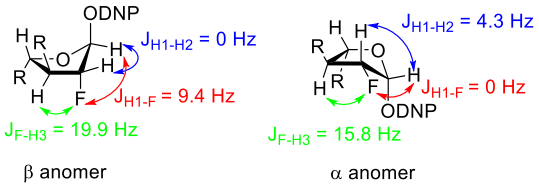

Scheme 36. Preferred envelope conformations of both diastereoisomers according to literature.[31] *The measured coupling constants between H-1, H-2,H-3 and F are represented in the scheme.*

Noteworthy, similar coupling constants are observed with comparable furanosides described in the literature. In that respect, the described H1-H2 and H1-F coupling constants of both isolated anomers of glycoside **7** by Q. Zhang and H.-W. Liu[35] are nearly identical to our synthesized anomeric equivalent **41α** and **41β**.

However, the apparent conformation of a furanoside is mainly an average of many conformations arising from envelope and twist interconversions and general coupling constants rules for pyranosides may not apply for furanosides.[48] We thus need a complementary technique to confirm the anomeric configuration of each molecule. The preferred characterization technique for this purpose is the nuclear Overhauser effect (NOE) observed in NMR. The principle of this technique is to detect interactions between protons through space and not through chemical bonds as for the coupling constants. By irradiating a specific nucleus (here the anomeric H-1 proton), it is possible to evidence the protons that are in close proximity.

In the NOE spectrum of the first analyzed anomer illustrated in Figure 10, a strong interaction with the H-2 proton and with an aromatic proton from the 2,4-dinitrophenyl group are observed. The same interactions are also observed in the NOE spectrum of the other anomer in Figure 11 and thus they cannot help us determine the anomeric configuration. However, a small interaction between H-1 with a proton located at 4.29 ppm can also be seen. This NMR shift corresponds to H-4 and according to the structure, it strongly suggests an α configuration as those two protons are both on the same face of the ring.

Concerning the NOE spectrum of the second anomer illustrated in Figure 11, no interaction can be seen between H-1 and any other proton with the exception of H-2 and an aromatic proton. The lack of interaction with H-4 allows us to confirm that this anomer has the opposite configuration of the first analyzed molecule and that it is indeed the β anomer.

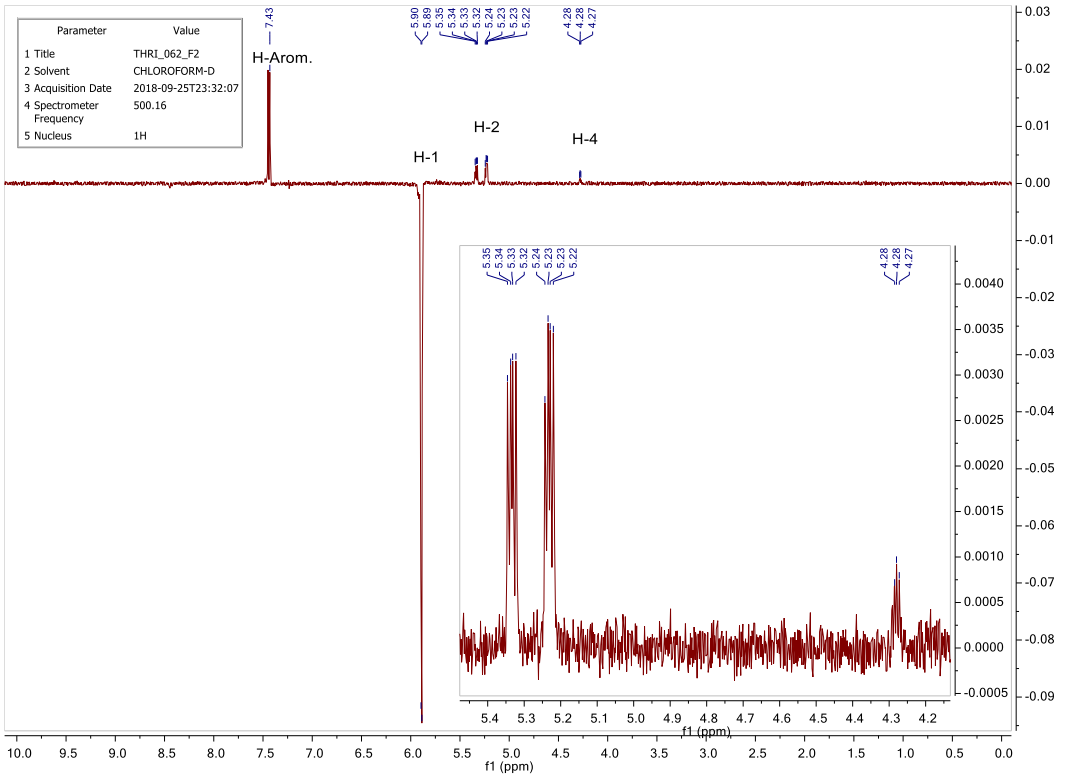

*Figure 10. [1]H NOE NMR spectrum of **41**$_{\alpha}$. The irradiated proton is H-1 and a small interaction with H-4 proton can be seen.*

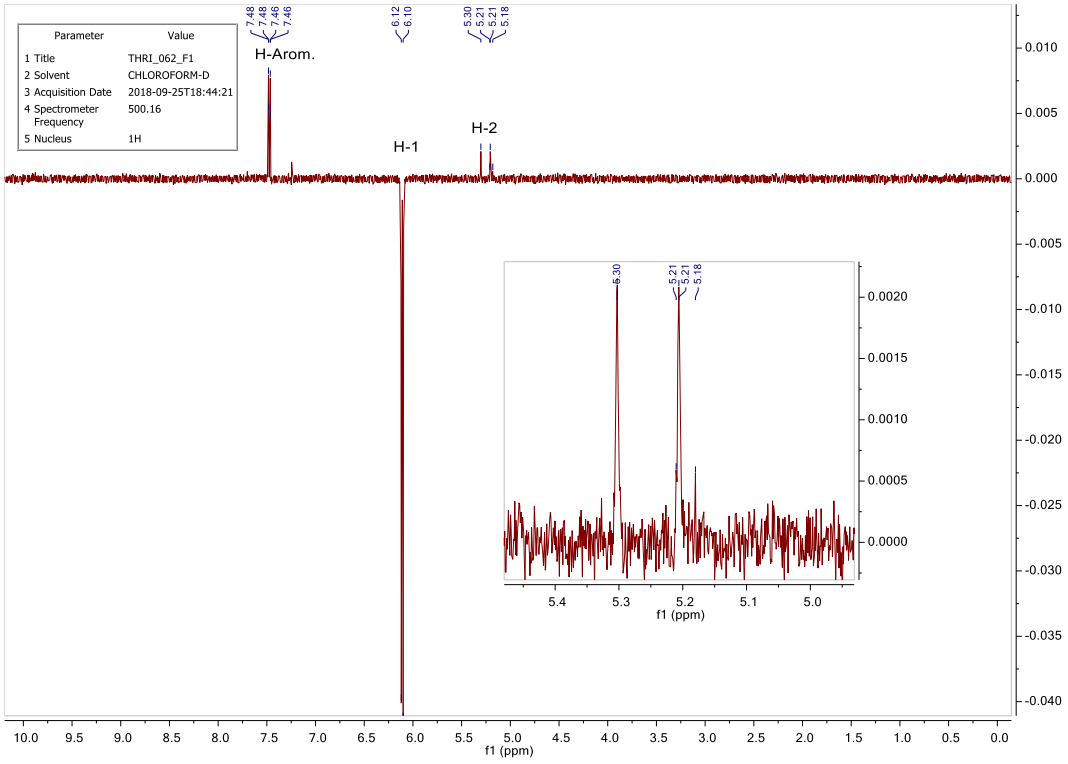

*Figure 11. [1]H NOE NMR spectrum of **41**$_{\beta}$. The irradiated proton is H-1 and apart interactions with H-2, no other interactions can be observed.*

Based on the analyses of ^{1}H-^{1}H, ^{1}H-^{19}F coupling constants and NOE spectra, we could thus assign the absolute configuration of both anomers of **41**.

III.6 Final deprotection

The last step of the synthesis is a mild deprotection of the last three acetyl functions. To perform this reaction, two different methods were tested. The first method is the so-called Zemplén deacetylation (Na in CH_3OH or CH_3ONa in CH_3OH) as used for the deprotection of glycoside **16**. Those conditions are described in the literature for the deprotection of the non-fluorinated D-galactofuranose coupled with 4-nitrophenol.[37] A different technique consists in using acetyl chloride in MeOH. This reaction is described in the literature for the deprotection of non-fluorinated glycosides coupled with 2,4-dinitrophenol.[49] The results obtained with those two different techniques can be found in Table 4.

Entry	Reagent	Equivalent	Conditions	Crude composition[a] (%)			Isolated yield (%)
				Target molecule	Degradation products	Starting Material	
1	MeONa	0.65	30 min. 0 °C	40	60	0	23
2	MeONa	0.1 → 0.4	90 min. 0 °C	24	62	14	/
3	AcCl	47.6	8 hours 0 °C and overnight at 4 °C	100	0	0	62

*Table 4. Deacetylation of glycoside **41β**. a) Assessed by ^{19}F-NMR.*

The first attempt at deprotecting the acetyl groups of glycoside **41β** was performed with catalytic amount of sodium methoxide in methanol (Table 4, entry 1). However, these conditions were found to be too harsh for the substrate as the reaction led to some degradation. The main degradation products being 2,4-dinitrophenolate and 1-*O*-methoxy-2-fluoro-D-galactopyanose (not isolated). Even if the amount of catalytic MeONa was reduced (entry 2), the degradation was still observed and the conversion was even worse.

The second technique uses acetyl chloride in methanol (entry 3). This reaction might seem unusual as acetyl chloride is more commonly used to actually esterify alcohols but it can have a different role if it is used in methanol. Indeed, methanol will react with AcCl to form MeOAc and by doing so, it will slowly generate HCl *in situ*. This last molecule will catalyze the transesterification of the acetyl groups to methanol which is in large excess. At the end, the

totally deprotected glycoside **1** will be obtained. This reaction was performed for 8 hours at 0 °C and then overnight at 4 °C (Scheme 37). The conversion was total and the obtained yield after column chromatography is 70 % for **1β** and 11 % for the **1α**. The difference in yield might be due to different stability of the two diastereoisomers.

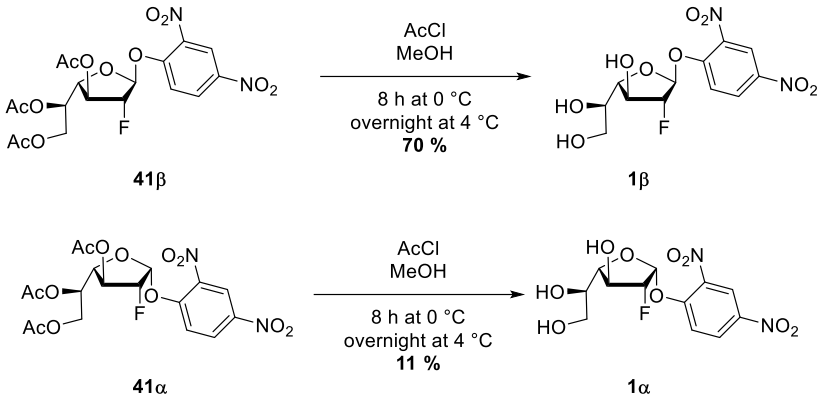

*Scheme 37. Deprotection of all acetyl groups on glycoside **41α** and **41β** with AcCl in MeOH.*

The target molecule being obtained in both anomeric configuration, precise amounts were weighed and were sent to the University of Lille. The team working on the novel glycosidase will be able to pursue their biochemical investigations on the enzyme. Finally, α-D-galactofuranoside **1α**, with the "wrong" anomeric position (the targeted enzyme is a β-glycosidase) will be used by the enzymologists as a control molecule.

IV. Conclusion

The objective of this master thesis was to find a working synthetic pathway to a mechanistic probe of a novel glycosidase from *Mycobacterium tuberculosis*. This probe would allow a better understanding of the novel enzyme at the molecular level. The structure of the probe **1β** (Scheme 38) has been designed according to the supposed retention of the anomeric configuration mechanism that is shared among many glycosidases. It is based on the structure of its natural substrate (D-galactan) but with two major modifications:

1) A fluorine atom at C-2 instead of the hydroxyl group
2) A good leaving group on the anomeric position

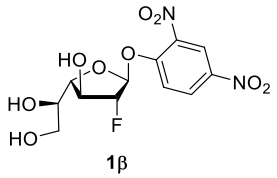

Scheme 38. Structure of the mechanistic probe.

As this molecule was not described in the literature, it was necessary to look for a viable synthetic route (Scheme 39).

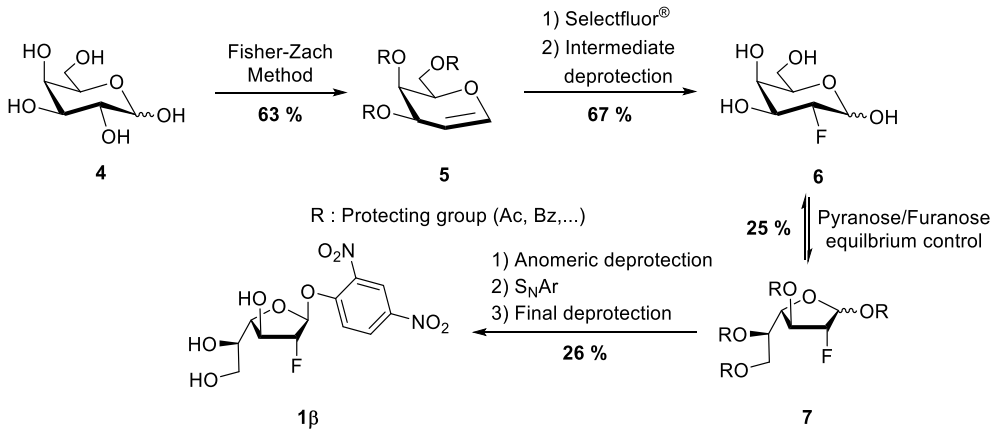

*Scheme 39. Synthetic route towards the synthesis of the molecular probe **1β** with the yield of each major step.*

The first synthesized molecule was D-galactal **5** which was obtained with no major issues. The only problem encountered for this synthesis was the low stability of the galactosyl bromide intermediate which simply implied to avoid an aqueous work-up. More recent conditions reporting a better yield were tested but they were less effective in our hands. Thus it has been concluded that the standard Fisher-Zach method was the best to follow.

Fluorination was performed with Selecfluor® to obtain 2-deoxy-2-fluoro-D-galactopyranose **6** with a moderate yield. Two different selectfluor salt were tested to see the impact of the

counterion on the reaction. The best yields were obtained with the commercial Selectfluor® salt (tetrafluoroborate counterion) while the modified salt (triflate counterion) gave a lower yield. The full deprotection of the acetyl function has been performed thanks to the Zemplén conditions with a very good yield.

Conversion from the pyranoside **6** to the furanoside **7** has been performed following conditions inspired by the seminal work of Q. Zhang and H.-W. Liu.[35] This reaction has been found to be reproducible with yields similar to the one reported in their article. As those yields were low, different reaction times were tested but unfortunately, they gave the same pyranoside/furanoside ratio.

The anomeric coupling of the fluorinated furanoside with a dinitrophenyl group was tested with two different approaches. The first one, based upon the direct Lewis acid catalyzed substitution of the anomeric acetate group by 4-nitrophenol, did not afford the desired glycoside under various reaction conditions. The second approach, based on a S_NAr reaction, required first the selective deprotection of the anomeric acetyl function. The usual conditions based on the use of nucleophilic amines such as DMAPA or hydrazine acetate did not work because they led to the formation of the pyranoside lactol. Instead, it was necessary to realize first an anomeric bromination followed by hydrolysis under basic conditions to obtain the furanoside lactol successfully with moderate yield. The S_NAr has been performed on this lactol with 1-fluoro-2,4-dinitrobenzene to obtain a mixture of α/β coupling products which were easily separated by chromatography. The final reaction was a mild deprotection of the acetyl functions. Sodium methoxide in catalytic amounts was found to be too harsh and lead to degradation while acetyl chloride in methanol allowed a mild deprotection with good yield for the desired anomer **1β**.

The objective of this master thesis is then fulfilled. Indeed, a synthetic route to the desired molecular probe has been found. Now that the target molecule has been synthesized, a biochemical investigation is ongoing within the laboratory of Dr. Guérardel (Université de Lille). The inhibition and inactivation properties of probe **1β** will be first assessed. In parallel, controlled co-crystallization experiments with the target galactofuranosidase and furanoside **1β** are under progress to obtain a 3D structure of the enzyme in complex with **1β**.

V. Outlooks

V.1 Planned enzymatic studies

As explained in the introduction, the synthesized molecular probe **1** should act as an inativator (Scheme 40). By binding to the catalytic site (K_i), the enzyme will catalyze the hydrolysis of the probe ($k_{inact.}$) which should release 2,4-dinitrophenol. It will allow the formation of a stable enzyme-probe complex that will not be able to process the next reaction which is the release of the free enzyme ($k_{release}$). According to this model, the intermediate E-I should accumulate as $k_{release}$ is much slower than $k_{inact.}$. As a result, inactivation of the enzyme should be observed in a time-dependent manner if the inactivation step is slow enough to fit in the timescale of an enzymatic assay.[50]

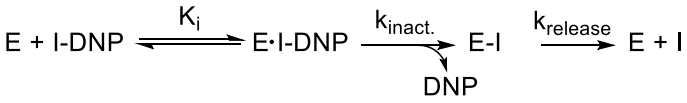

Scheme 40. Reaction scheme of the target glycosidase (E) with the molecular probe (I-DNP). K_I is the non-covalent binding rate constant between the probe and the enzyme, $k_{inact.}$ is the reaction rate of the first inversion step and $k_{release}$ is the reaction rate of the third inversion step.

The kinetic study of the enzyme in the presence of the probe has to be based on the evaluation of a time-dependent inhibition. The usual test consists in incubating the enzyme with the potential inactivator for different time periods and then evaluating the residual activity of the enzyme with a non-fluorinated substrate such as 2,4-dinitrophenyl-D-galactofuranose. A decrease in residual activity over time of incubation with the inhibitor should be observed. According to the reaction scheme presented in Scheme 40, the inactivation rate should follow simple pseudo first-order kinetics.[51] The plot of the residual activity against the time of incubation should fit a single exponential from which can be obtained a first-order rate constant. To obtain K_i and $k_{inact.}$, the same experiment has to be done at different concentrations of the inhibitor to draw a plot of the reciprocal first-rate constant versus the reciprocal inhibitor concentration. This plot should give a straight line from which K_i and $k_{inact.}$ can be extracted.

It is important to mention that for this test to be successful, it is necessary to screen the conditions of inhibition (concentration of enzymes, of inhibitors, T°,…) as the time necessary to completely suppress the activity of the enzyme depends a lot on both the nature of the inactivator and the enzyme.[52]

V.2 Synthesis of di-fluorinated D-galactofuranose

An interesting outlook would be the synthesis of a di-fluorinated molecular probe. The introduction of a second fluorine atom at C-2 can enhance or alter dramatically the activity in biological processes.[53] Our laboratory is especially interested in this question because we observed, on another enzyme of TB's cell wall biosynthesis, a dramatic effect on the inhibition or behavior of a monofluorinated substrate analogue compared to a polyfluorinated one.[54,55]

The synthesis of the difluorinated-D-galactopyranose is described in the literature. It is a three-step synthesis starting from tri-*O*-acetyl-D-galactal **5**. First **5** is fluorinated with Selectfluor® in presence of $MgBr_2$ (a source of bromide). Then the obtained molecule **42** undergoes elimination with Et_3N to form a fluorinated galactal **43**. Finally, this last intermediate reacts once again with Selectfluor® to add the second fluorine atom and form molecule **44**. Those reactions have already been done in the laboratory and the obtained yield for each step after purification is given in Scheme 41.

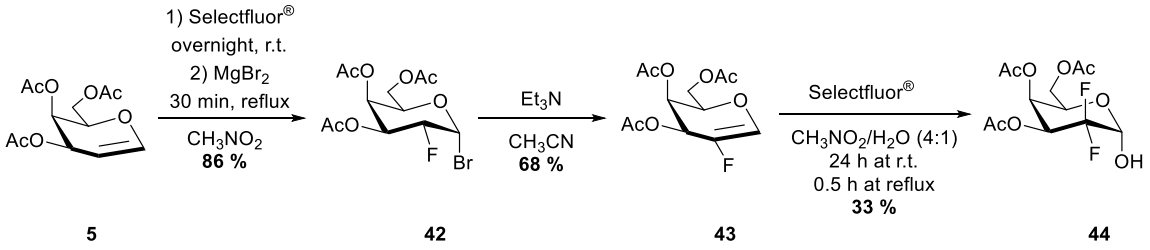

*Scheme 41. Synthetic pathway to difluorinated galactopyranose **44**.*

It would be interesting to investigate if the equilibrium between pyranoside and furanoside can also be shifted at high temperature. And if it is the case, it would be interesting to know if a simple column chromatography would allow a separation between pyranoside and furanoside products. To do so, glycoside **44** needs however to be first fully deprotected. A first attempt of deprotection has been done under the Zemplén conditions previously used. Unfortunately, the results of this reaction was not satisfactory as the reaction was not complete. It would probably need more investigation to find suitable conditions in terms of reaction time and purification technique.

VI. Experimental part

VI.1 Generalities

The molecular weights of the different molecules have been calculated with the software ChemDraw® 17.1.

The NMR spectra used for the characterization of the synthesized molecules were recorded either on a JEOL JNM EX-400 (at 400 MHz for ^{1}H, 100 MHz for ^{13}C and 377 MHz for ^{19}F) or on a JEOL KNM EX-500 (at 500 MHz for ^{1}H, 126 MHz for ^{13}C and 471 MHz for ^{19}F). All the spectra were realized in $CDCl_3$, CD_3OD or D_2O. The chemical shifts (δ) are quoted in parts per million (ppm) and are calibrated with the solvent residual peak ($CDCl_3$: ^{1}H 7.26 ppm, ^{13}C 77.0 ppm, CD_3OD: ^{1}H 3.31 ppm, ^{13}C 49.0 ppm, D_2O: ^{1}H 4.79 ppm). The chemical shifts of ^{19}F NMR spectra are uncorrected.

Each ^{1}H NMR spectrum is described in the following manner: chemical shift (ppm), multiplicity, coupling constants (Hz), integration.

The ^{13}C spectra are ^{1}H decoupled. The chemical shift is reported with the eventual coupling constants with the ^{19}F nucleus.

The multiplicity is reported in the following manner: s = singlet, d = doublet, t = triplet, m = multiplet.

All the 1-D spectra are analyzed thanks to MestReNova® 12 and all the 2-D spectra (COSY (^{1}H, ^{1}H), HMQC (^{13}C, ^{1}H)) are analyzed thanks to Delta® 5.2.1.

The carbon (and corresponding hydrogen) numbering follows the classical numbering of carbohydrates with the position 1 being the anomeric carbon. For the aryl substituents at the anomeric position, the quaternary aromatic carbon attached to the oxygen is assigned *ipso*. The other carbons are assigned *ortho, meta* and *para* respectively (Scheme 42). In the assignation of each nucleus, an “A” corresponds to the α anomer while a “B” corresponds to the β anomer of the same molecule.

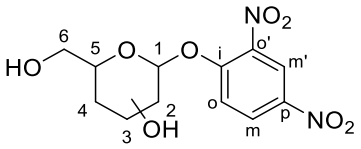

Scheme 42. Carbohydrate numbering.

The HRMS spectra were performed on a Bruker MaXis mass spectrometer Q-TOF by the "Fédération de recherche" ICOA/CBM (FR2708) platform of Orléans in France. The analytes were dissolved in a suitable solvent at a concentration of 1 mg/mL and diluted 500 times in methanol. The diluted solution (1 µL) were delivered to the ESI source by a Dionex Ultimate 3000 RSLC chain used in FIA (Flow Injection Analysis) mode at a flow rate of 200 µL/min. with a mixture of CH_3CN + 0.1 % of HCO_2H (65/35) for positive mode and without formic acid for negative mode. The injection volume is 0.2 µL. ESI conditions were as follows: capillary voltage was set at 4.5 kV; dry nitrogen was used as a nebulizing gas at 0.6 bars and as a drying gas at 200 °C at a rate of 7.0 mL/min. The ESI-MS was recorded at 1 Hz in the range of 50-3000 m/z. The calibration was performed with ESI-TOF tuning mix from Agilent and corrected using lock at m/z 299.294457 (methyl stearate) and 1221.990638 (HP-1221).The data were processed using Bruker DataAnalysis 4.1 software.

The infrared spectra were acquired on a Perkin-Elmer Spectrum II FT-IR System UATR on neat compounds mounted with a diamond crystal. The selected absorption bands are reported by wavenumber (cm^{-1}). The spectra were measured between wavenumbers of 4000-450 cm^{-1}.

The TLCs were performed with aluminum-baked 0.2 mm thick Merck Silica gel $60F_{254}$ plates. The compounds were detected by one of the following methods:

- Fluorescence quenching detection at 254 nm.
- Dipping into a 5 % phosphomolybdic acid solution in ethanol and subsequent heating.
- Dipping into a solution of ceric (IV) ammonium nitrate (10 g/L), ammonium molybdate tetrahydrate (50 g/L) in 50 mL of concentrated sulfuric acid and 450 mL of water. Heating is subsequently applied.

Retention factors (R_f) are indicated with the corresponding eluent used.

The flash chromatographies were performed on silica gel using Davisil® (particle size 40-63 µm, 60 Å) in usual conditions (± 30 g of silica for 1 g of crude). The solvents were at least of technical grade and distilled prior to use. The indicated mixture ratios are given as volumic percentages.

The reagents and chemicals were obtained from Merck, Fischer, ABCR, Carbosynth and were used without purification if not stated. The reactions were performed using purified and dried solvents if necessary. Dichloromethane and toluene were dried through a MBraun SPS system. CH_3CN, Pyridine, Et_3N were distilled from CaH_2 and stored over 4 Å molecular sieves. DMF,

CH_3NO_2 and MeOH were bought anhydrous and stored over 4 Å molecular sieves. Deionized water was used for reaction work-up. Dowex® 50WX8 was rinsed with aqueous 1M HCl and then rinsed with H_2O until neutral pH.

All reactions were carried out under an argon atmosphere in a round bottom flask closed by a septum and a rubber balloon filled up with argon, and stirred with a Teflon stirring rod.

VI.2 Synthesis and protocols

VI.2.1 tri-*O*-acetyl-D-galactal

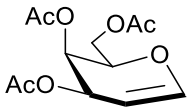

In a dried flask, D-galactose (0,17 g, 0.94 mmol) was suspended in acetic anhydride (100 mL, 1064 mmol, 7.6 eq.) under argon atmosphere. The suspension was cooled to 0 °C and then perchloric acid (0.6 mL, 6.9 mmol, 0.05 eq.) was added dropwise under stirring. Then, D-galactose was added by portion of 5 g every 15 minutes (25 g total, 140 mmol, 1 eq.). The reaction was left to warm to room temperature and was monitored by TLC. After 2 hours, the reaction was finished and the crude had turned orange. Bromhydric acid (110 mL, 33 % in AcOH, 637 mmol, 4.6 eq.) was added dropwise to the solution and stirring was kept going on. After 1 hour, the reaction was complete (monitored by TLC). To avoid degradation of the product, no work-up was done and the crude was concentrated *in vacuo* to obtain a thick brownish syrup (a sodium hydroxide trap was set up to protect the pump and the laboratory from corrosive vapors).

The previous brownish syrup was added to a suspension of zinc powder (63.17 g, 966 mmol, 6,9 eq., Mesh 12) in AcOH/H_2O (50 % v/v, 200 mL) first cooled to -15 °C. After 1 hour of stirring at 0 °C, TLC showed completion of the reaction. The crude was diluted with 265 mL of CH_2Cl_2 and filtered over Celite® to remove the excess zinc powder. Then the organic phase was washed with ice-cold distilled water (3 x 80 mL), saturated $NaHCO_3$ (2 x 50 mL) and brine (1 x 50 mL). The organic phase was dried over $MgSO_4$, filtered and concentrated *in vacuo* to obtain an orange oil. The crude oil was purified by silica gel chromatography (EtOAc/Cyclohexane (1:2)) to obtain D-galactal as a colorless syrup (yield = 63 %). Analytical data collaborated with those described in the literature.[56]

- **Formula :** $C_{12}H_{16}O_7$
- **Molecular weight :** 272.25 g/mol
- **R_f :** 0.68 (EtOAc/n-Hexane 1:1)
- **Aspect :** Colorless syrup
- **^{1}H NMR** (500 MHz, $CDCl_3$) **:** δ 6.46 (dd, J = 6.3, 1.8 Hz, 1H, H-1), 5.59 – 5.51 (m, 1H, H-3), 5.46 – 5.39 (m, 1H, H-4), 4.73 (ddd, J = 6.3, 2.7, 1.5 Hz, 1H, H-2), 4.35 – 4.30 (m, 1H, H-5), 4.29 – 4.19 (m, 2H, H-6 + H-6'), 2.13 (s, 3H, Ac), 2.09 (s, 3H, Ac), 2.03 (s, 3H, Ac)
- **^{13}C NMR** (126 MHz, $CDCl_3$) **:** δ 170.76 (Ac), 170.48 (Ac), 170.33 (Ac), 145.56 (C-1), 98.97 (C-2), 72.91 (C-5), 64.01 (C-3), 63.84 (C-4), 62.08 (C-6), 20.98 (Ac), 20.93 (Ac), 20.83 (Ac).
- **HRMS (ESI) :** *m/z* Calculated for $C_{12}H_{16}O_7$ $[M+Na]^+$: 295.0788; found : 295.0790; δ = 0.6 ppm

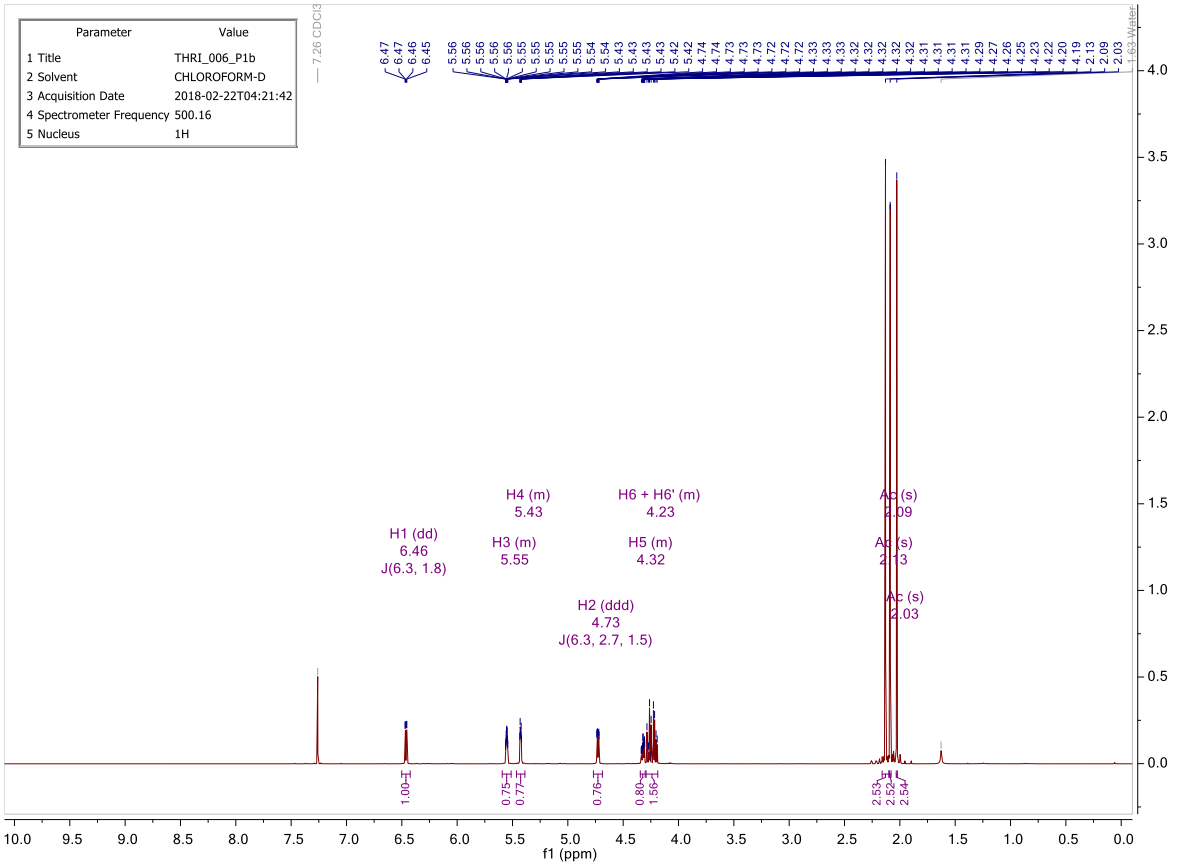

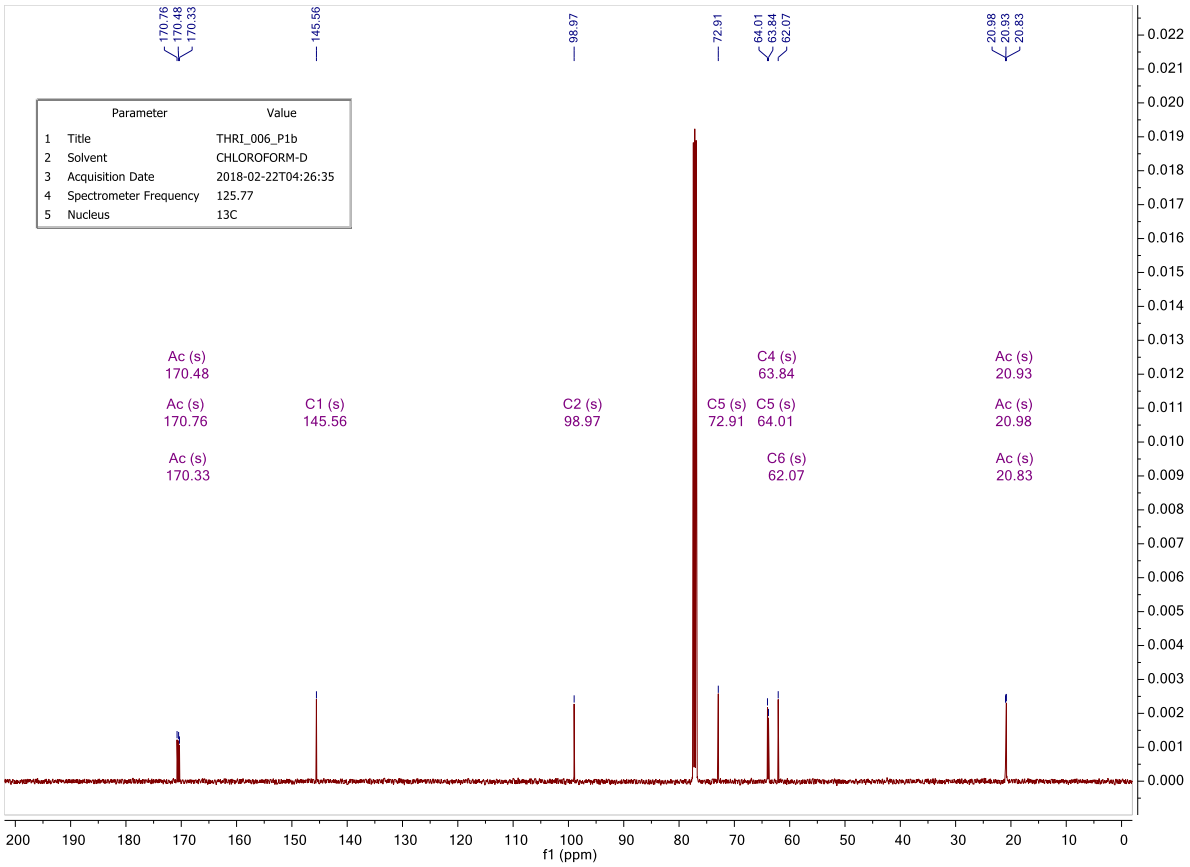
170.76
170.48
170.33
145.56
98.97
72.91
64.01
63.84
62.07
20.98
20.93
20.83
Parameter Value
1 Title THRI_006_P1b
2 Solvent CHLOROFORM-D
3 Acquisition Date 2018-02-22T04:26:35
4 Spectrometer Frequency 125.77
5 Nucleus 13C
Ac (s) 170.48
Ac (s) 170.76
Ac (s) 170.33
C1 (s) 145.56
C2 (s) 98.97
C5 (s) 72.91
C5 (s) 64.01
C4 (s) 63.84
C6 (s) 62.07
Ac (s) 20.93
Ac (s) 20.98
Ac (s) 20.83
f1 (ppm)

VI.2.2 3,4,6-tri-*O*-acetyl-2-deoxy-2-fluoro-D-galactopyranose

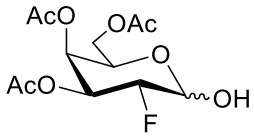

Selectfluor® (37.16 g, 105 mmol, 1.2 eq.) was added to a solution of D-galactal (23.8 g, 87.4 mmol, 1 eq.) in a mixture of nitromethane/water (195 mL, 5:1 (v/v)) with stirring. After completion of the reaction (monitored by TLC, usually 3 hours), the mixture was heated to reflux (100 °C) for 30 minutes. Then, the reaction was cooled back to room temperature and the crude was concentrated *in vacuo*. The obtained gel was diluted in CH_2Cl_2 and then filtered. The organic phase was then concentrated *in vacuo* and purification by silica gel chromatography (EtOAc/Cyclohexane (1:2)) afforded a colorless syrup (yield = 68 %, α/β = 2:1). Analytical data collaborated with those described in the literature.[57]

- **Formula :** $C_{12}H_{17}O_8F$
- **Molecular weight :** 308.26 g/mol
- **R_f :** 0.47 (EtOAc/n-Hexane 1:1)
- **Aspect :** Colorless syrup
- **^{1}H NMR** (500 MHz, $CDCl_3$) **:** δ 5.54 (d, J = 3.7 Hz, 1H, H-1$_\alpha$), 5.51 – 5.44 (m, 2H, H-3$_\alpha$, H-4$_\alpha$), 5.42 (ddd, J = 3.7, 2.6, 1.2 Hz, 1H, H-4$_\beta$), 5.12 (ddd, J = 12.8, 9.9, 3.6 Hz, 1H, H-3$_\beta$), 4.91 (dd, J = 7.6, 3.8 Hz, 1H, H-1$_\beta$), 4.78 (ddd, J = 50.2, 10.0, 3.7 Hz, 1H, H-2$_\alpha$), 4.49 (ddd, J = 51.5, 9.9, 7.6 Hz, 1H, H-2$_\beta$), 4.49 (td, J = 6.4, 0.8 Hz, 1H, H-5$_\alpha$), 4.12 (s, 1H, H-6$_\beta$), 4.11 (s, 1H, H-6'$_\beta$), 4.10 (d, J = 2.2 Hz, 1H, H-6$_\alpha$), 4.08 (d, J = 2.6 Hz, 1H, H-6'$_\alpha$), 3.98 (ddd, J = 7.0, 6.2, 1.2 Hz, 1H, H-5$_\beta$), 3.43 (s, 1H, OH$_\alpha$), 2.14 (s, 3H, Ac), 2.14 (s, 3H, Ac), 2.06 (s, 3H, Ac), 2.05 (s, 3H, Ac), 2.05 (s, 3H, Ac), 2.04 (s, 3H, Ac).
- **^{13}C NMR** (126 MHz, $CDCl_3$) **:** δ 170.76 (Ac), 170.73 (Ac), 170.29 (Ac), 170.26 (Ac), 95.02 (d, J = 23.5 Hz, C-1$_\beta$), 90.86 (d, J = 21.5 Hz, C-1$_\alpha$), 89.22 (d, J = 186.7 Hz, C-2$_\beta$), 85.84 (d, J = 189.2 Hz, C-2$_\alpha$), 71.07 (d, J = 18.6 Hz, C-3$_\beta$), 71.06 (C-5$_\beta$), 68.84 (d, J = 7.8 Hz, C-4$_\alpha$), 67.96 (d, J = 19.1 Hz, C-3$_\alpha$), 67.94 (C-4$_\beta$), 66.55 (C-5$_\beta$), 61.77 (C-6$_\alpha$), 61.54 (C-6$_\beta$), 20.86 (Ac), 20.83 (Ac), 20.73 (Ac), 20.70 (Ac).
- **^{19}F NMR** (471 MHz, $CDCl_3$) : δ -206.65 (dddd, J = 51.6, 12.9, 3.9, 2.6 Hz, F$_\beta$), -207.14 (ddd, J = 50.2, 11.0, 3.5 Hz, F$_\alpha$).
- **HRMS (ESI) :** *m/*z Calculated for $C_{12}H_{17}O_8F$ $[M+Na]^+$: 331.0799; found : 331.0801; δ = 0.6 ppm

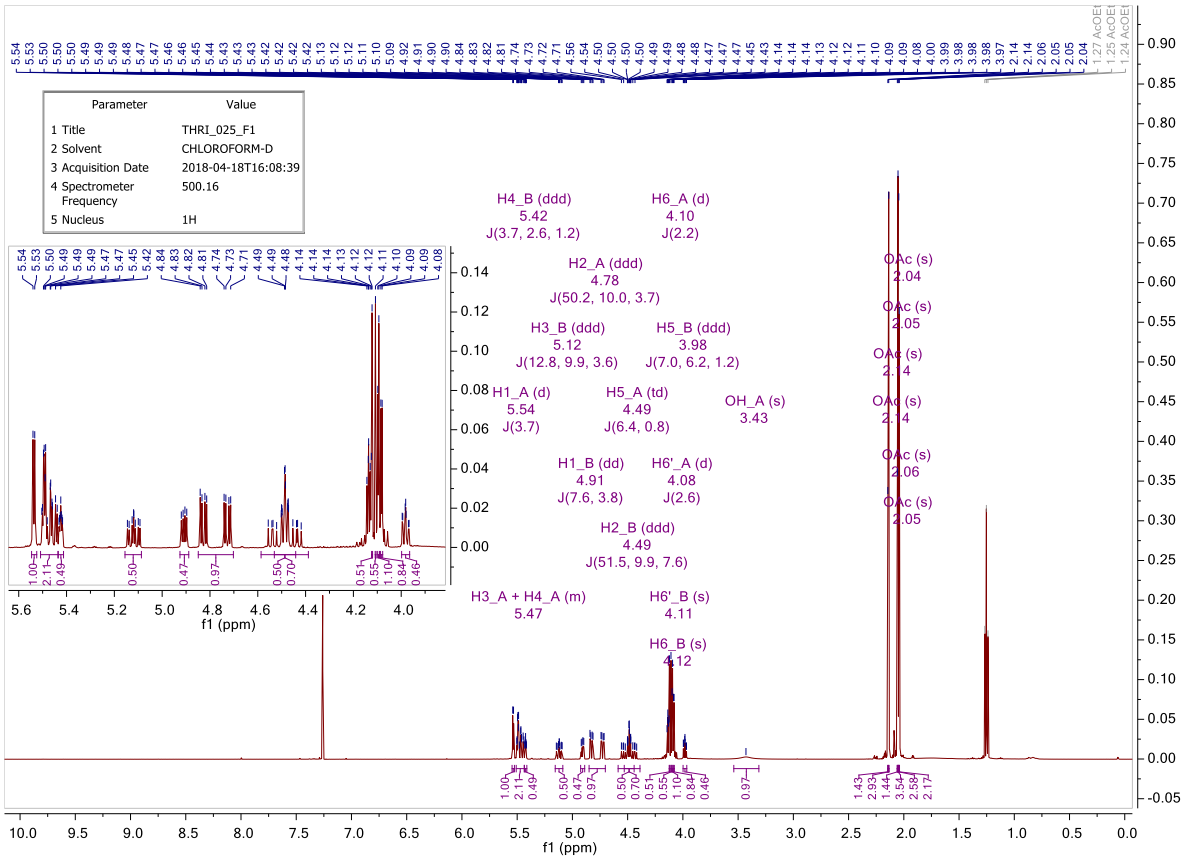
Parameter Value
1 Title THRI_025_F1
2 Solvent CHLOROFORM-D
3 Acquisition Date 2018-04-18T16:08:39
4 Spectrometer Frequency 500.16
5 Nucleus 1H
H4_B (ddd) 5.42 J(3.7, 2.6, 1.2)
H6_A (d) 4.10 J(2.2)
H2_A (ddd) 4.78 J(50.2, 10.0, 3.7)
H3_B (ddd) 5.12 J(12.8, 9.9, 3.6)
H5_B (ddd) 3.98 J(7.0, 6.2, 1.2)
H1_A (d) 5.54 J(3.7)
H5_A (td) 4.49 J(6.4, 0.8)
OH_A (s) 3.43
H1_B (dd) 4.91 J(7.6, 3.8)
H6'_A (d) 4.08 J(2.6)
H2_B (ddd) 4.49 J(51.5, 9.9, 7.6)
H3_A + H4_A (m) 5.47
H6'_B (s) 4.11
H6_B (s) 4.12
OAc (s) 2.04
OAc (s) 2.05
OAc (s) 2.04
OAc (s) 2.04
OAc (s) 2.06
OAc (s) 2.05
f1 (ppm)

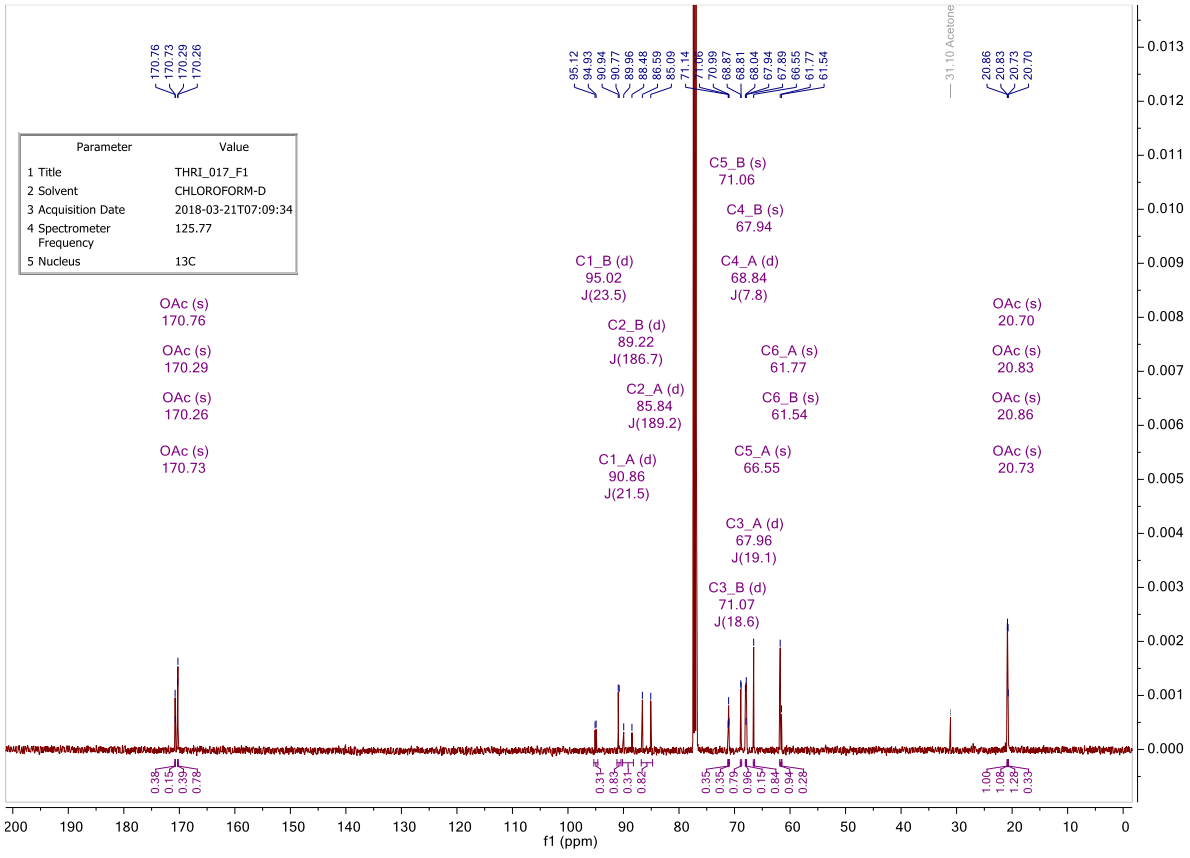
Parameter Value
1 Title THRI_017_F1
2 Solvent CHLOROFORM-D
3 Acquisition Date 2018-03-21T07:09:34
4 Spectrometer Frequency 125.77
5 Nucleus 13C
C5_B (s) 71.06
C4_B (s) 67.94
C1_B (d) 95.02 J(23.5)
C4_A (d) 68.84 J(7.8)
C2_B (d) 89.22 J(186.7)
C6_A (s) 61.77
C2_A (d) 85.84 J(189.2)
C6_B (s) 61.54
C1_A (d) 90.86 J(21.5)
C5_A (s) 66.55
C3_A (d) 67.96 J(19.1)
C3_B (d) 71.07 J(18.6)
OAc (s) 170.76
OAc (s) 170.29
OAc (s) 170.26
OAc (s) 170.73
OAc (s) 20.70
OAc (s) 20.83
OAc (s) 20.86
OAc (s) 20.73
f1 (ppm)

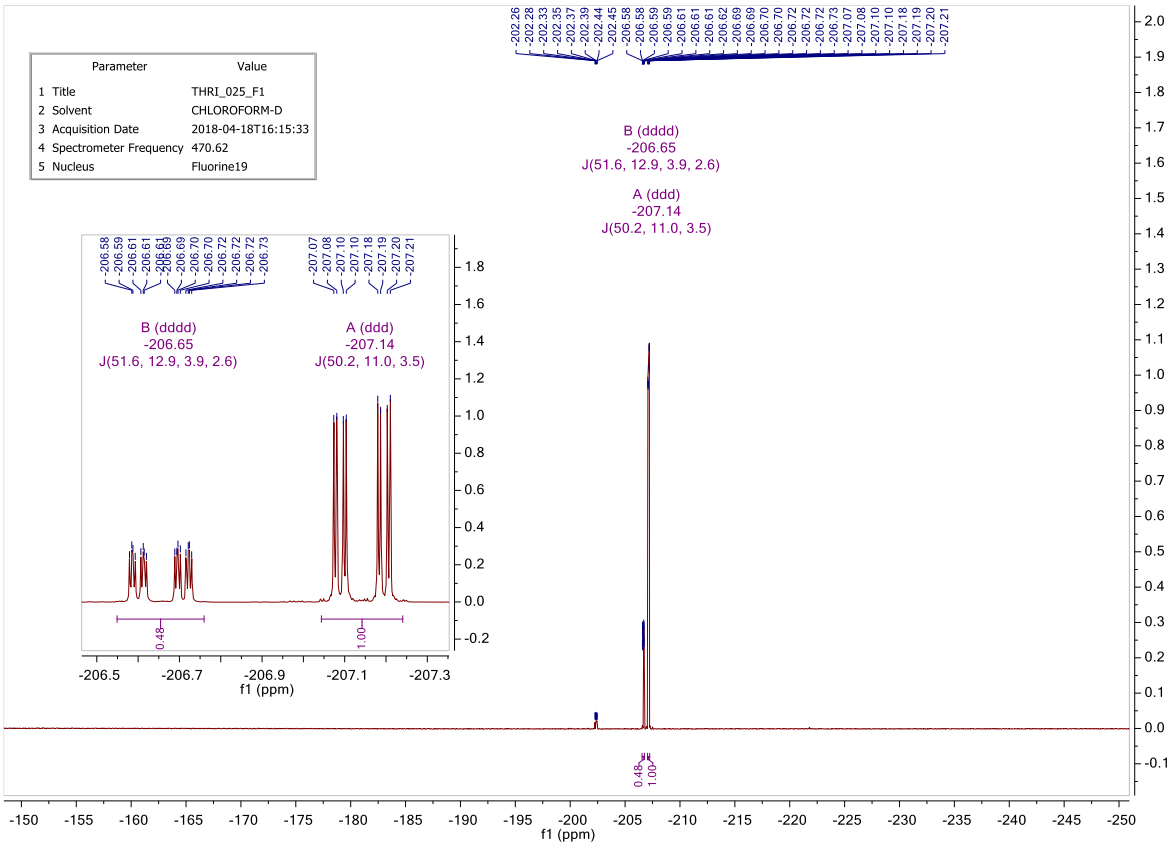
Parameter Value
1 Title THRI_025_F1
2 Solvent CHLOROFORM-D
3 Acquisition Date 2018-04-18T16:15:33
4 Spectrometer Frequency 470.62
5 Nucleus Fluorine19
B (dddd)
-206.65
J(51.6, 12.9, 3.9, 2.6)
A (ddd)
-207.14
J(50.2, 11.0, 3.5)
f1 (ppm)

VI.2.3 Selectfluor bis-triflate

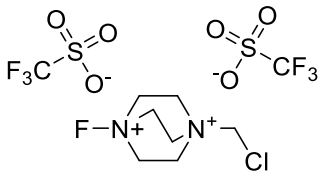

In a dried flask, Selectfluor bis-tetrafluoroborate (1,00 g, 2.82 mmol, 1 eq.) was suspended in dry acetonitrile (40 mL) under argon atmosphere. The suspension was cooled to 0 °C and then trimethylsilyltrifluoromethanesulfonate (1.12 mL, 6.20 mmol, 2.2 eq.) was added dropwise to the mixture. The reaction was left overnight at room temperature under stirring. After evaporation of the solvent *in vacuo*, the solid was suspended in diethyl ether (100 mL), filtered and washed abundantly with Et_2O. The white solid obtained was dried *in vacuo* to obtain selectfluor bis-triflate (yield = 91 %).

- **Formula :** $C_9H_{14}O_6N_2S_2F_7Cl$
- **Molecular weight :** 478.77 g/mol
- **Aspect :** White powder
- **^{1}H NMR** (500 MHz, D_2O) **:** δ 5.52 (s, 2H, -*CH_2*-Cl), 4.98 (q, J = 7.4 Hz, 6H, -*CH_2*-NF), 4.52 (t, J = 7.6 Hz, 6H, -*CH_2*-NCH_2Cl).
- **^{13}C NMR** (126 MHz, D_2O) **:** δ 68.98 (-*CH_2*-Cl), 57.33-57.21 (-*CH_2*-NF), 53.70 (-*CH_2*-NCH_2Cl).
- **^{19}F NMR** (471 MHz, D_2O) **:** δ 47.68 (F-N), -78.87 (CF_3).

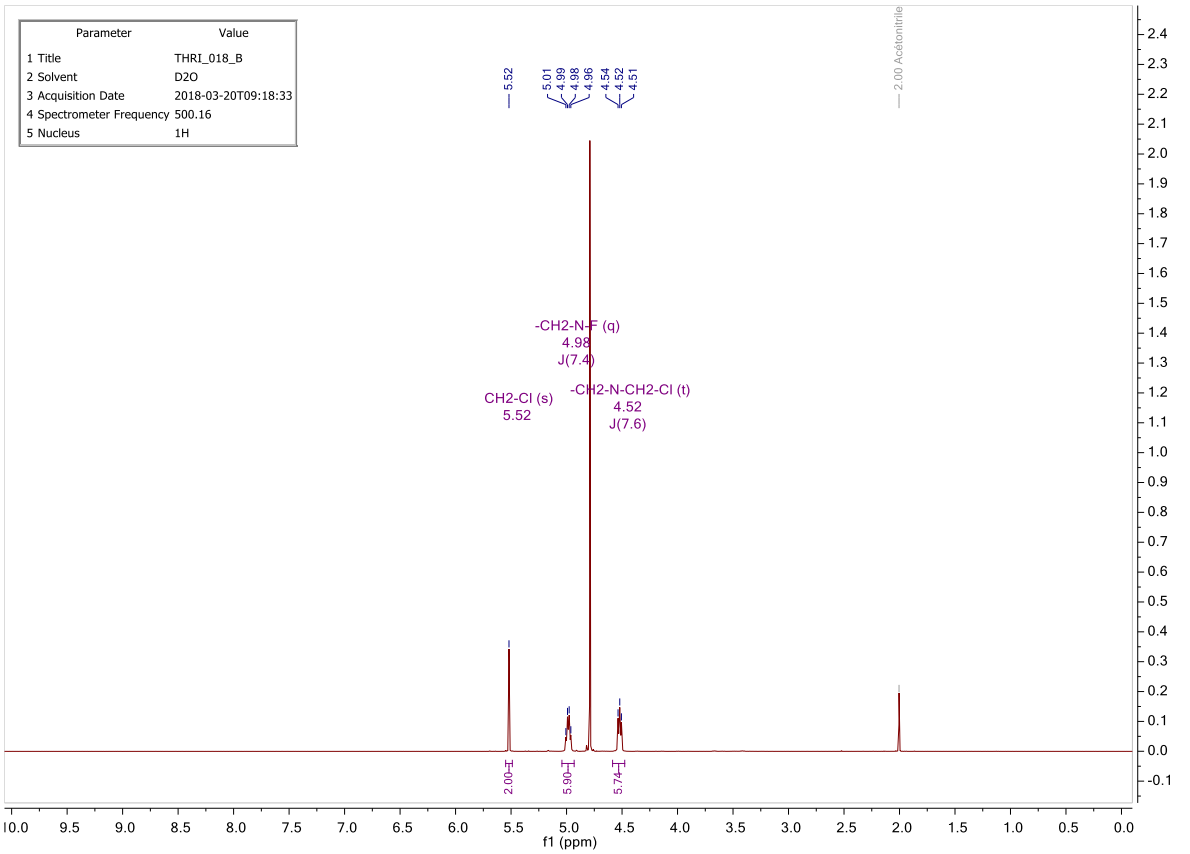
Parameter Value
1 Title THRI_018_B
2 Solvent D2O
3 Acquisition Date 2018-03-20T09:18:33
4 Spectrometer Frequency 500.16
5 Nucleus 1H
5.52
5.01
4.99
4.98
4.96
4.54
4.52
4.51
2.00 Acétonitrile
-CH2-N-F (q)
4.98
J(7.4)
CH2-Cl (s)
5.52
-CH2-N-CH2-Cl (t)
4.52
J(7.6)
2.00
5.90
5.74
f1 (ppm)

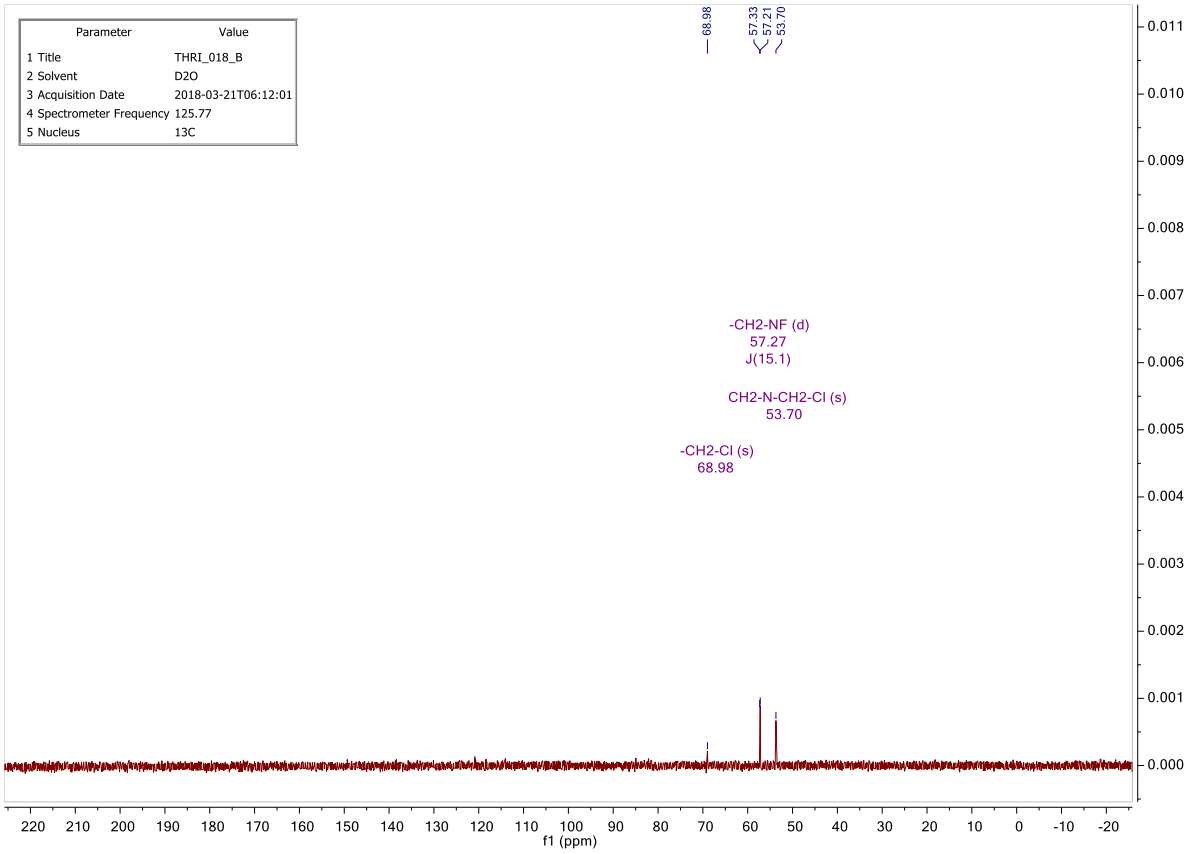
Parameter Value
1 Title THRI_018_B
2 Solvent D2O
3 Acquisition Date 2018-03-21T06:12:01
4 Spectrometer Frequency 125.77
5 Nucleus 13C
68.98
57.33
57.21
53.70
-CH2-NF (d)
57.27
J(15.1)
CH2-N-CH2-Cl (s)
53.70
-CH2-Cl (s)
68.98
f1 (ppm)

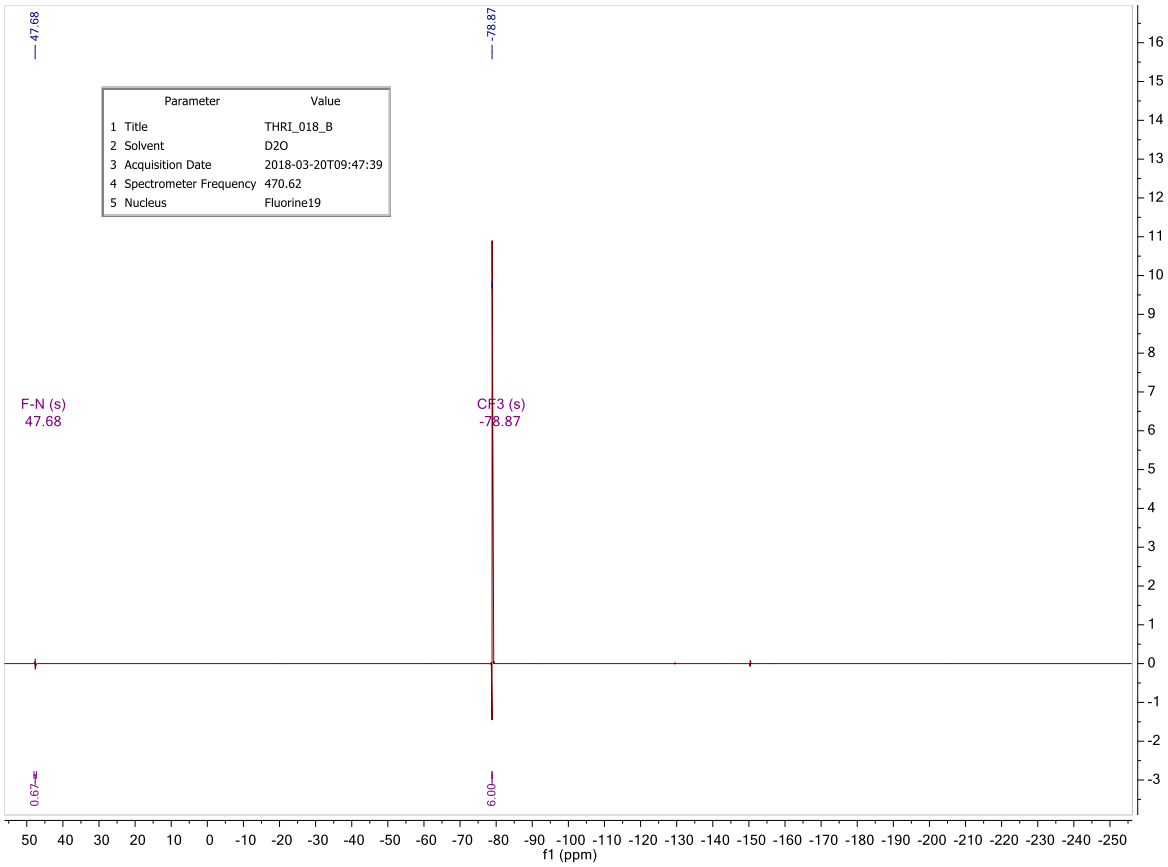
47.68
-78.87
Parameter Value
1 Title THRI_018_B
2 Solvent D2O
3 Acquisition Date 2018-03-20T09:47:39
4 Spectrometer Frequency 470.62
5 Nucleus Fluorine19
F-N (s)
47.68
CF3 (s)
-78.87
0.67
6.00
f1 (ppm)

VI.2.4 2-deoxy-2-fluoro-D-galactopyranose

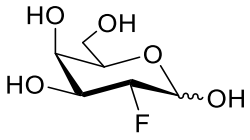

Under stirring at room temperature sodium methoxide (967 mg, 17.9 mmol, 0.3 eq.) was added to a solution of 3,4,6-tri-*O*-acetyl-2-deoxy-2-fluoro-D-galactopyranose (18.39 g, 59.7 mmol, 1 eq.) in MeOH (184 mL). When all the starting material has been consumed (monitored by TLC, usually 30 minutes), the crude was concentrated *in vacuo*, diluted in a small amount of distilled water and then eluted on a column of Dowex® 50WX8 (previously washed with HCl 1M and then with water). The filtrate was concentrated *in vacuo* to obtain a white solid after a night at rest (yield = 99 %, α/β = 1:2). Analytical data collaborated with those described in the literature.[58]

- **Formula :** $C_6H_{11}O_5F$
- **Molecular weight :** 182.15 g/mol
- **R_f :** 0.13 ($MeOH/CH_2Cl_2$ 1:9)
- **Aspect :** white solid
- **^{1}H NMR** (500 MHz, CD_3OD) **:** δ 5.26 (d, J = 3.9 Hz, 1H, H-1$_\alpha$), 4.61 (dd, J = 7.7, 3.5 Hz, 1H, H-1$_\beta$), 4.53 (ddd, J = 50.6, 9.7, 3.9 Hz, 1H, H-2$_\alpha$), 4.22 (ddd, J = 52.1, 9.4, 7.6 Hz, 1H, H-2$_\beta$), 4.02 – 3.94 (m, 2H, H-3$_\alpha$ + H-5$_\alpha$), 3.92 (td, J = 3.8, 1.3 Hz, 1H, H-4$_\alpha$), 3.84 (td, J = 3.4, 1.1 Hz, 1H, H-4$_\beta$), 3.72 – 3.63 (m, 5H, H-3$_\beta$ + H-6$_\beta$ + H-6'$_\beta$ + H-6$_\alpha$ + H-6'$_\alpha$), 3.52 (ddd, J = 6.7, 5.4, 1.1 Hz, 1H, H-5$_\beta$).
- **^{13}C NMR** (126 MHz, CD_3OD) **:** δ 96.10 (d, J = 23.5 Hz, C-1$_\beta$), 94.15 (d, J= 180.7 Hz, C-2$_\beta$), 91.69 (d, J = 91.69 Hz, C-1$_\alpha$), 90.58 (d, J = 184.0 Hz, C-2$_\alpha$), 76.66 (C-5$_\beta$), 73.25 (d, J = 17.2 Hz, C-3$_\beta$), 71.61 (d, J = 8.3 Hz, C-4$_\alpha$), 71.51 (C-5$_\alpha$), 70.97 (d, J = 8.9 Hz, C-4$_\beta$), 69.24 (d, J = 17.3 Hz, C-3$_\alpha$), 62.38 (C-6$_\alpha$), 62.24 (C-6$_\beta$).
- **^{19}F NMR** (471 MHz, CD_3OD) : δ -208.84 (ddt, *J* = 52.1, 13.9, 3.0 Hz, F$_\beta$), -209.86 (ddd, *J* = 51.1, 11.9, 4.4 Hz, F$_\alpha$).
- **HRMS (ESI) :** *m/*z Calculated for $C_6H_{11}O_5F$ $[M+Na]^+$: 205.0482 ; found : 205.0481; δ = 0.8 ppm

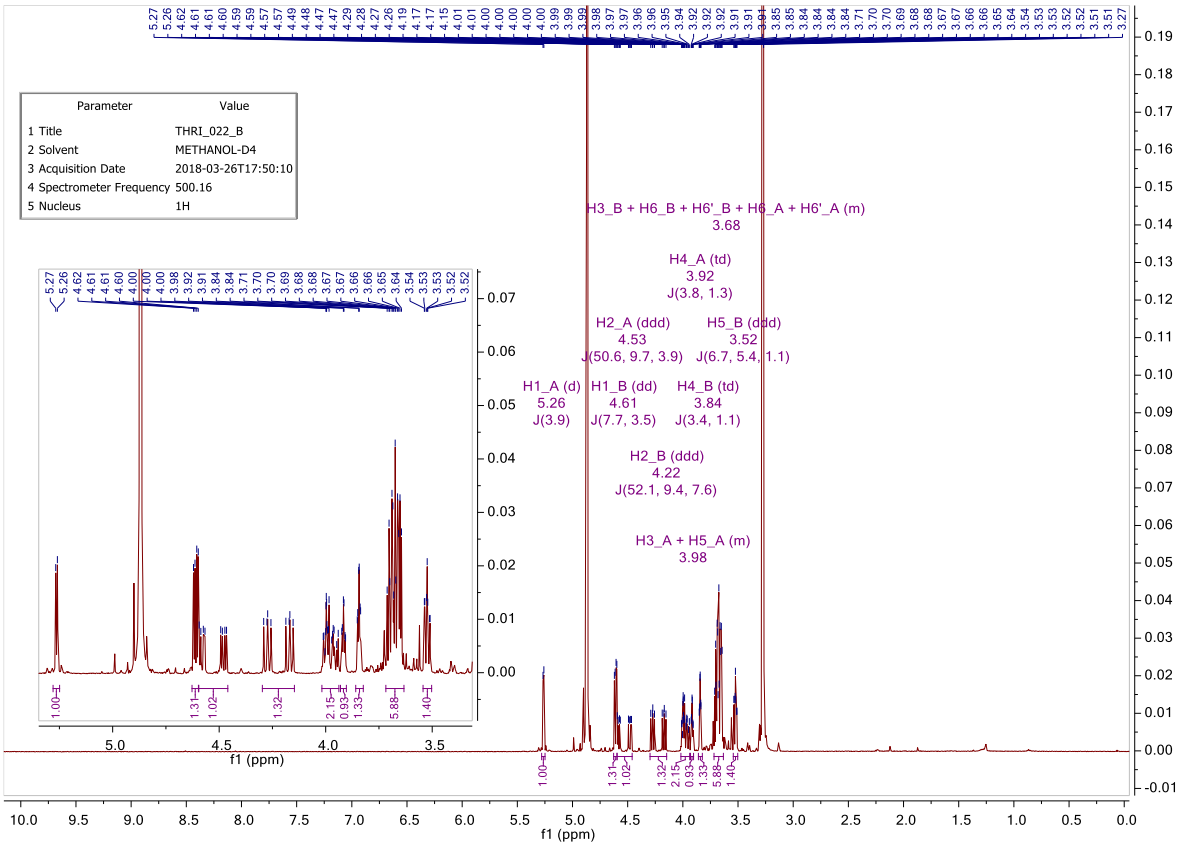
Parameter Value
1 Title THRI_022_B
2 Solvent METHANOL-D4
3 Acquisition Date 2018-03-26T17:50:10
4 Spectrometer Frequency 500.16
5 Nucleus 1H
H3_B + H6_B + H6'_B + H6_A + H6'_A (m)
3.68
H4_A (td)
3.92
J(3.8, 1.3)
H2_A (ddd)
4.53
J(50.6, 9.7, 3.9)
H5_B (ddd)
3.52
J(6.7, 5.4, 1.1)
H1_A (d)
5.26
J(3.9)
H1_B (dd)
4.61
J(7.7, 3.5)
H4_B (td)
3.84
J(3.4, 1.1)
H2_B (ddd)
4.22
J(52.1, 9.4, 7.6)
H3_A + H5_A (m)
3.98
f1 (ppm)

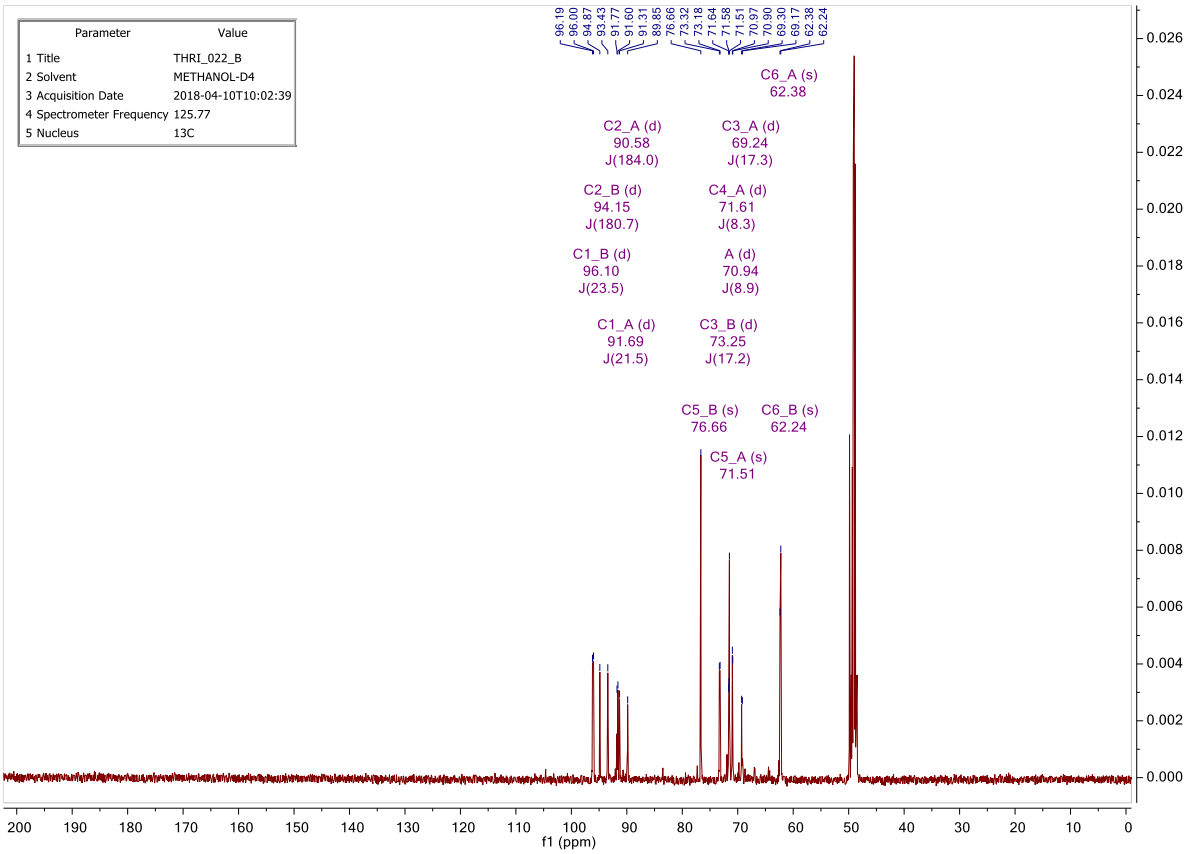
Parameter Value
1 Title THRI_022_B
2 Solvent METHANOL-D4
3 Acquisition Date 2018-04-10T10:02:39
4 Spectrometer Frequency 125.77
5 Nucleus 13C
C6_A (s)
62.38
C2_A (d)
90.58
J(184.0)
C3_A (d)
69.24
J(17.3)
C2_B (d)
94.15
J(180.7)
C4_A (d)
71.61
J(8.3)
C1_B (d)
96.10
J(23.5)
A (d)
70.94
J(8.9)
C1_A (d)
91.69
J(21.5)
C3_B (d)
73.25
J(17.2)
C5_B (s)
76.66
C6_B (s)
62.24
C5_A (s)
71.51
f1 (ppm)

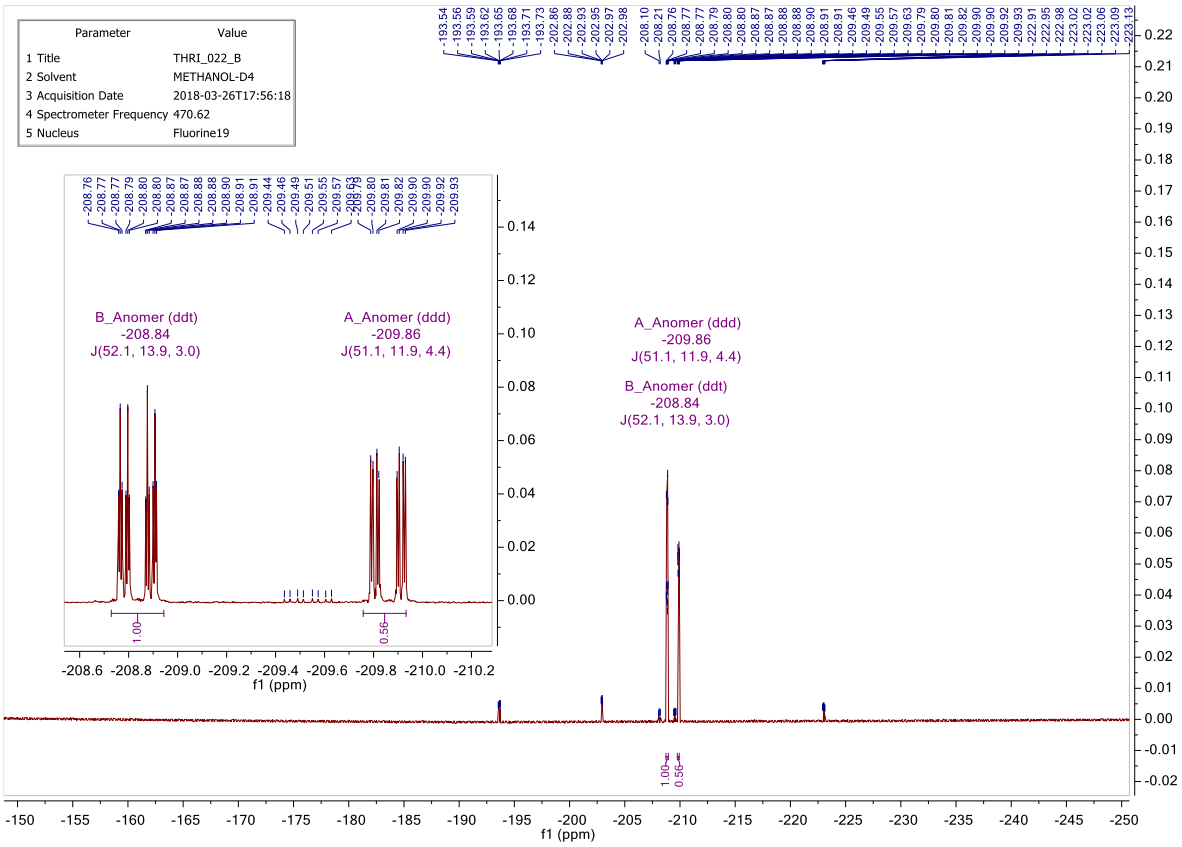
Parameter Value
1 Title THRI_022_B
2 Solvent METHANOL-D4
3 Acquisition Date 2018-03-26T17:56:18
4 Spectrometer Frequency 470.62
5 Nucleus Fluorine19
B_Anomer (ddt)
-208.84
J(52.1, 13.9, 3.0)
A_Anomer (ddd)
-209.86
J(51.1, 11.9, 4.4)
A_Anomer (ddd)
-209.86
J(51.1, 11.9, 4.4)
B_Anomer (ddt)
-208.84
J(52.1, 13.9, 3.0)
1.00
0.56
f1 (ppm)

VI.2.5 1,3,4,6-tetra-*O*-acetyl-2-deoxy-2-fluoro-D-galactopyranose

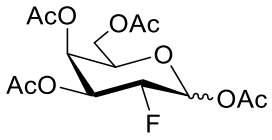

In a dried flask, 3,4,6-tri-*O*-acetyl-2-deoxy-2-fluoro-D-galactopyranose (50 mg, 0.16 mmol, 1 eq.) was dissolved in pyridine (0.5 mL, 38.76 mmol, 242.2 eq.) under argon atmosphere. Acetic anhydride (18 µL, 0.19 mmol, 1.2 eq.) and DMAP (14 mg, 0.11 mmol, 0.7 eq.) were added to the solution. The mixture was left under stirring at room temperature and the reaction was monitored by TLC. When the reaction was completed, saturated $NaHCO_3$ (5 mL) was added to the crude. The aqueous phase was then extracted with CH_2Cl_2 (3 x 5mL). The organic phases were gathered, dried over $MgSO_4$, filtered and concentrated *in vacuo* to afford a pale orange solid (69 mg, α/β = 3:2, containing impurities). Analytical data collaborated with those described in the literature.[59]

- **Formula :** $C_{14}H_{19}O_9F$
- **Molecular weight :** 350.30 g/mol
- **R_f :** 0.71 (EtOAc/n-hexane 1:1)
- **Aspect :** Pale orange solid
- **^{1}H NMR** (500 MHz, $CDCl_3$) **:** δ 6.46 (d, J = 3.9 Hz, 1H, H-1$_\alpha$), 5.79 (dd, J = 8.0, 4.1 Hz, 1H, H-1$_\beta$), 5.52 (td, J = 3.4, 1.4 Hz, 1H, H-4$_\alpha$), 5.45 (ddd, J = 3.7, 2.6, 1.1 Hz, 1H, H-4$_\beta$), 5.41 (ddd, J = 11.0, 10.2, 3.5 Hz, 1H, H-3$_\alpha$), 5.17 (ddd, J = 13.2, 9.8, 3.5 Hz, 1H, H-3$_\beta$), 4.89 (ddd, J = 49.2, 10.2, 3.9 Hz, 1H, H-2$_\alpha$), 4.65 (ddd, J = 51.5, 9.9, 8.1 Hz, 1H, H-2$_\beta$), 4.31 (tdd, J = 6.7, 1.5, 0.6 Hz, 1H, H-5$_\alpha$), 4.12 (dd, J = 6.5, 5.4 Hz, 1H, H-6$_\alpha$), 4.12 – 4.02 (m, 4H, H-5$_\beta$, H-6'$_\alpha$, H-6$_\beta$, H-6$_\beta$), 2.19 (s, 3H, Ac), 2.19 (s, 3H, Ac), 2.15 (s, 6H, Ac), 2.06 (s, 3H, Ac), 2.06 (s, 3H, Ac), 2.04 (s, 3H, Ac), 2.04 (s, 3H, Ac).
- **^{13}C NMR** (126 MHz, $CDCl_3$) **:** δ 170.48 (Ac), 170.21 (Ac), 170.09 (Ac), 170.05 (Ac), 169.96 (Ac), 169.00 (Ac), 168.97 (Ac), 91.67 (d, J = 24.7 Hz, C-1$_\beta$), 89.06 (d, J = 22.9 Hz, C-1$_\alpha$), 87.79 (d, J = 188.4 Hz, C-2$_\beta$), 84.24 (d, 191.0 Hz, C-2$_\alpha$), 71.83 (C-5$_\beta$), 71.06 (d, J = 18.8, C-3$_\beta$), 68.66 (C-5$_\alpha$), 68.27 (d, J = 18.8 Hz, C-3$_\alpha$), 67.99 (d, J = 7.7 Hz, C-4$_\alpha$), 67.53 (d, J = 7.9 Hz, C-4$_\beta$), 61.08 (C-6$_\alpha$), 60.94 (C-6$_\beta$), 21.02 (Ac), 20.96 (Ac), 20.77 (Ac), 20.67 (Ac).
- **^{19}F NMR** (471 MHz, $CDCl_3$) **:** δ -207.95 (ddt, J = 52.0, 12.9, 3.5 Hz, F$_\beta$), -208.95 (ddd, J = 49.3, 11.1, 3.3 Hz, F$_\alpha$).
- **HRMS (ESI) :** *m/*z Calculated for $C_{14}H_{19}O_9F$ $[M+Na]^+$: 373.0905 ; found : 373.0907; δ = 0.6 ppm

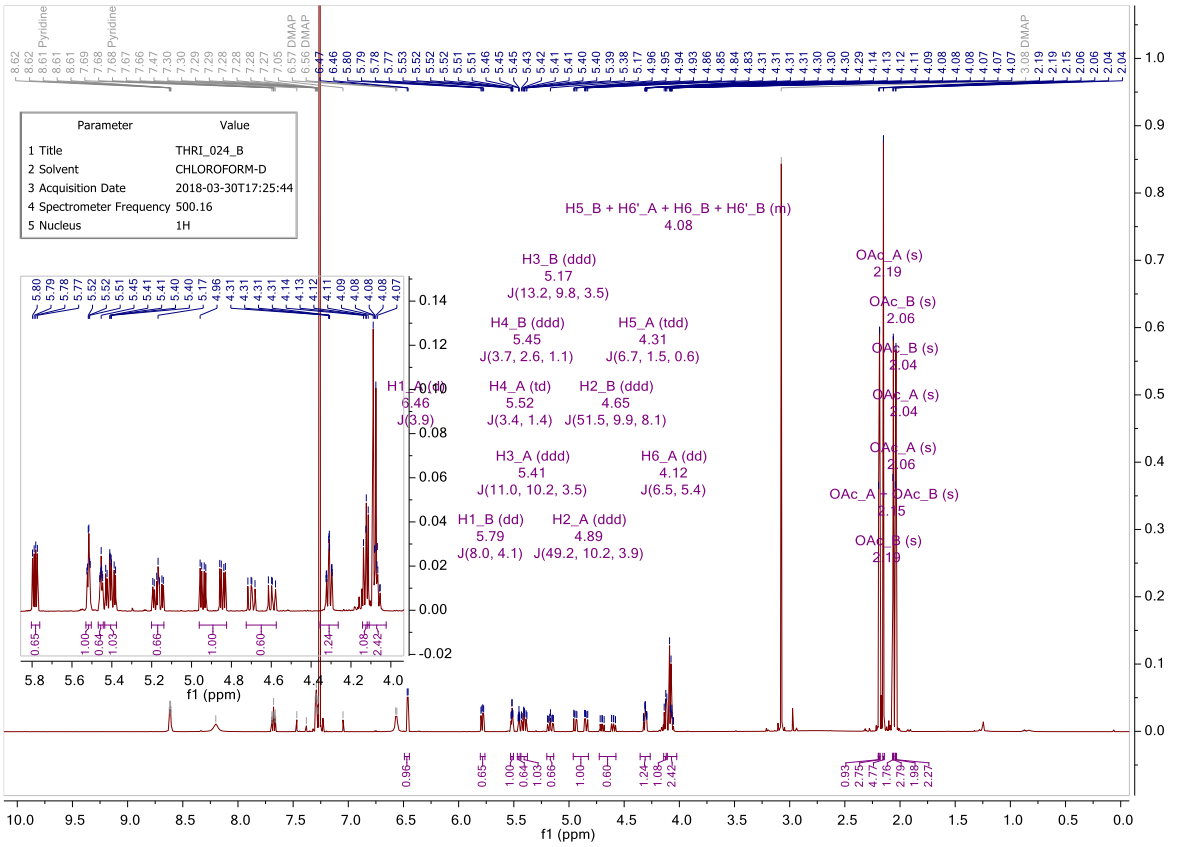
Parameter Value
1 Title THRI_024_B
2 Solvent CHLOROFORM-D
3 Acquisition Date 2018-03-30T17:25:44
4 Spectrometer Frequency 500.16
5 Nucleus 1H
H5_B + H6'_A + H6_B + H6'_B (m)
4.08
H3_B (ddd)
5.17
J(13.2, 9.8, 3.5)
H4_B (ddd)
5.45
J(3.7, 2.6, 1.1)
H5_A (tdd)
4.31
J(6.7, 1.5, 0.6)
H1_A (d)
6.46
J(3.9)
H4_A (td)
5.52
J(3.4, 1.4)
H2_B (ddd)
4.65
J(51.5, 9.9, 8.1)
H3_A (ddd)
5.41
J(11.0, 10.2, 3.5)
H6_A (dd)
4.12
J(6.5, 5.4)
H1_B (dd)
5.79
J(8.0, 4.1)
H2_A (ddd)
4.89
J(49.2, 10.2, 3.9)
OAc_A (s)
2.19
OAc_B (s)
2.06
OAc_B (s)
2.04
OAc_A (s)
2.04
OAc_A (s)
2.06
OAc_A + OAc_B (s)
4.5
f1 (ppm)

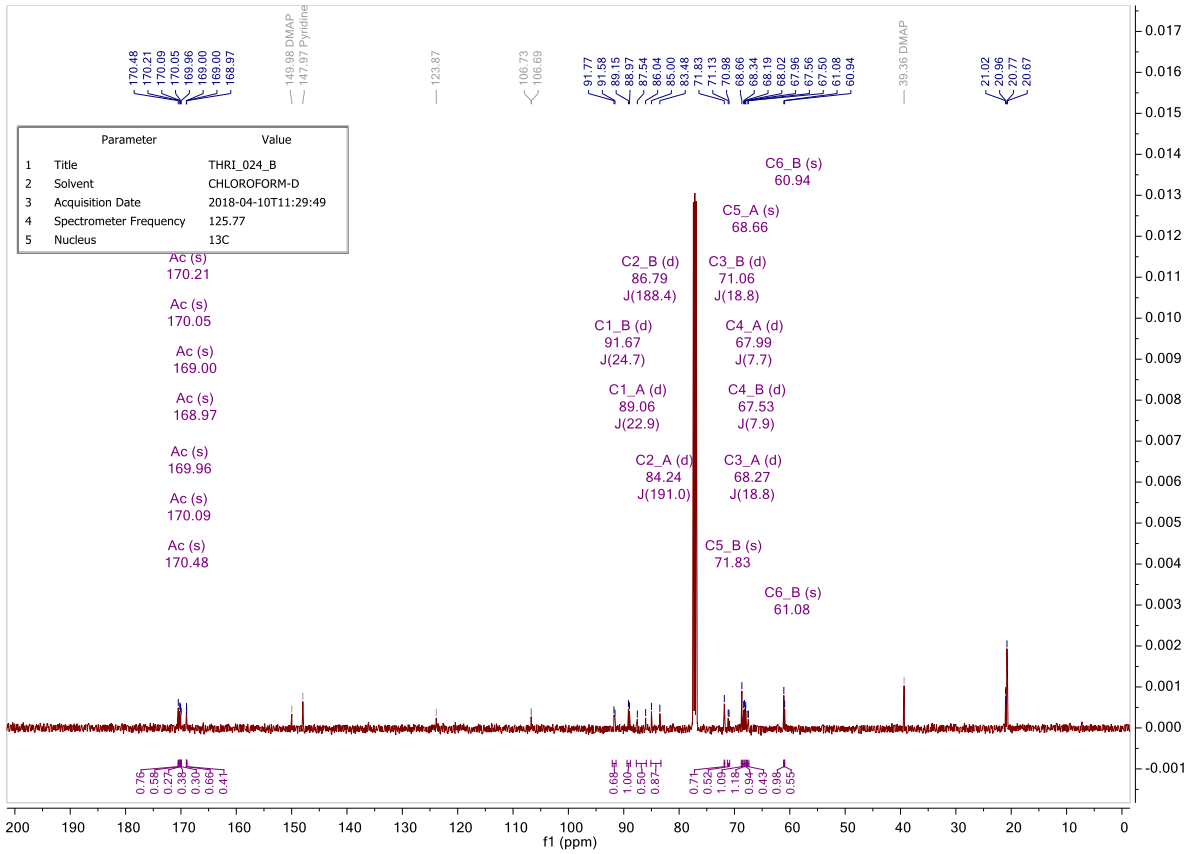
Parameter Value
1 Title THRI_024_B
2 Solvent CHLOROFORM-D
3 Acquisition Date 2018-04-10T11:29:49
4 Spectrometer Frequency 125.77
5 Nucleus 13C
C6_B (s)
60.94
C5_A (s)
68.66
C2_B (d)
86.79
J(188.4)
C3_B (d)
71.06
J(18.8)
C1_B (d)
91.67
J(24.7)
C4_A (d)
67.99
J(7.7)
C1_A (d)
89.06
J(22.9)
C4_B (d)
67.53
J(7.9)
C2_A (d)
84.24
J(191.0)
C3_A (d)
68.27
J(18.8)
C5_B (s)
71.83
C6_B (s)
61.08
Ac (s)
170.21
Ac (s)
170.05
Ac (s)
169.00
Ac (s)
168.97
Ac (s)
169.96
Ac (s)
170.09
Ac (s)
170.48
f1 (ppm)

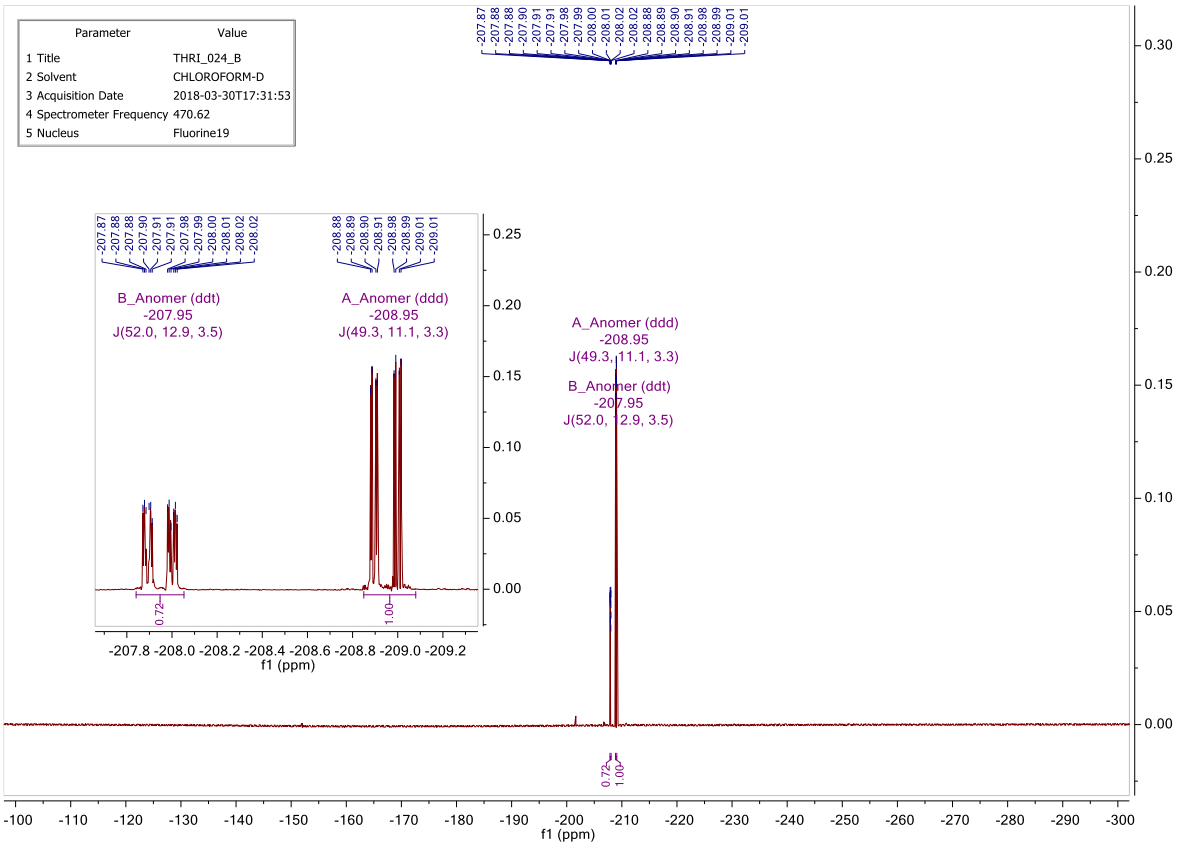
Parameter Value
1 Title THRI_024_B
2 Solvent CHLOROFORM-D
3 Acquisition Date 2018-03-30T17:31:53
4 Spectrometer Frequency 470.62
5 Nucleus Fluorine19
B_Anomer (ddt)
-207.95
J(52.0, 12.9, 3.5)
A_Anomer (ddd)
-208.95
J(49.3, 11.1, 3.3)
A_Anomer (ddd)
-208.95
J(49.3, 11.1, 3.3)
B_Anomer (ddt)
-207.95
J(52.0, 12.9, 3.5)
0.72
1.00
f1 (ppm)

VI.2.6 1,3,5,6-tetra-*O*-acetyl-2-deoxy-2-fluoro-D-galactofuranose

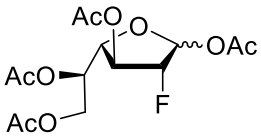

In a dried flask, 2-deoxy-2-fluro-D-galactopyranose (100 mg, 0.55 mmol, 1 eq.) was dissolved in distilled pyridine (1.44 mL, 17.9 mmol, 32.6 eq.) under argon atmosphere. The solution was heated to reflux at 110 °C for 2 hours with moderate stirring. Then, acetic anhydride (0.87 mL, 9.17 mmol, 16.7 eq.) was added dropwise to the reaction mixture which was left for an additional 1 h 30 at 110 °C. Then the mixture was allowed to cool down to room temperature. The crude was concentrated *in vacuo* and purified by silica gel chromatography (eluted with EtOAc/Cyclohexane (1:2)). The furanoses products eluted second after pyranoses products. After concentration *in vacuo*, a light yellow syrup was obtained (yield = 25 %).

First fraction was mainly composed of the α anomer (60 % α-furanose, 10 % β-furanose, 10 % α-pyranose, 9 % β-pyranose, 11 % others) while the second fraction was mainly composed of the β anomer (13 % α-furanose, 84 % β-furanose, 3 % impurity). Analytical data collaborated with those described in the literature.[35]

- **Formula :** $C_{14}H_{19}O_9F$
- **Molecular weight :** 350.30 g/mol
- **R_f :** 0.53 (EtOAc/n-Hexane 1:1)
- **Aspect :** Light yellow syrup
- **^{1}H NMR** (500 MHz, $CDCl_3$) :
  - α-anomer : δ 6.30 (d, *J* = 4.5 Hz, 1H, H-1), 5.59 (dt, *J* = 16.1, 6.1 Hz, 1H, H-3), 5.28 (td, *J* = 5.9, 4.3 Hz, 1H, H-5), 5.12 (ddd, *J* = 51.9, 6.2, 4.5 Hz, 1H, H-2), 4.30 (dd, *J* = 12.1, 4.3 Hz, 1H, H-6), 4.19 – 4.10 (m, 2H, H-6' + H-4), 2.17 (s, 3H, Ac), 2.13 (s, 3H, Ac), 2.12 (s, 3H, Ac), 2.05 (s, 3H, Ac).
  - β-anomer : δ 6.37 (dd, *J* = 10.8, 0.9 Hz, 1H, H-1), 5.41 (ddd, *J* = 6.9, 4.4, 3.2 Hz, 1H, H-5), 5.14 (ddt, *J* = 21.4, 4.6, 1.1 Hz, 1H, H-3), 4.97 (dd, *J* = 49.1, 1.0 Hz, 1H, H-2), 4.38 (dd, *J* = 4.6, 3.3 Hz, 1H, H-4), 4.32 (dd, *J* = 11.9, 4.4 Hz, 1H, H-6), 4.24 (dd, *J* = 11.9, 6.9 Hz, 1H, H-6'), 2.13 (s, 3H, Ac), 2.12 (s, 3H, Ac), 2.11 (s, 3H, Ac), 2.06 (s, 3H, Ac).
- **^{13}C NMR** (126 MHz, $CDCl_3$) **:**
  - α-anomer : δ 170.56 (Ac), 169.96 (Ac), 169.79 (Ac), 169.57 (Ac), 92.82 (d, *J* = 50.7 Hz, C-1), 91.94 (d, *J* = 135.1 Hz, C-2), 79.27 (d, *J* = 7.8 Hz, C-4), 73.83 (d, *J* = 24.3 Hz, C-3), 70.17 (C-5), 62.14 (C-6), 21.17 (Ac), 20.91 (Ac), 20.79 (Ac), 20.77 (Ac).

- β-anomer : δ 170.67 (Ac), 169.36 (Ac), 169.81 (Ac), 169.09 (Ac), 99.01 (d, *J* = 37.9 Hz, C-1), 97.42 (d, *J* = 185.3 Hz, C-2), 83.33 (C-4), 76.38 (d, *J* = 30.7 Hz, C-3), 69.22 (C-5), 62.60 (C-6), 21.04 (Ac), 20.81 (Ac), 20.69 (Ac).

- **^{19}F NMR** (471 MHz, $CDCl_3$) :
  - α-anomer : δ -205.72 (dd, J = 51.8, 16.2 Hz).
  - β-anomer : δ -190.53 (dd, J = 49.1, 21.4, 10.8 Hz)
- **HRMS (ESI) :** *m/*z Calculated for $C_{14}H_{19}O_9F$ $[M+Na]^+$: 373.0905 ; found : 373.0904; δ = 0.4 ppm

α anomer spectra:

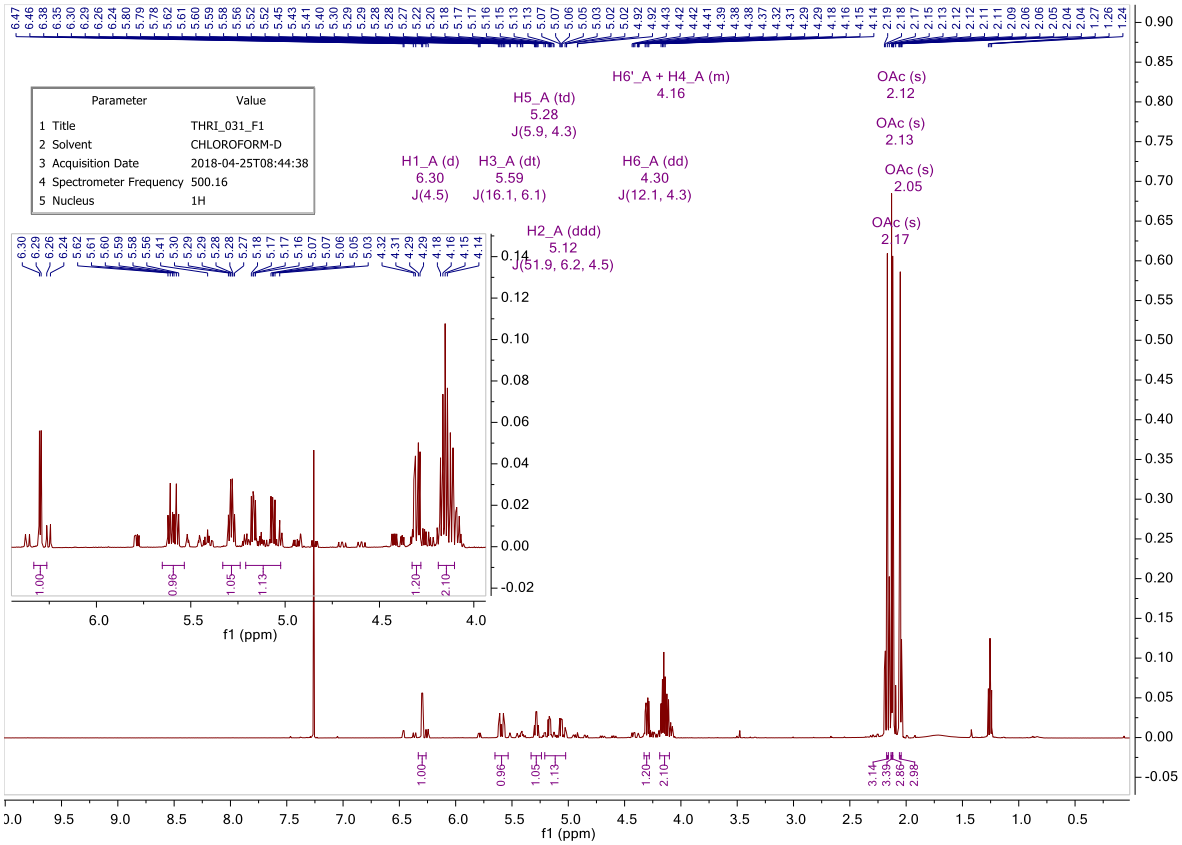

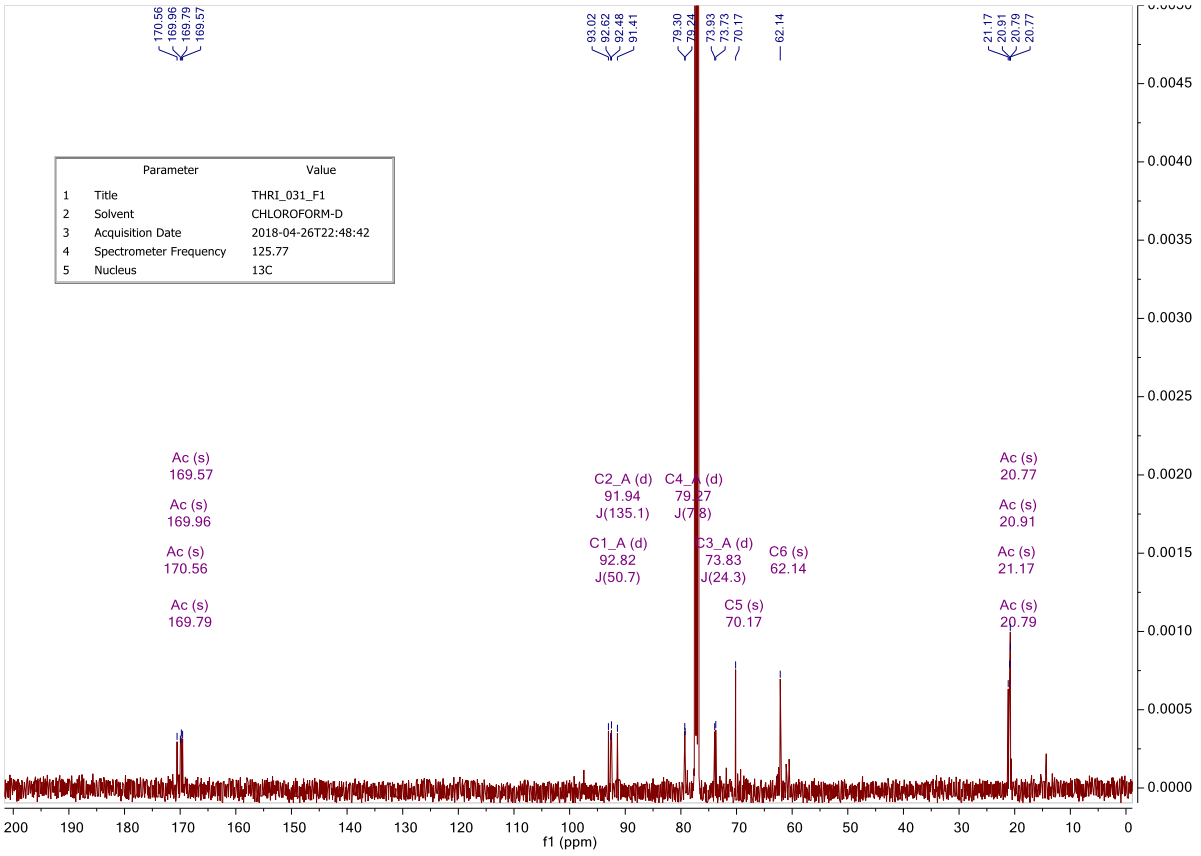
170.56
169.96
169.79
169.57
93.02
92.62
92.48
91.41
79.30
79.24
73.93
73.73
70.17
62.14
21.17
20.91
20.79
20.77
Parameter Value
1 Title THRI_031_F1
2 Solvent CHLOROFORM-D
3 Acquisition Date 2018-04-26T22:48:42
4 Spectrometer Frequency 125.77
5 Nucleus 13C
Ac (s) 169.57
Ac (s) 169.96
Ac (s) 170.56
Ac (s) 169.79
C2_A (d) 91.94 J(135.1)
C4_A (d) 79.27 J(7.8)
C1_A (d) 92.82 J(50.7)
C3_A (d) 73.83 J(24.3)
C6 (s) 62.14
C5 (s) 70.17
Ac (s) 20.77
Ac (s) 20.91
Ac (s) 21.17
Ac (s) 20.79
f1 (ppm)

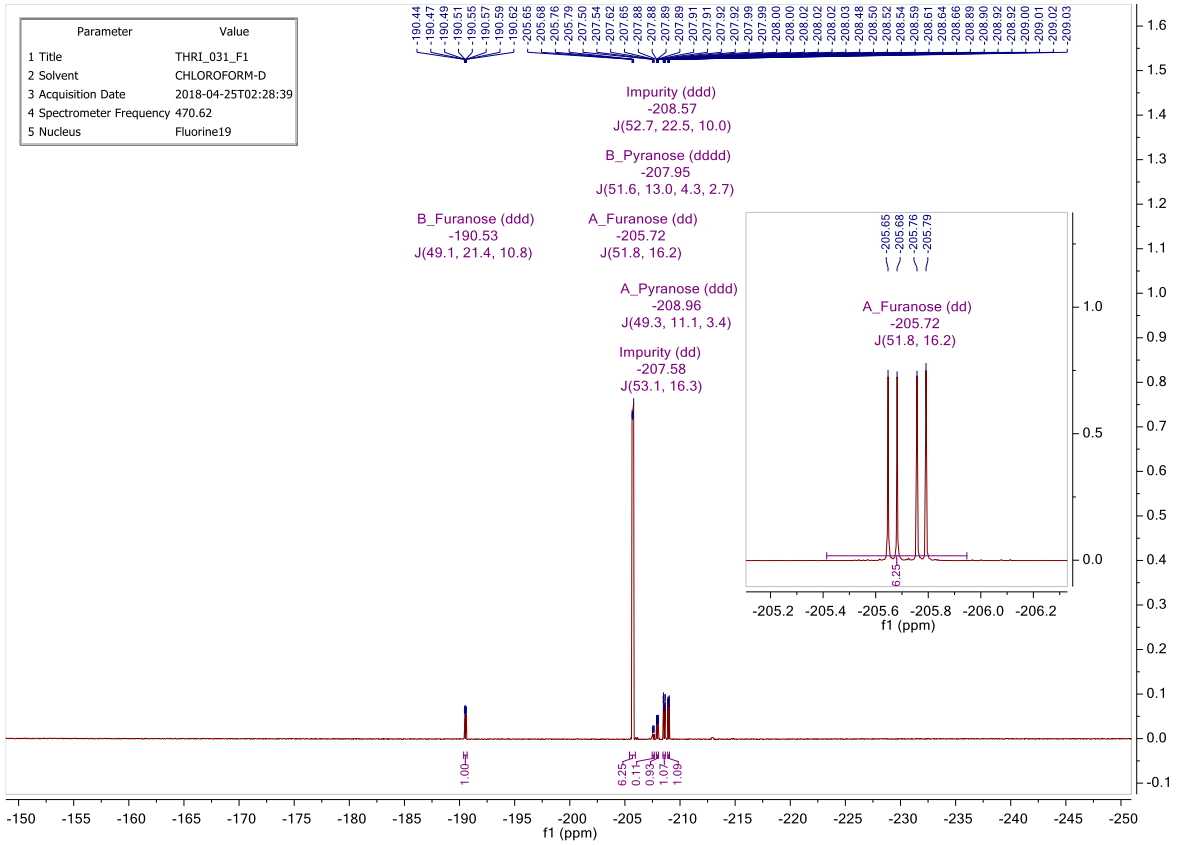
Parameter Value
1 Title THRI_031_F1
2 Solvent CHLOROFORM-D
3 Acquisition Date 2018-04-25T02:28:39
4 Spectrometer Frequency 470.62
5 Nucleus Fluorine19
Impurity (ddd) -208.57 J(52.7, 22.5, 10.0)
B_Pyranose (dddd) -207.95 J(51.6, 13.0, 4.3, 2.7)
B_Furanose (ddd) -190.53 J(49.1, 21.4, 10.8)
A_Furanose (dd) -205.72 J(51.8, 16.2)
A_Pyranose (ddd) -208.96 J(49.3, 11.1, 3.4)
Impurity (dd) -207.58 J(53.1, 16.3)
A_Furanose (dd) -205.72 J(51.8, 16.2)
f1 (ppm)

β anomer spectra:

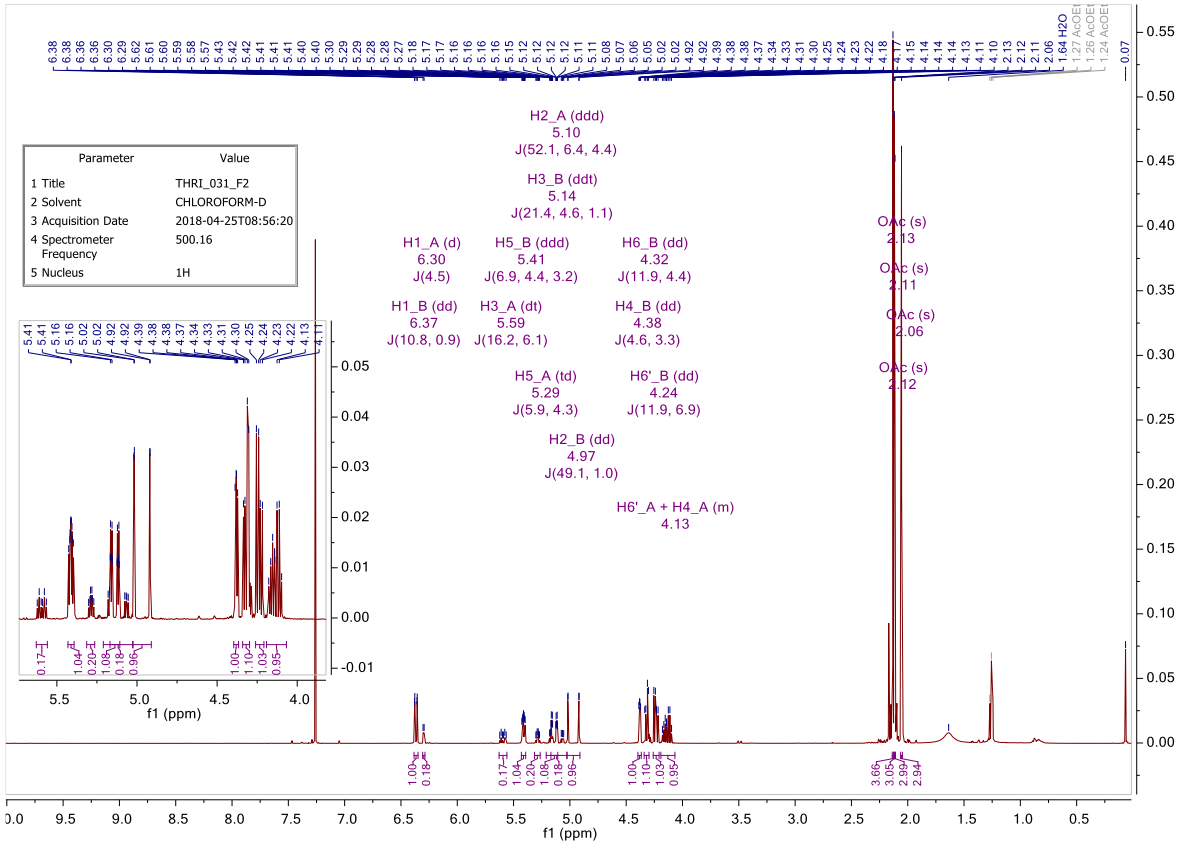

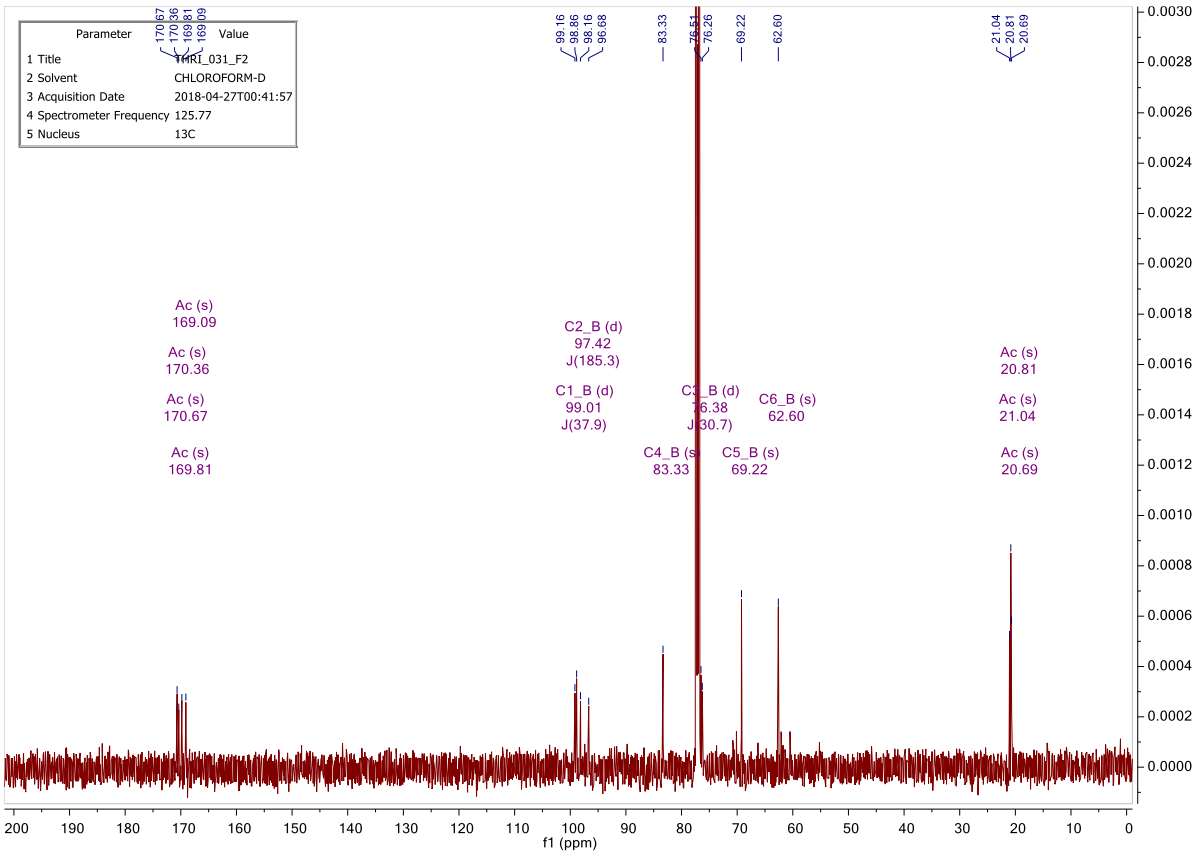

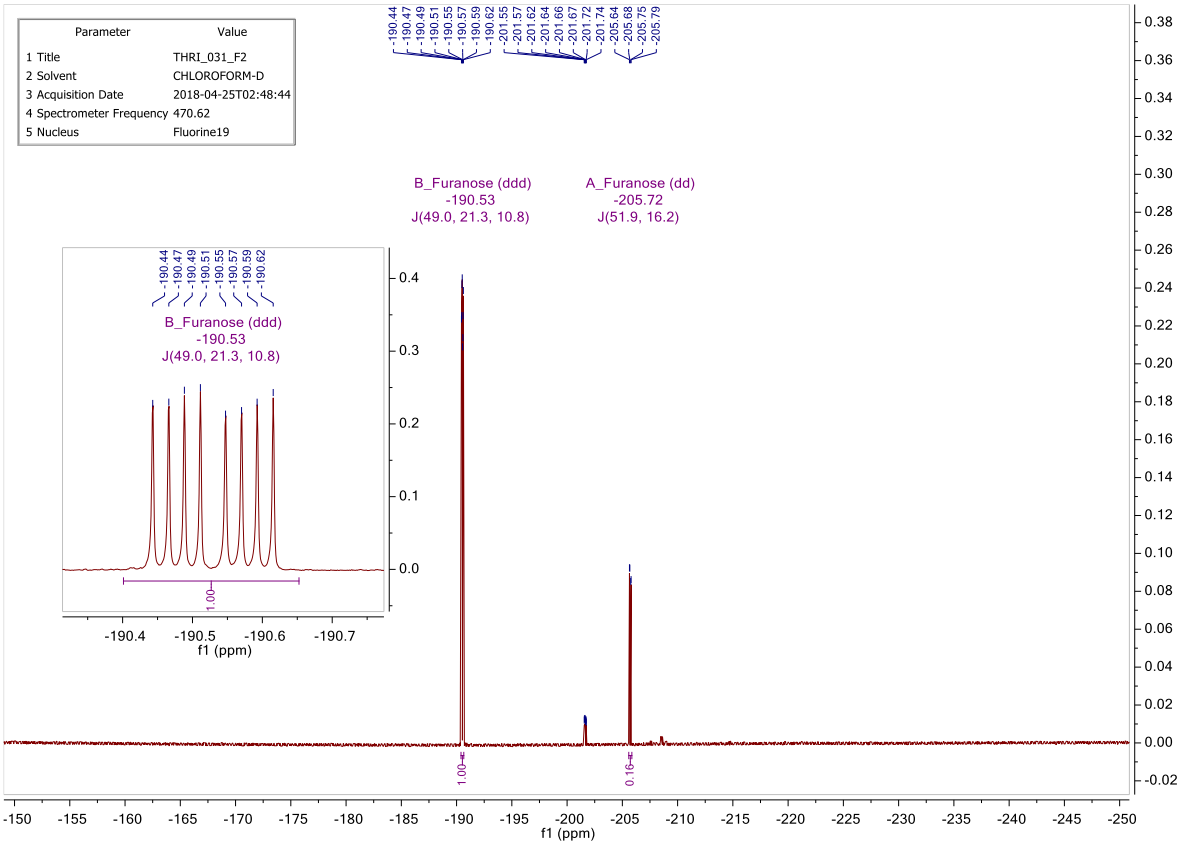
Parameter Value
1 Title THRI_031_F2
2 Solvent CHLOROFORM-D
3 Acquisition Date 2018-04-25T02:48:44
4 Spectrometer Frequency 470.62
5 Nucleus Fluorine19
-190.44 -190.47 -190.49 -190.51 -190.55 -190.57 -190.59 -190.62
-201.55 -201.57 -201.62 -201.64 -201.66 -201.67 -201.72 -201.74
-205.64 -205.68 -205.75 -205.79
B_Furanose (ddd)
-190.53
J(49.0, 21.3, 10.8)
A_Furanose (dd)
-205.72
J(51.9, 16.2)
1.00
0.16
f1 (ppm)

VI.2.7 3,5,6-tri-*O*-acetyl-2-deoxy-2-fluoro-D-galactofuranose

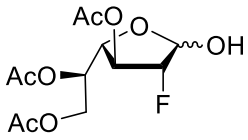

In a dried flask, 1,3,5,6-tetra-*O*-acetyl-2-deoxy-2-fluoro-D-galactofuranose (469 mg, 1,34 mmol, 1 eq.) was dissolved in distilled CH_2Cl_2 (4,7 mL) under argon atmosphere. The reagent was cooled to 0 °C before the dropwise addition of HBr 33 % in AcOH (1,24 mL, 21,7 mmol, 16,3 eq.) under stirring. The reaction was left overnight at room temperature. After concentration of the crude *in vacuo*, the residue was diluted in DCM (25 mL), washed with saturated $NaHCO_3$ (3 x 25 mL), brine (1 x 25 mL), dried over $MgSO_4$, filtrated and concentrated *in vacuo* for the next step. The obtained orange oil was dissolved in a 10:1 mixture of Acetone/H_2O (5 mL) and then Ag_2CO_3 (369mg, 1,34 mmol, 1 eq.) was added to the solution under stirring. After 90 minutes of reaction time at room temperature, the crude was filtered on silica and concentrated to dryness. Purification by silica gel chromatography ((EtOAc/Cyclohexane (1:2)) afforded a colorless syrup (64 % yield, α/β = 1:9).

- **Formula :** $C_{12}H_{17}O_8F$
- **Molecular weight :** 308.26 g/mol
- **R_f :** 0.35 (EtOAc/Cyclohexane 1:1)
- **Aspect :** Colorless syrup
- **^{1}H NMR** (500 MHz, $CDCl_3$) : δ 5.59 (dd, *J* = 10.7, 3.4 Hz, 1H, H-1), 5.41 (ddd, *J* = 6.9, 4.7, 3.5 Hz, 1H, H-4), 5.08 (ddd, *J* = 22.0, 4.7, 1.8 Hz, 1H, H-3), 4.92 (dd, *J* = 49.4, 1.0 Hz, 1H, H-2), 4.42 (dd, *J* = 4.8, 3.5 Hz, 1H, H-5), 4.34 (dd, *J* = 11.7, 4.7 Hz, 1H, H-6), 4.21 (dd, *J* = 11.8, 6.9 Hz, 1H, H-6'), 3.00 (t, *J* = 3.4 Hz, 1H, OH), 2.13 (s, 3H, Ac), 2.11 (s, 3H, Ac), 2.06 (s, 3H, Ac).
- **^{13}C NMR** (126 MHz, $CDCl_3$) : δ 170.76 (Ac), 170.41 (Ac), 170.08 (Ac), 100.47 (d, J = 35.5 Hz, C-1), 98.16 (d, J = 183.1 Hz, C-2), 81.56 (C-4), 76.90 (d, J = 30.4 Hz, C-3), 69.55 (C-5), 62.63 (C-6), 20.89 (Ac), 20.88 (Ac), 20.81 (Ac).
- **^{19}F NMR** (471 MHz, $CDCl_3$) : δ -190.72 (dddd, J = 49.4, 22.4, 10.7, 2.2 Hz, F_β), -205.43 (ddd, J = 50.7, 16.5, 8.9 Hz, F_α).
- **HRMS (ESI) :** *m/*z Calculated for $C_{12}H_{17}FO_8$ $[M+Na]^+$: 331.0799; found : 331.0800; δ = 0.1 ppm

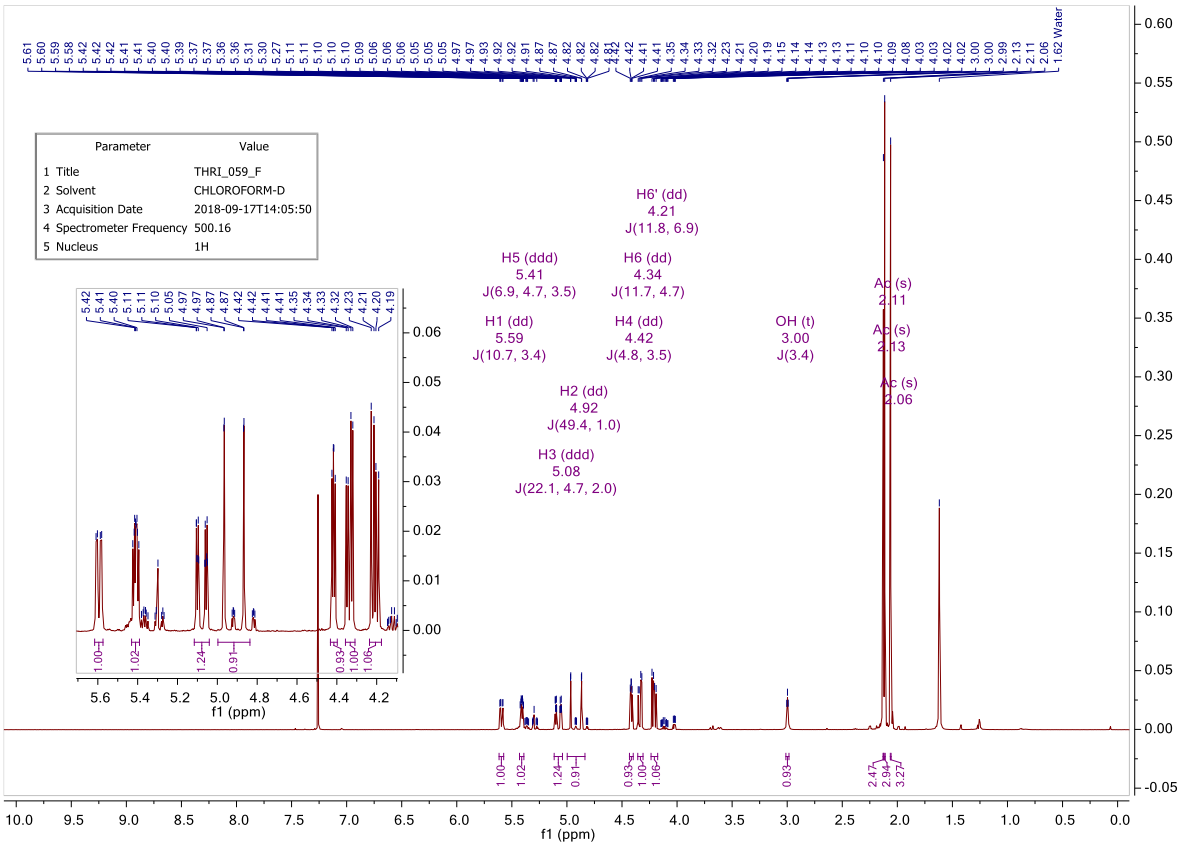
Parameter Value
1 Title THRI_059_F
2 Solvent CHLOROFORM-D
3 Acquisition Date 2018-09-17T14:05:50
4 Spectrometer Frequency 500.16
5 Nucleus 1H
H6' (dd)
4.21
J(11.8, 6.9)
H5 (ddd)
5.41
J(6.9, 4.7, 3.5)
H6 (dd)
4.34
J(11.7, 4.7)
H1 (dd)
5.59
J(10.7, 3.4)
H4 (dd)
4.42
J(4.8, 3.5)
OH (t)
3.00
J(3.4)
Ac (s)
2.11
Ac (s)
2.13
Ac (s)
2.06
H2 (dd)
4.92
J(49.4, 1.0)
H3 (ddd)
5.08
J(22.1, 4.7, 2.0)
f1 (ppm)

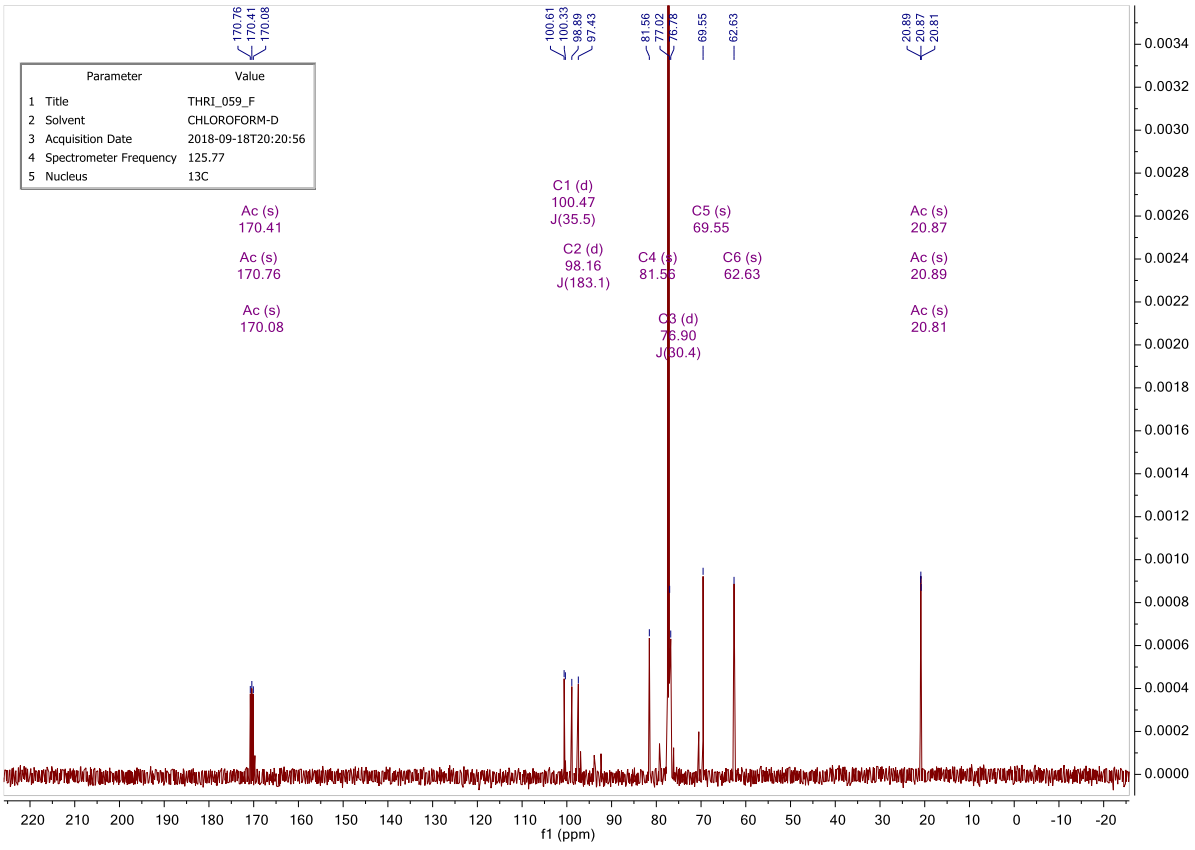
Parameter Value
1 Title THRI_059_F
2 Solvent CHLOROFORM-D
3 Acquisition Date 2018-09-18T20:20:56
4 Spectrometer Frequency 125.77
5 Nucleus 13C
C1 (d)
100.47
J(35.5)
C2 (d)
98.16
J(183.1)
C3 (d)
76.90
J(30.4)
C4 (s)
81.56
C5 (s)
69.55
C6 (s)
62.63
Ac (s)
170.41
Ac (s)
170.76
Ac (s)
170.08
Ac (s)
20.87
Ac (s)
20.89
Ac (s)
20.81
f1 (ppm)

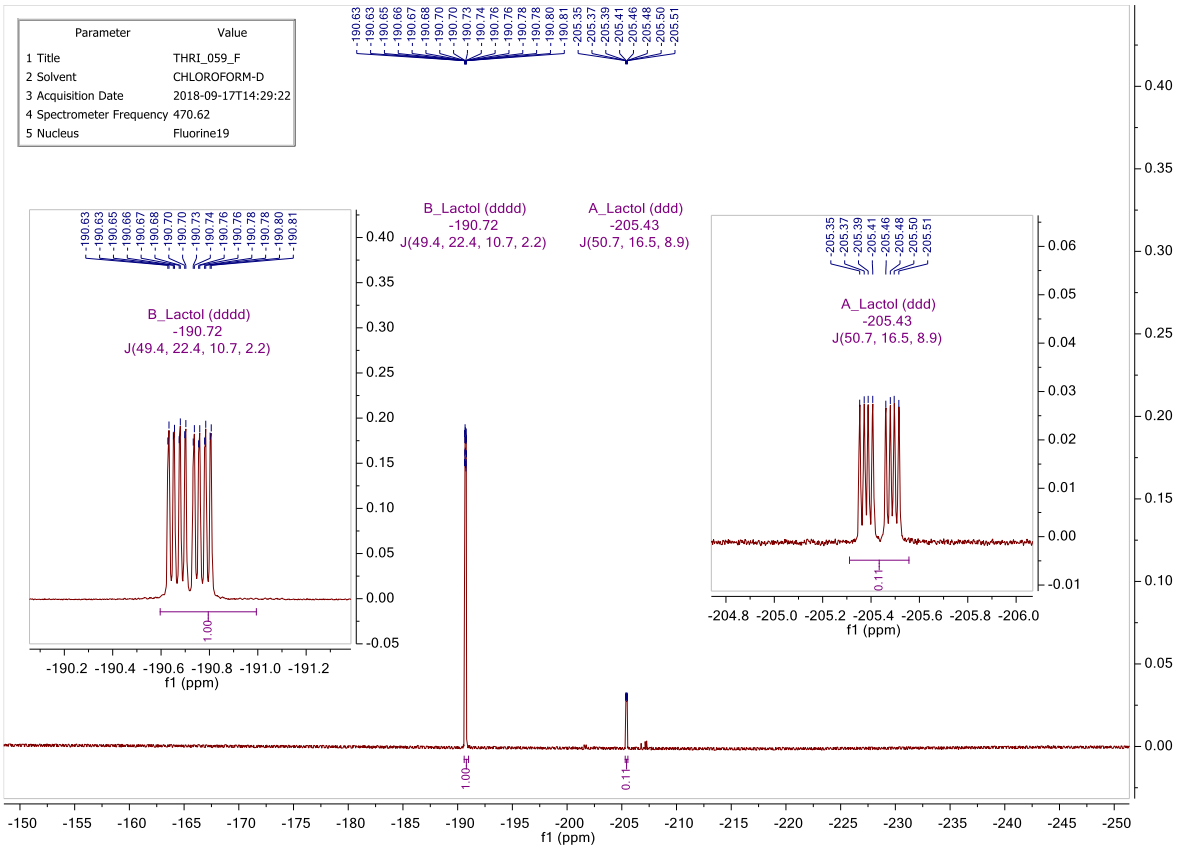
Parameter Value
1 Title THRI_059_F
2 Solvent CHLOROFORM-D
3 Acquisition Date 2018-09-17T14:29:22
4 Spectrometer Frequency 470.62
5 Nucleus Fluorine19
B_Lactol (dddd)
-190.72
J(49.4, 22.4, 10.7, 2.2)
A_Lactol (ddd)
-205.43
J(50.7, 16.5, 8.9)
f1 (ppm)

VI.2.8 1-*O*-(o,p-dinitrophenyl)-3,5,6-tri-*O*-acetyl-2-deoxy-2-fluoro-α-D-galactofuranose and 1-*O*-(o,p-dinitrophenyl)-3,5,6-tri-*O*-acetyl-2-deoxy-2-fluoro-β-D-galactofuranose

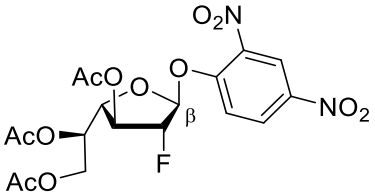

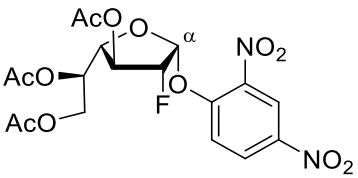

In a dried flask, 3,5,6-tri-*O*-acetyl-2-deoxy-2-fluoro-D-galactofuranose (220 mg, 0.71 mmol, 1 eq.) and 1,4-diazabicyclo[2.2.2]octane (248 mg, 2.21 mmol, 1.1 eq.) were dissolved in 2.9 mL of dry CH_3CN under argon atmosphere. 1-fluoro-2,4-dinitrobenzene (99 µL, 0.79 mmol, 1.1 eq.) was added dropwise to the solution and the reaction was left under stirring at room temperature for 2 h 30. The crude was concentrated *in vacuo* and then diluted in CH_2Cl_2 (72 mL), washed with HCl 1M (2 x 72 mL) and with H_2O (1 x 72 mL), dried with $MgSO_4$, filtrated and concentrated *in vacuo*. Purification was performed by silica gel chromatography (EtOAc/Cyclohexane (1:2)). To remove the yellow tint of the purified fraction, a work-up with saturated $NaHCO_3$ was performed. The two anomers could be separated as a pale yellow syrup (Yield: α anomer = 27 %, β anomer = 30 %).

- **Formula :** $C_{18}H_{19}FN_2O_{12}$
- **Molecular weight :** 474.35 g/mol
- **R_f :**
  - α anomer : 0.30 (EtOAc/Cyclohexane 1:1)
  - β anomer : 0.72 (EtOAc/Cyclohexane 1:1)
- **Aspect :** Light yellow syrup
- **^{1}H NMR** (500 MHz, Chloroform-*d*) :
  - α anomer : δ 8.78 (d, J = 2.7 Hz, 1H, H-m'), 8.44 (dd, J = 9.2, 2.8 Hz, 1H, H-m), 7.45 (d, J = 9.3 Hz, 1H, H-o), 5.90 (d, J = 4.3 Hz, 1H, H-1), 5.73 (dt, J = 15.9, 7.0 Hz, 1H, H-3), 5.29 (ddd, J = 51.4, 7.2, 4.4 Hz, 1H, H-2), 5.31 – 5.26 (m, 1H, H-5), 4.29 (dd, J = 6.7, 3.8 Hz, 1H, H-4), 4.22 (dd, J = 11.6, 5.5 Hz, 1H, H-6), 4.03 (dd, J = 11.6, 6.4 Hz, 1H, H-6'), 2.15 (s, 3H, Ac), 2.04 (s, 3H, Ac), 1.96 (s, 3H, Ac).
  - β anomer : δ 8.74 (d, J = 2.7 Hz, 1H, H-m'), 8.45 (dd, J = 9.3, 2.8 Hz, 1H, H-m), 7.47 (d, J = 9.3 Hz, 1H, H-o), 6.11 (d, J = 9.4 Hz, 1H, H-1), 5.46 (ddd, J = 6.9, 4.9, 3.3 Hz, 1H, H-5), 5.25 (dd, J = 48.5, 0.9 Hz, 1H, H-2), 5.17 (ddd, J = 20.0, 3.9, 0.8 Hz, 1H, H-3), 4.45 (t, J = 3.6 Hz, 1H, H-4), 4.28 (dd, J = 11.8, 4.9 Hz, 1H, H-6), 4.20 (dd, J = 11.8, 7.0 Hz, 1H, H-6'), 2.17 (s, 3H), 2.11 (s, 3H), 2.02 (s, 3H).

- **^{13}C NMR** (126 MHz, Chloroform-*d*) :
  - α anomer : δ 170.47 (Ac), 169.79 (Ac), 169.74 (Ac), 153.76 (C-i), 141.80 (C-p), 139.95 (C-o'), 128.95 (C-m), 122.02 (C-m'), 117.14 (C-o), 97.92 (d, *J* = 17.2 Hz, C-1), 91.53 (d, *J* = 207.8 Hz, C-2), 80.15 (d, *J* = 8.1 Hz, C-4), 72.92 (d, *J* = 23.7 Hz, C-3), 69.07 (C-5), 61.78 (C-6), 20.80 (Ac), 20.69 (Ac), 20.53 (Ac).
  - β anomer : δ 170.55 (Ac), 170.23 (Ac), 170.20 (Ac), 153.00 (C-i), 148.05 (C-p), 141.84 (C-o'), 128.93 (C-m), 121.88 (C-m'), 117.25 (C-o), 103.94 (d, J = 36.7 Hz, C-1), 96.98 (d, J = 185.2 Hz, C-2), 84.57 (C-4), 75.87 (d, J = 30.5 Hz, C-3), 69.09 (C-5), 62.30 (C-6), 20.84 (Ac), 20.81 (Ac), 20.66 (Ac).
- **^{19}F NMR** (471 MHz, Chloroform-*d*) :
  - α : δ -205.99 (dd, J = 51.5, 15.8 Hz).
  - β : δ -192.66 (ddd, J = 48.5, 19.9, 9.4 Hz).
- **FTIR** : (β anomer)
  - 1537.7 cm^{-1} (N-O assymetrical stretching)
  - 1345.2 cm^{-1} (N-O symmetrical stretching)
- **HRMS (ESI) :** *m/z* Calculated for $C_{18}H_{19}FN_2O_{12}$ $[M+Na]^+$: 497.0814; found : 497.0808; δ = 1.2 ppm

α anomer spectra:

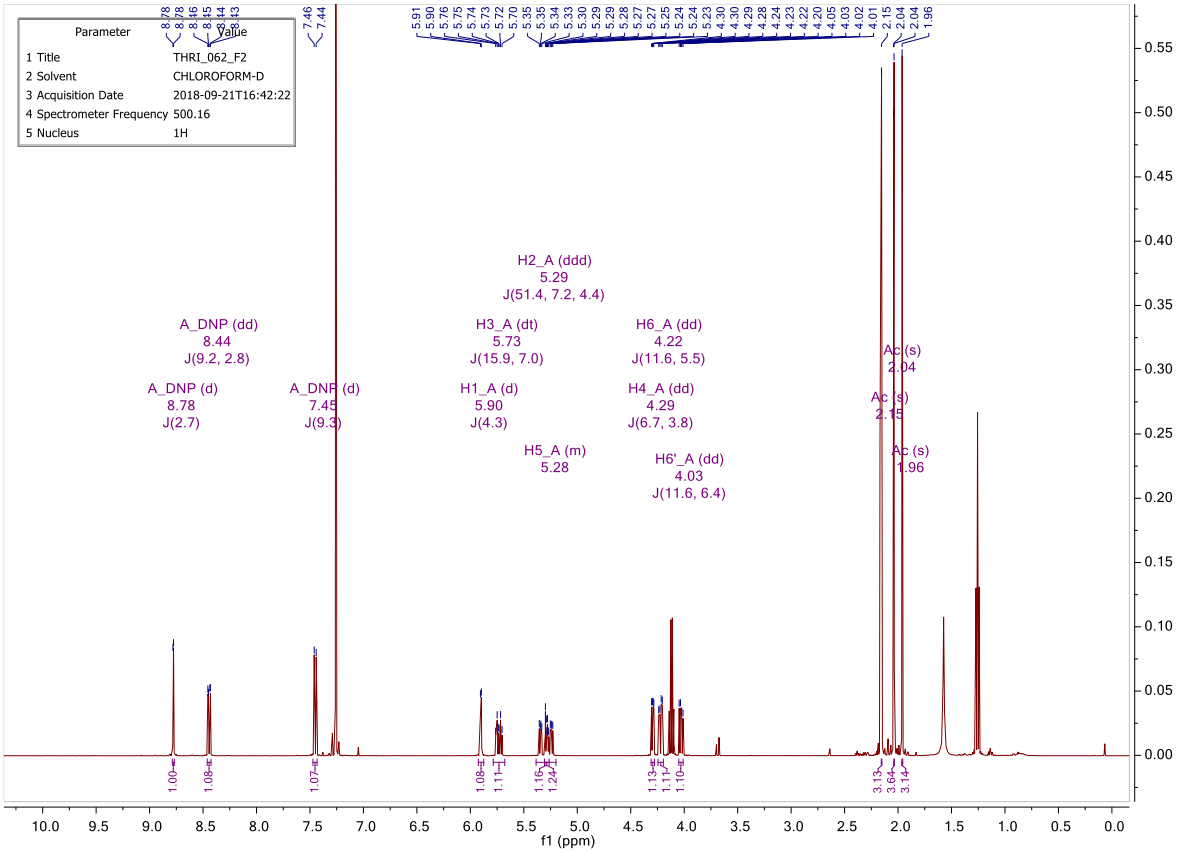

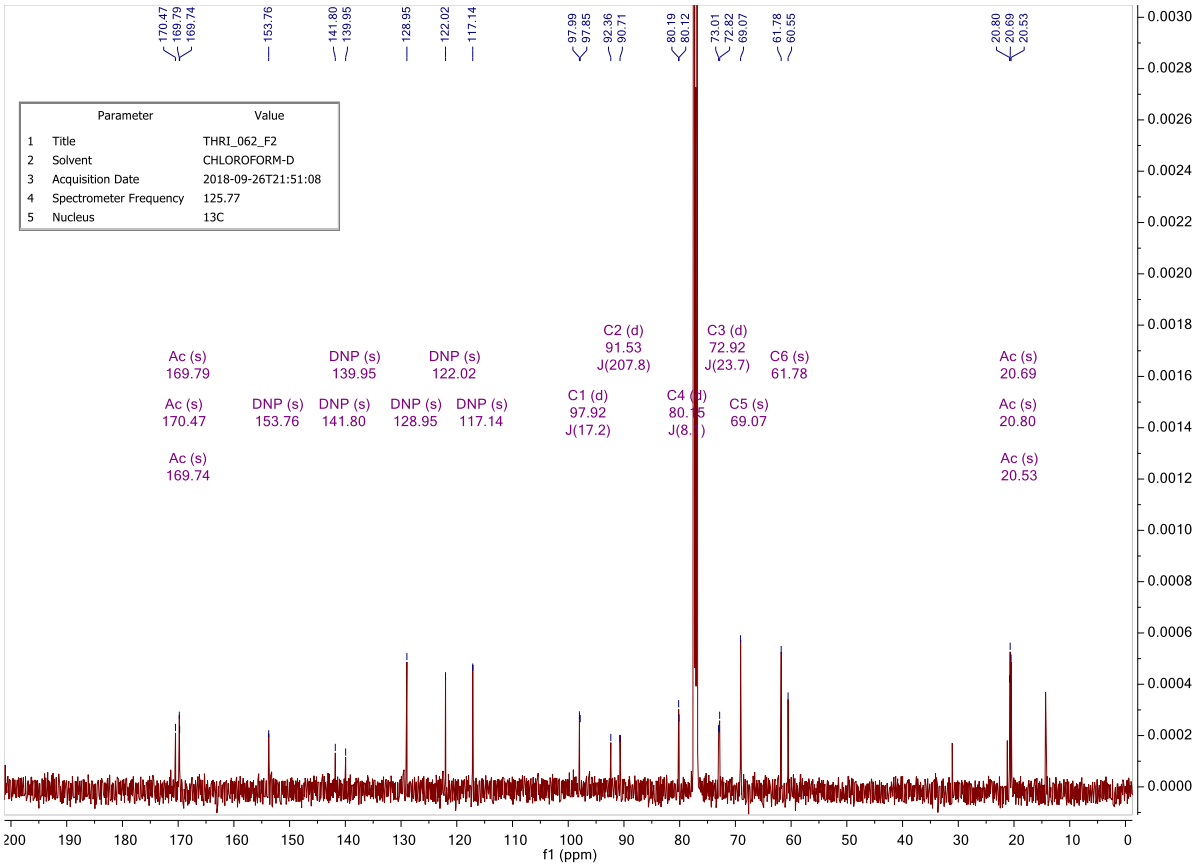
170.47
169.79
169.74
153.76
141.80
139.95
128.95
122.02
117.14
97.99
97.85
92.36
90.71
80.19
80.12
73.01
72.82
69.07
61.78
60.55
20.80
20.69
20.53
Parameter Value
1 Title THRI_062_F2
2 Solvent CHLOROFORM-D
3 Acquisition Date 2018-09-26T21:51:08
4 Spectrometer Frequency 125.77
5 Nucleus 13C
Ac (s) 169.79
Ac (s) 170.47
Ac (s) 169.74
DNP (s) 153.76
DNP (s) 139.95
DNP (s) 141.80
DNP (s) 128.95
DNP (s) 122.02
DNP (s) 117.14
C2 (d) 91.53 J(207.8)
C1 (d) 97.92 J(17.2)
C4 (d) 80.15 J(8.1)
C3 (d) 72.92 J(23.7)
C5 (s) 69.07
C6 (s) 61.78
Ac (s) 20.69
Ac (s) 20.80
Ac (s) 20.53
f1 (ppm)

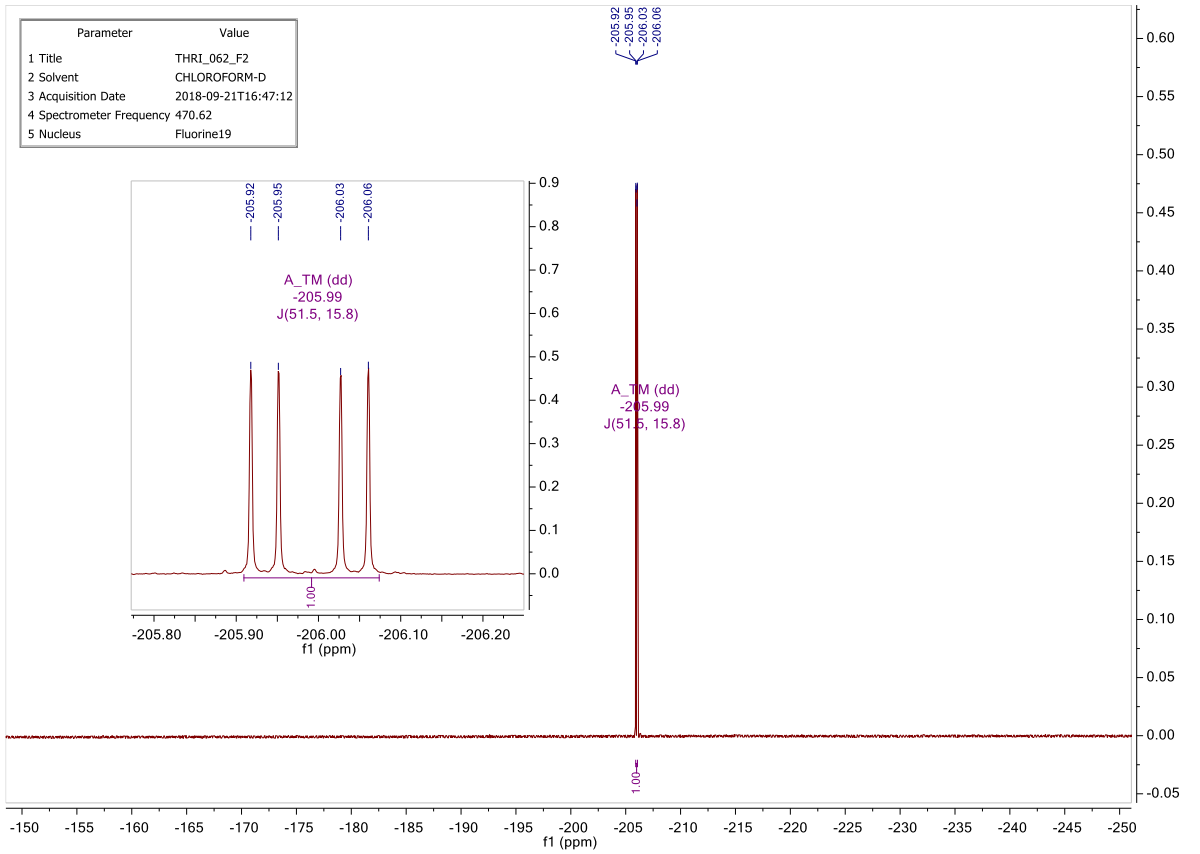
Parameter Value
1 Title THRI_062_F2
2 Solvent CHLOROFORM-D
3 Acquisition Date 2018-09-21T16:47:12
4 Spectrometer Frequency 470.62
5 Nucleus Fluorine19
-205.92
-205.95
-206.03
-206.06
A_TM (dd) -205.99 J(51.5, 15.8)
1.00
f1 (ppm)

β anomer spectra:

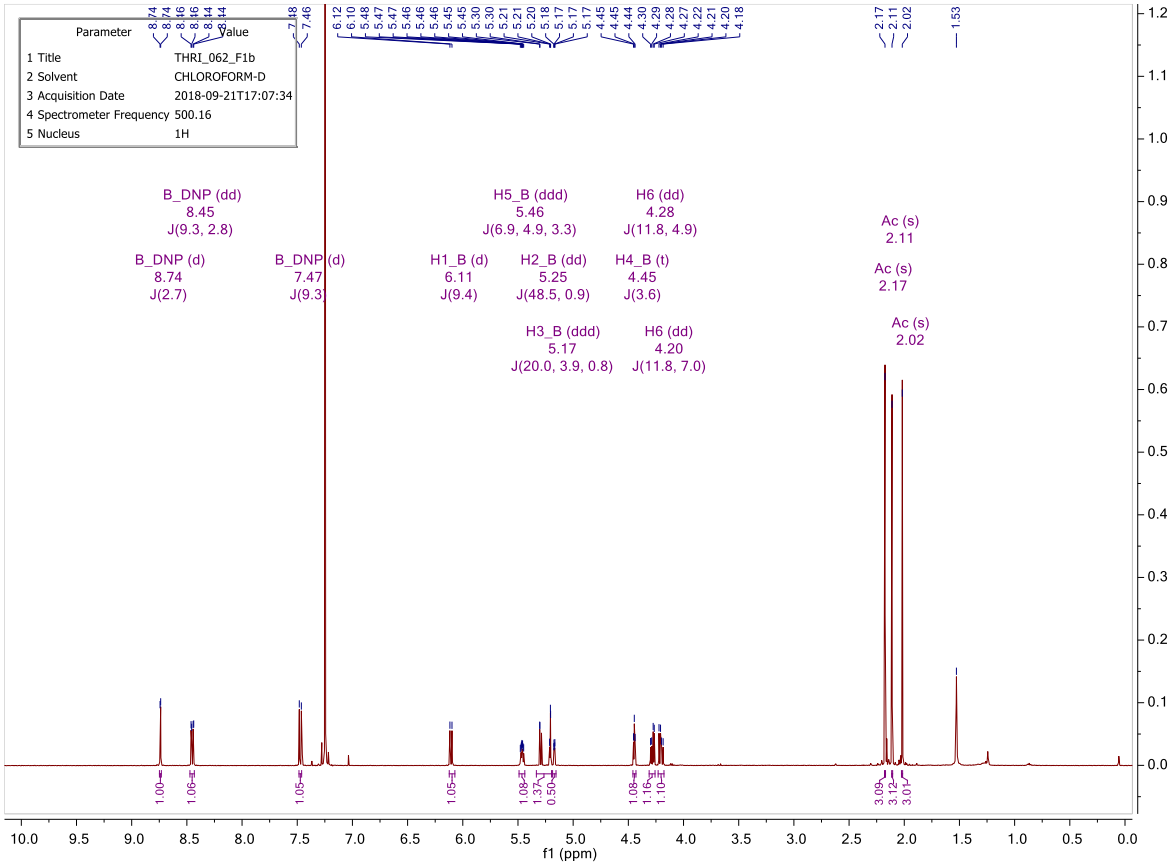

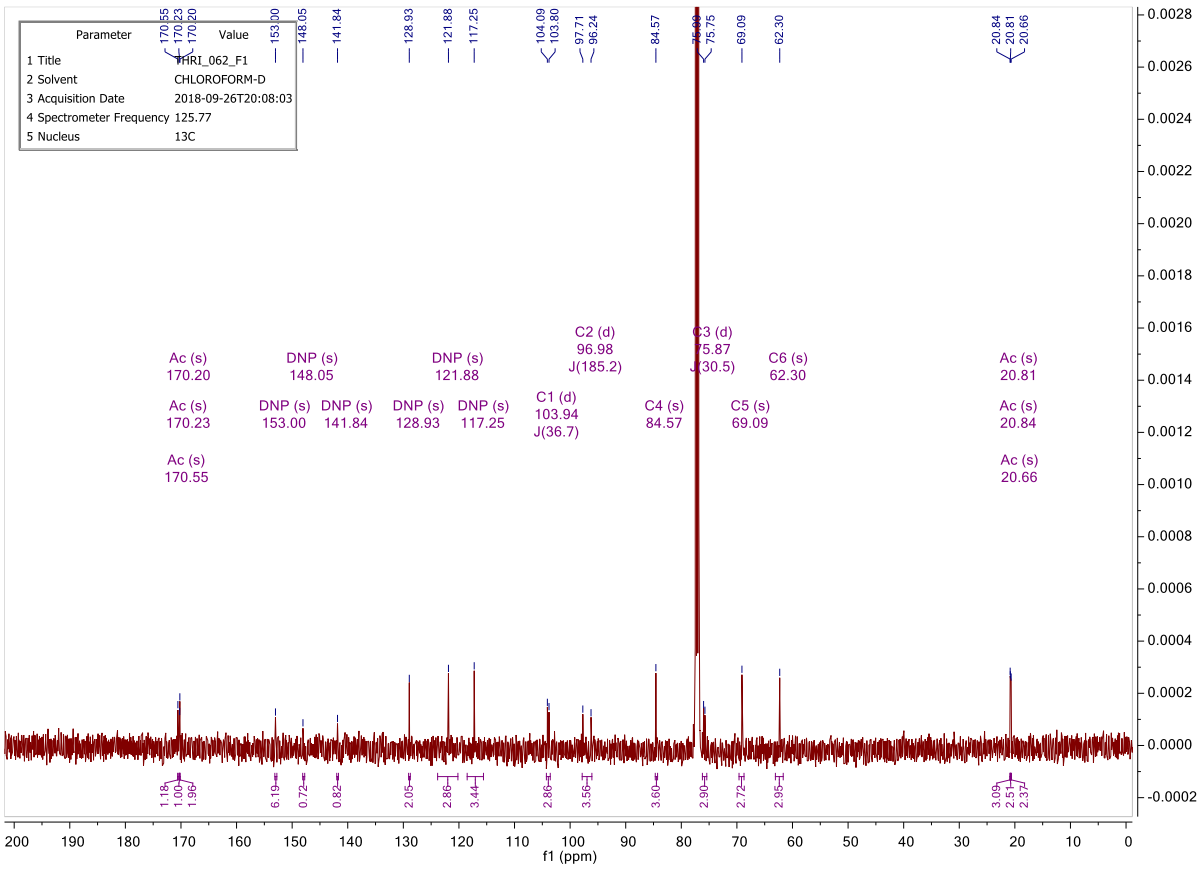

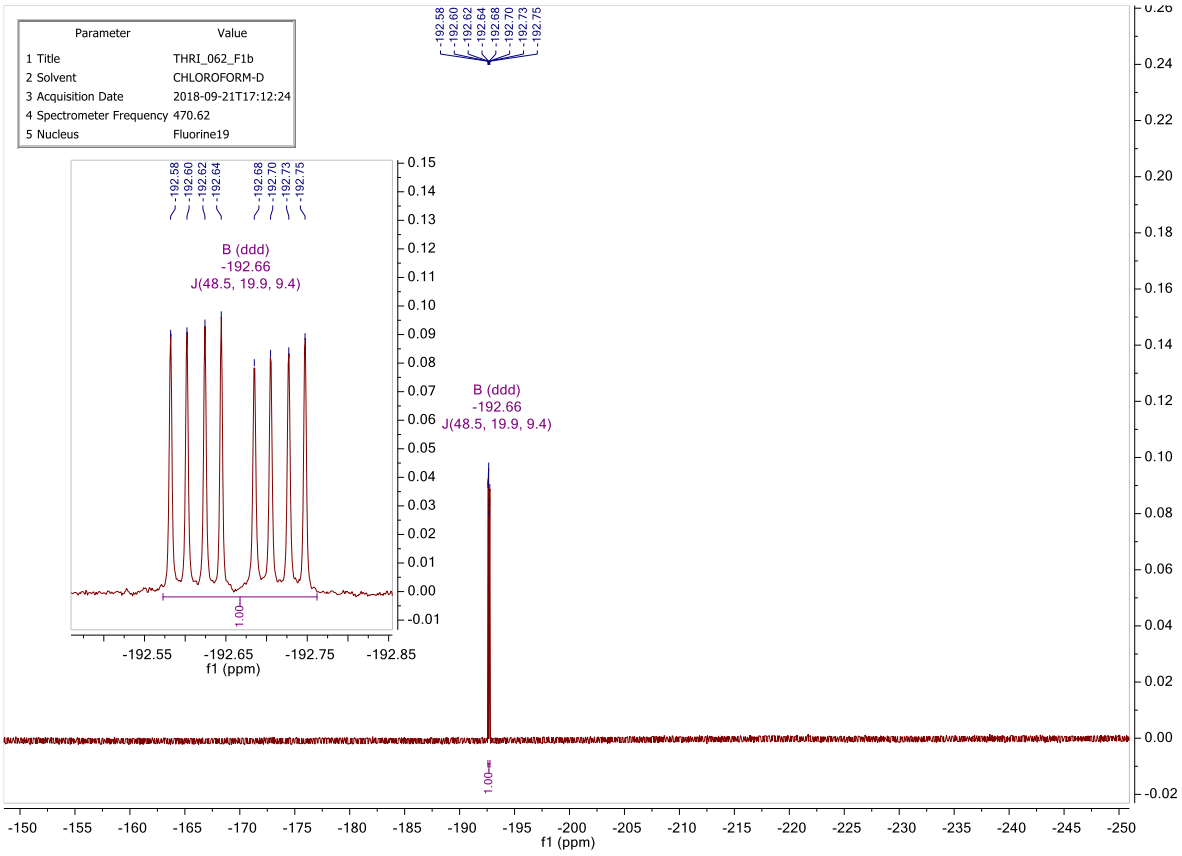
Parameter Value
1 Title THRI_062_F1b
2 Solvent CHLOROFORM-D
3 Acquisition Date 2018-09-21T17:12:24
4 Spectrometer Frequency 470.62
5 Nucleus Fluorine19
B (ddd)
-192.66
J(48.5, 19.9, 9.4)
f1 (ppm)

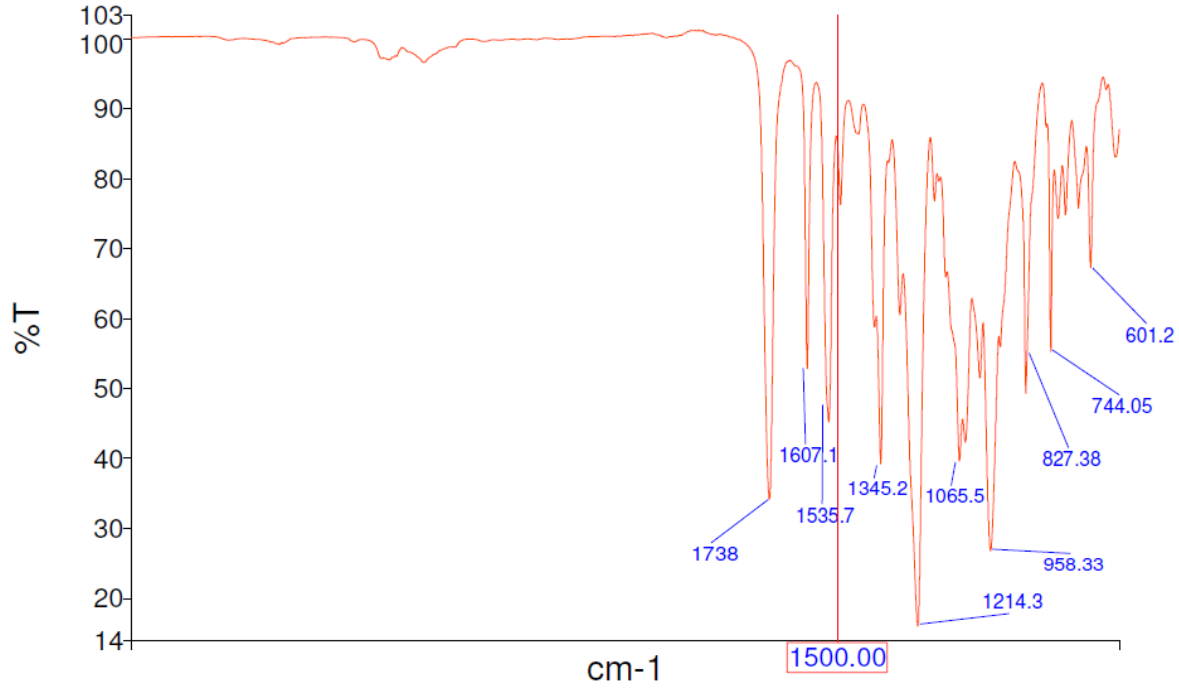
%T
cm-1
1738
1607.1
1535.7
1345.2
1065.5
1214.3
958.33
827.38
744.05
601.2
1500.00

VI.2.9 1-*O*-(o,p-dinitrophenyl)-2-deoxy-2-fluoro-β-D-galactofuranose

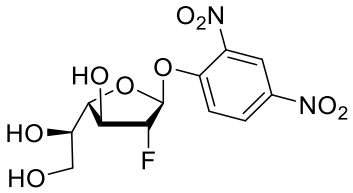

In a dried flask, 1-*O*-(o,p-dinitrophenyl)-3,5,6-tri-*O*-acetyl-2-deoxy-2-fluoro-D-galactofuranose (185 mg, 0.39 mmol, 1 eq.) was dissolved in anhydrous MeOH (16.9 mL) under argon atmosphere. After cooling of the solution to 0 °C, acetyl chloride (1.32 mL, 18.6 mmol, 47.6 eq.) was added dropwise and the reaction was left under stirring for 8 hours at 0 °C and then one night at 4 °C. TLC showed total consumption of the starting material (R_f: 0.84) and apparition of only one product (R_f: 0.30). A short silica column (MeOH/$CHCl_3$ (1:9)) afforded a yellow syrup (70 % yield).

- **Formula :** $C_{12}H_{13}FN_2O_9$
- **Molecular weight :** 348.24 g/mol
- **R_f :** 0.30 (MeOH/$CHCl_3$ 1:9)
- **Aspect :** Yellow syrup
- **^{1}H NMR** (500 MHz, CD_3OD) : δ 8.76 (d, *J* = 2.8 Hz, 1H, H-m'), 8.49 (dd, *J* = 9.3, 2.8 Hz, 1H, H-m), 7.68 (d, *J* = 9.3 Hz, 1H, H-o), 6.15 (dt, *J* = 11.6, 1.0 Hz, 1H, H-1), 5.18 (ddd, *J* = 51.8, 3.3, 1.1 Hz, 1H, H-2), 4.47 (dddd, *J* = 25.9, 7.4, 3.3, 0.8 Hz, 1H, H-3), 4.16 (dd, *J* = 7.5, 3.2 Hz, 1H, H-4), 3.77 (td, *J* = 6.4, 3.2 Hz, 1H, H-5), 3.64 – 3.55 (m, 2H, H-6 + H-6').
- **^{13}C NMR** (126 MHz, CD_3OD) : δ 154.94 (C-i), 142.85 (C-p), 141.43 (C-o'), 129.68 (C-m), 122.37 (C-m'), 119.42 (C-o), 106.22 (d, *J* = 39.1 Hz, C-1), 103.45 (d, *J* = 184.3 Hz, C-2), 85.74 (d, *J* = 5.7 Hz, C-4), 76.25 (d, *J* = 25.7 Hz, C-3), 71.48 (C-5), 64.00 (C-6).
- **^{19}F NMR** (471 MHz, CD_3OD) : δ -193.52 (ddd, *J* = 51.8, 25.9, 11.6 Hz, F_β).
- **FTIR** :
  - 1529.8 cm^{-1} (N-O assymetrical stretching)
  - 1345.2 cm^{-1} (N-O symmetrical stretching)
- **HRMS (ESI) :** *m/*z Calculated for $C_{12}H_{13}FN_2O_9$ $[M+Na]^+$: 371.0497; found : 371.0496; δ = 0.4 ppm

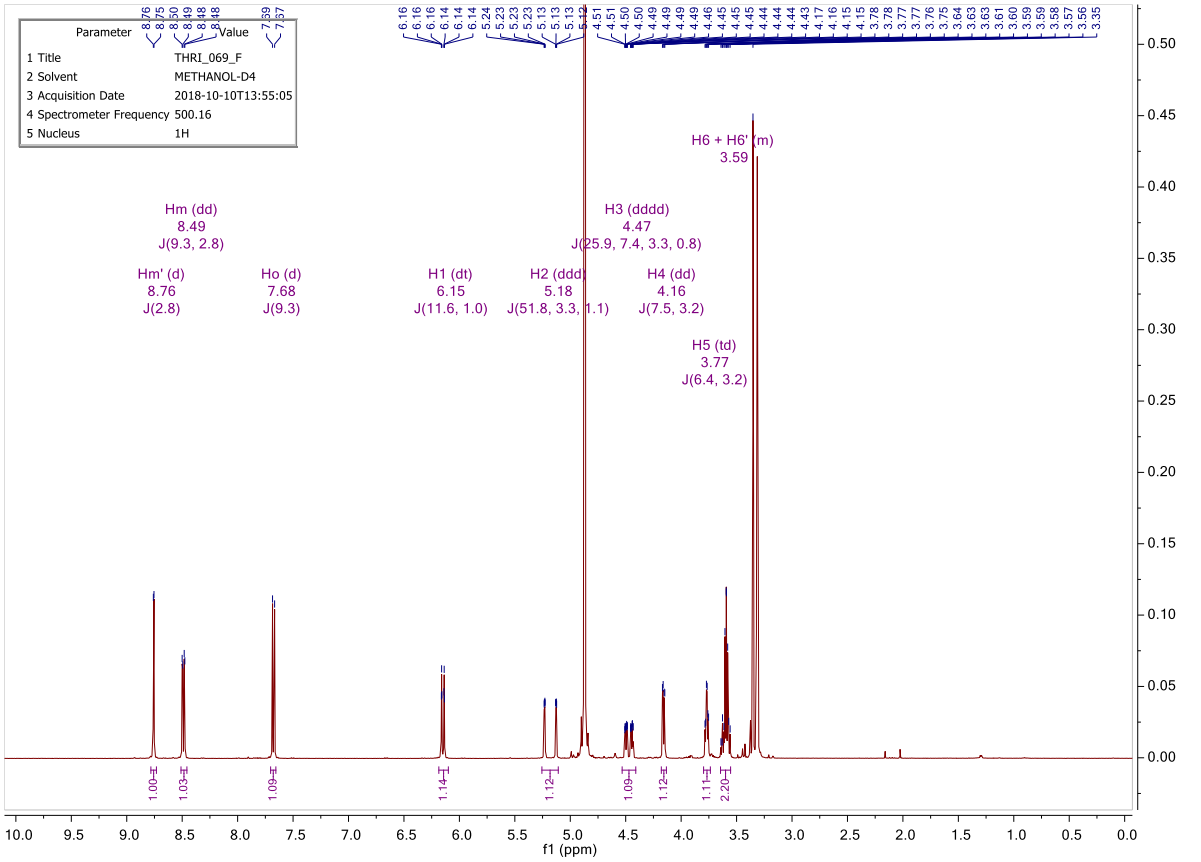
Parameter Value
1 Title THRI_069_F
2 Solvent METHANOL-D4
3 Acquisition Date 2018-10-10T13:55:05
4 Spectrometer Frequency 500.16
5 Nucleus 1H
Hm (dd)
8.49
J(9.3, 2.8)
Hm' (d)
8.76
J(2.8)
Ho (d)
7.68
J(9.3)
H1 (dt)
6.15
J(11.6, 1.0)
H2 (ddd)
5.18
J(51.8, 3.3, 1.1)
H3 (dddd)
4.47
J(25.9, 7.4, 3.3, 0.8)
H4 (dd)
4.16
J(7.5, 3.2)
H5 (td)
3.77
J(6.4, 3.2)
H6 + H6' (m)
3.59
f1 (ppm)

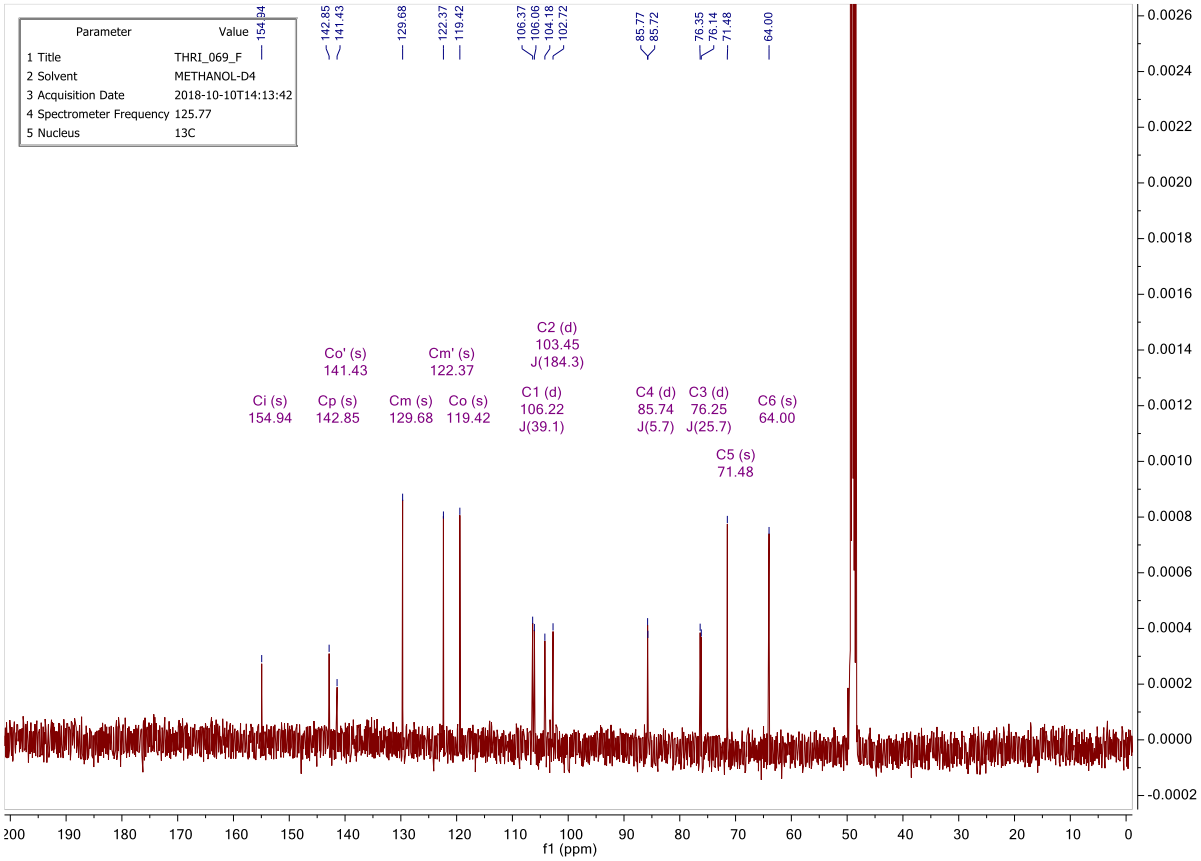
Parameter Value
1 Title THRI_069_F
2 Solvent METHANOL-D4
3 Acquisition Date 2018-10-10T14:13:42
4 Spectrometer Frequency 125.77
5 Nucleus 13C
Ci (s)
154.94
Cp (s)
142.85
Co' (s)
141.43
Cm (s)
129.68
Co (s)
119.42
Cm' (s)
122.37
C1 (d)
106.22
J(39.1)
C2 (d)
103.45
J(184.3)
C4 (d)
85.74
J(5.7)
C3 (d)
76.25
J(25.7)
C5 (s)
71.48
C6 (s)
64.00
f1 (ppm)

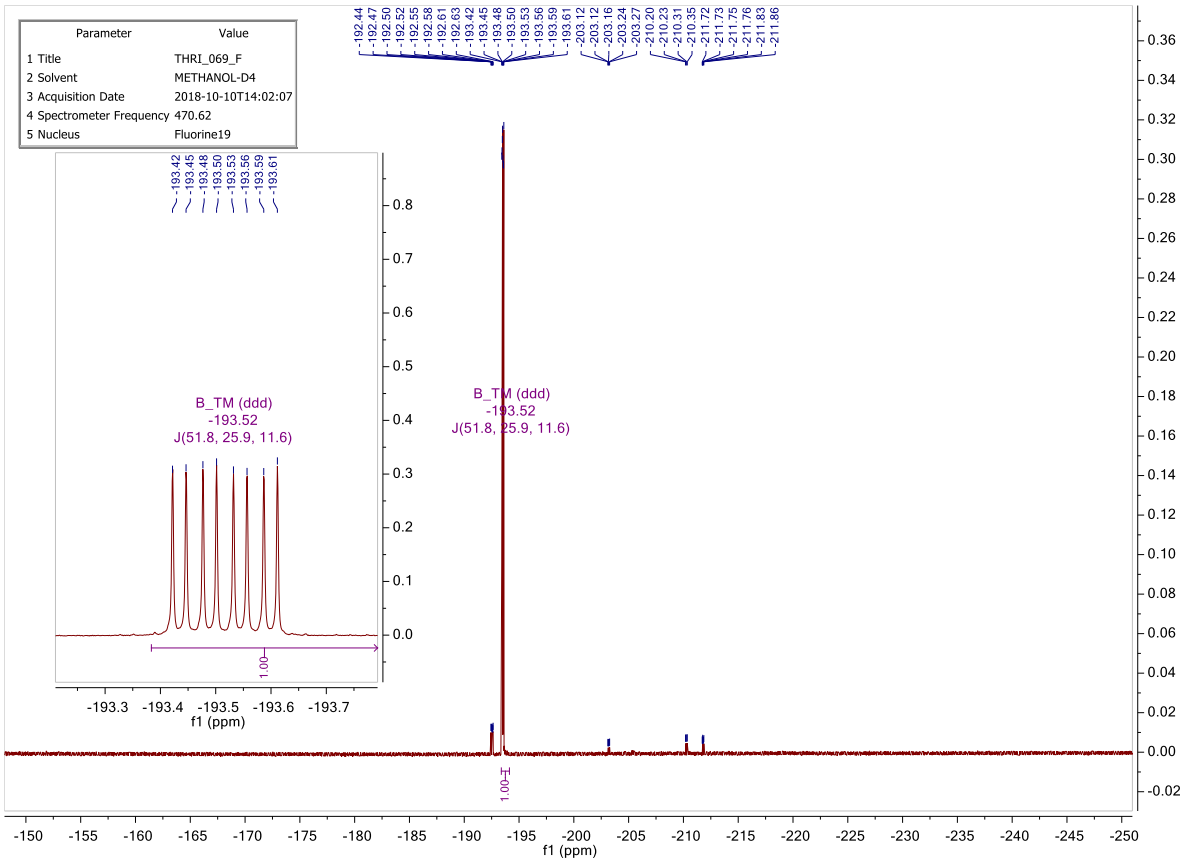
Parameter Value
1 Title THRI_069_F
2 Solvent METHANOL-D4
3 Acquisition Date 2018-10-10T14:02:07
4 Spectrometer Frequency 470.62
5 Nucleus Fluorine19
B_TM (ddd)
-193.52
J(51.8, 25.9, 11.6)
f1 (ppm)

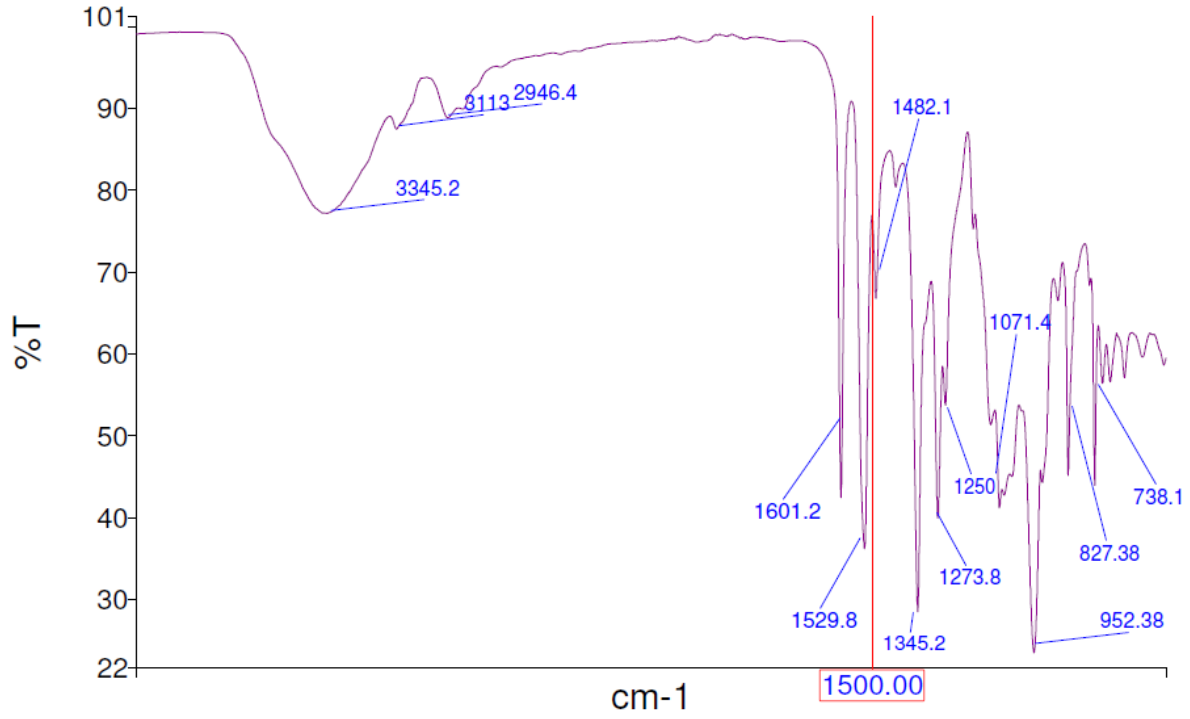
%T
cm-1
3345.2
3113
2946.4
1482.1
1071.4
1601.2
1250
738.1
827.38
1273.8
1529.8
1345.2
952.38
1500.00

VI.2.10 1-*O*-(o,p-dinitrophenyl)-2-deoxy-2-fluoro-α-D-galactofuranose

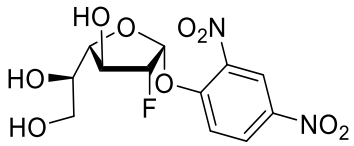

In a dried flask, 1-*O*-(o,p-dinitrophenyl)-3,5,6-tri-*O*-acetyl-2-deoxy-2-fluoro-D-galactofuranose (166 mg, 0.35 mmol, 1 eq.) was dissolved in anhydrous MeOH (15.2 mL) under argon atmosphere. After cooling of the solution to 0 °C, acetyl chloride (1.19 mL, 16.6 mmol, 47.6 eq.) was added dropwise and the reaction was left under stirring for 8 hours at 0 °C and then one night at 4 °C. TLC showed total consumption of the starting material (R_f: 0.69) and apparition of only one product (R_f: 0.27). A short silica column (MeOH/$CHCl_3$ (1:9)) afforded a yellow syrup (11 % yield).

- **Formula :** $C_{12}H_{13}FN_2O_9$
- **Molecular weight :** 348.24 g/mol
- **R_f :** 0.27 (MeOH/$CHCl_3$ 1:9)
- **Aspect :** Yellow syrup
- **^{1}H NMR** (500 MHz, CD_3OD) : δ 8.70 (d, *J* = 2.8 Hz, 1H, H-m'), 8.43 (dd, *J* = 9.3, 2.8 Hz, 1H, H-m), 7.59 (d, *J* = 9.3 Hz, 1H, H-o), 6.08 (dd, *J* = 4.2, 1.6 Hz, 1H, H-1), 5.07 (ddd, *J* = 52.4, 7.9, 4.2 Hz, 1H, H-2), 4.62 (dt, *J* = 17.1, 7.7 Hz, 1H, H-3), 3.92 (dd, *J* = 7.7, 4.6 Hz, 1H, H-4), 3.61 (dt, *J* = 6.7, 5.1 Hz, 1H, H-5), 3.52 (dd, *J* = 11.2, 5.5 Hz, 1H, H-6), 3.46 (dd, *J* = 11.2, 6.7 Hz, 1H, H-6').
- **^{13}C NMR** (126 MHz, CD_3OD) : δ 155.38 (C-i), 142.36 (C-p), 141.21 (C-p'), 129.56 (C-m), 122.28 (C-m'), 118.86 (C-o), 99.40 (d, J = 17.5 Hz, C-1), 95.88 (d, J = 202.5 Hz, C-2), 84.07 (d, J = 10.1 Hz, C-4), 72.72 (d, J = 20.9 Hz, C-3), 72.66 (C-5), 63.62 (C-6).
- **^{19}F NMR** (471 MHz, CD_3OD) : δ -210.19 (ddt, J = 52.3, 17.2, 1.9 Hz).
- **HRMS (ESI) :** *m/z* Calculated for $C_{12}H_{13}FN_2O_9$ $[M+Na]^+$: 371.0497; found : 371.0499; δ = 0.3 ppm

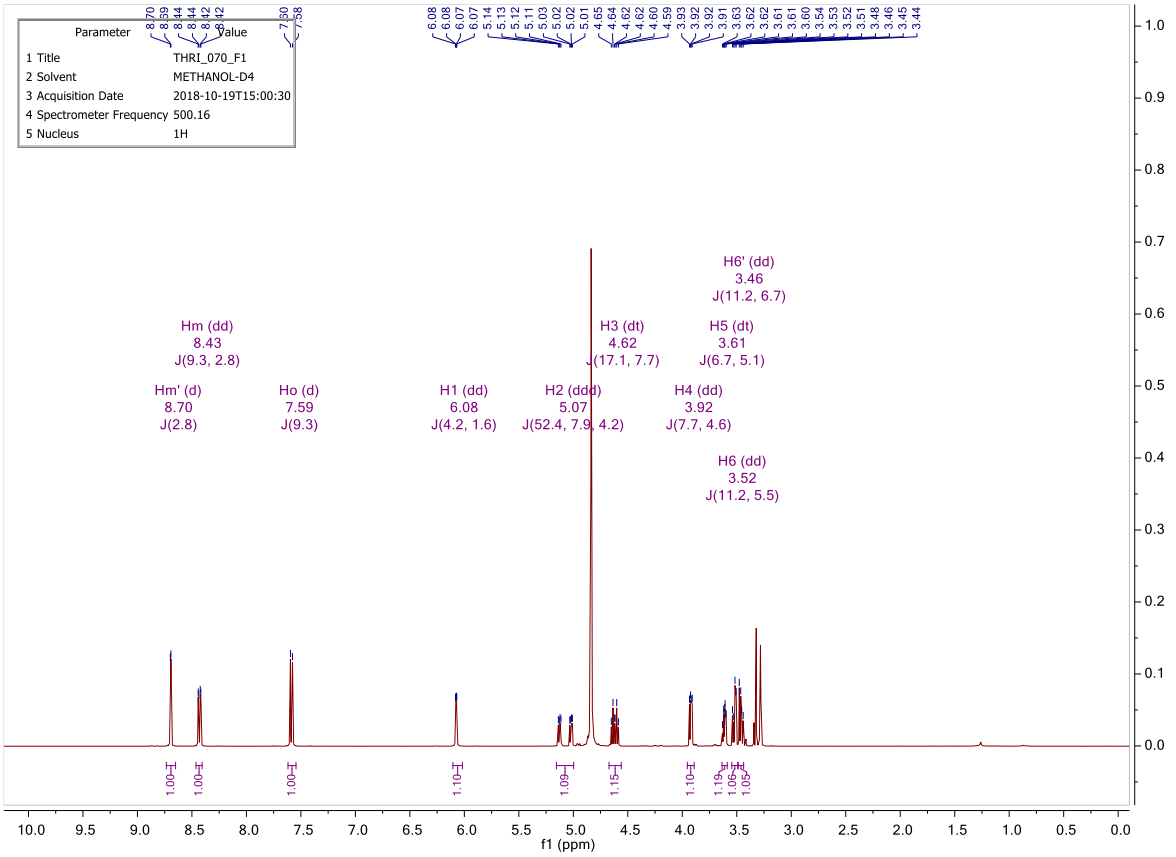
Parameter Value
1 Title THRI_070_F1
2 Solvent METHANOL-D4
3 Acquisition Date 2018-10-19T15:00:30
4 Spectrometer Frequency 500.16
5 Nucleus 1H
Hm (dd)
8.43
J(9.3, 2.8)
Hm' (d)
8.70
J(2.8)
Ho (d)
7.59
J(9.3)
H1 (dd)
6.08
J(4.2, 1.6)
H2 (ddd)
5.07
J(52.4, 7.9, 4.2)
H3 (dt)
4.62
J(17.1, 7.7)
H4 (dd)
3.92
J(7.7, 4.6)
H5 (dt)
3.61
J(6.7, 5.1)
H6' (dd)
3.46
J(11.2, 6.7)
H6 (dd)
3.52
J(11.2, 5.5)
f1 (ppm)

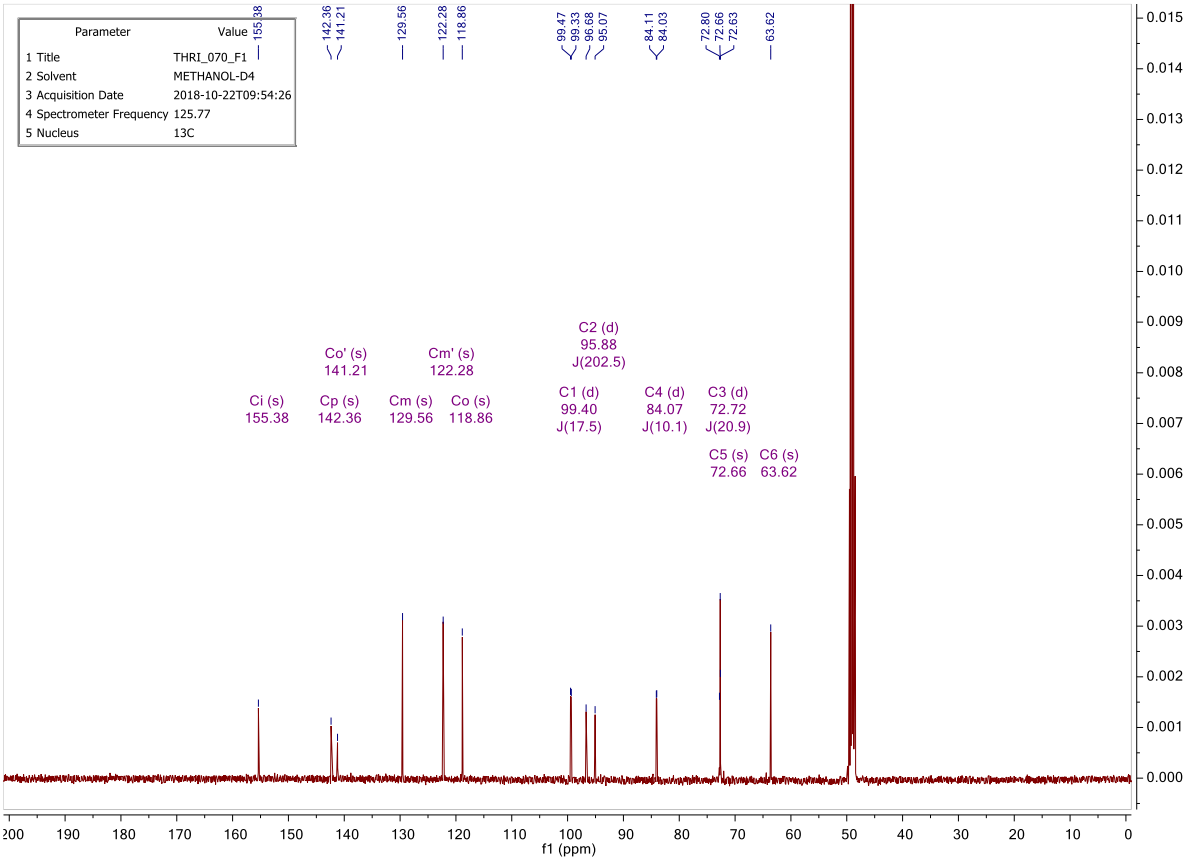
Parameter Value
1 Title THRI_070_F1
2 Solvent METHANOL-D4
3 Acquisition Date 2018-10-22T09:54:26
4 Spectrometer Frequency 125.77
5 Nucleus 13C
Ci (s)
155.38
Cp (s)
142.36
Co' (s)
141.21
Cm (s)
129.56
Cm' (s)
122.28
Co (s)
118.86
C1 (d)
99.40
J(17.5)
C2 (d)
95.88
J(202.5)
C4 (d)
84.07
J(10.1)
C3 (d)
72.72
J(20.9)
C5 (s)
72.66
C6 (s)
63.62
f1 (ppm)

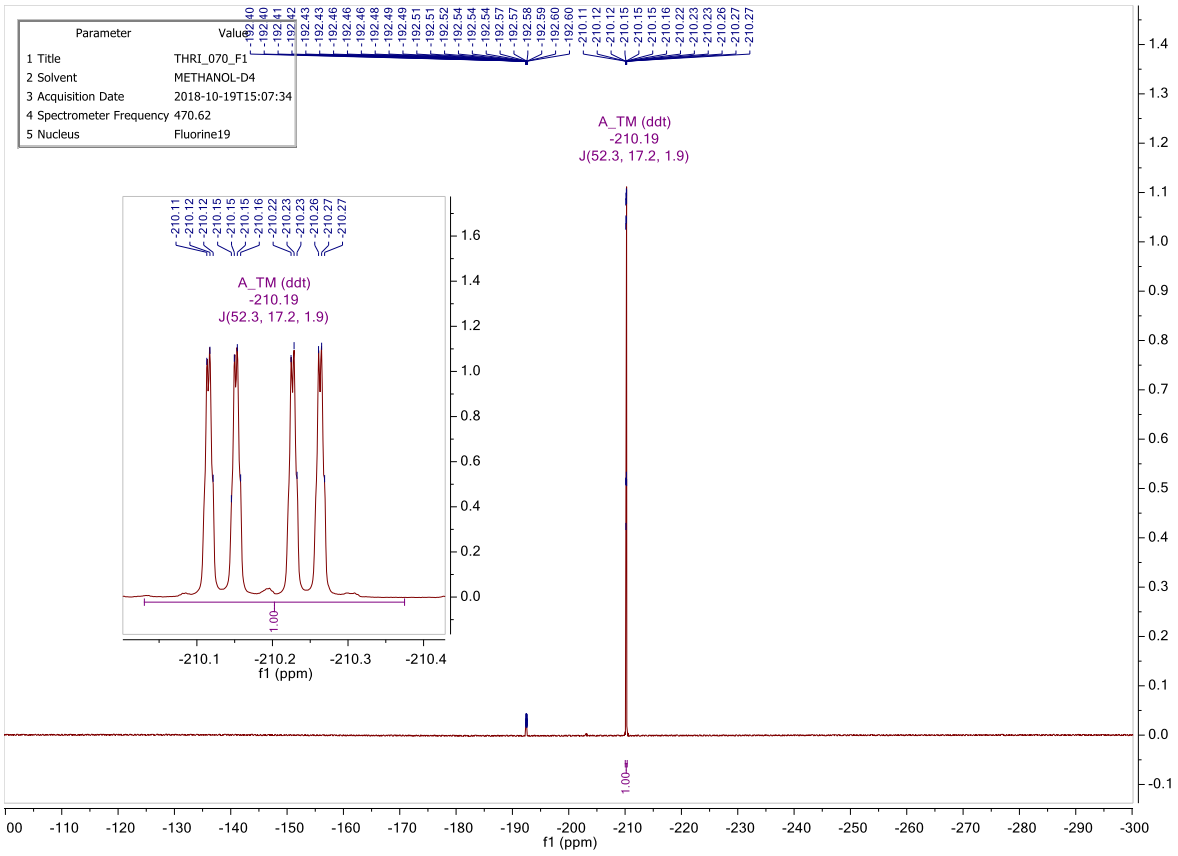
Parameter Value
1 Title THRI_070_F1
2 Solvent METHANOL-D4
3 Acquisition Date 2018-10-19T15:07:34
4 Spectrometer Frequency 470.62
5 Nucleus Fluorine19
A_TM (ddt)
-210.19
J(52.3, 17.2, 1.9)
1.00
f1 (ppm)

VI.2.11 3,4,6-tri-*O*-acetyl-2-deoxy-2-fluoro-α-D-galactopyranosyl bromide

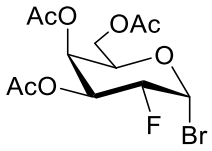

In a dried flask, per-*O*-acetyl-D-galactal (5.30 g, 19.5 mmol, 1 eq.) was dissolved in dry CH_3NO_2 (145 mL) under argon atmosphere. Selectfluor® (10.34 g, 29.2 mmol, 1.5 eq.) was added to the solution and the mixture was left under stirring overnight at room temperature. Then anhydrous $MgBr_2$ (7.17 g, 38.9 mmol, 2 eq.) was added to the mixture which was heated to reflux for 30 minutes. After addition, the reaction mixture had taken a yellow color. Once the reaction had cooled down to room temperature, the crude was treated with brine (200 mL) and the aqueous phase was extracted with EtOAc (2 X 150 mL). The organic phases were combined, dried over $MgSO_4$, filtrated and concentrated *in vacuo*. Purification was done with silica gel chromatography (Cyclohexane/EtOAc (6:4)) to obtain a yellow syrup (86% yield). Analytical data collaborated with those described in the literature.[60]

- **Formula :** $C_{12}H_{16}BrFO_7$
- **Molecular weight :** 371.16 g/mol
- **R_f :** 0.63 (EtOAc/Cyclohexane 1:1)
- **Aspect :** Yellow syrup
- **^{1}H NMR** (500 MHz, $CDCl_3$) : δ 6.61 (ddd, *J* = 4.2, 1.1, 0.6 Hz, 1H, H-1), 5.53 (td, *J* = 3.4, 1.4 Hz, 1H, H-4), 5.47 (td, *J* = 10.0, 3.5 Hz, 1H, H-3), 4.76 (ddd, *J* = 50.1, 10.0, 4.2 Hz, 1H, H-2), 4.51 (tdd, *J* = 6.4, 1.4, 0.7 Hz, 1H, H-5), 4.17 (dd, *J* = 11.5, 6.3 Hz, 1H, H-6), 4.11 (dd, *J* = 12.2, 6.1 Hz, 1H, H-6'), 2.14 (s, 3H, Ac), 2.06 (s, 3H, Ac), 2.05 (s, 3H, Ac).
- **^{13}C NMR** (126 MHz, $CDCl_3$) : δ 170.45 (Ac), 169.87 (Ac), 169.84 (Ac), 86.92 (d, *J* = 25.4 Hz, C-1), 84.29 (d, *J* = 195.2 Hz, C-2), 71.34 (C-5), 69.06 (d, *J* = 18.0 Hz, C-3), 67.59 (d, *J* = 7.6 Hz, C-4), 60.76 (C-6), 20.75 (Ac), 20.69 (Ac), 20.62 (Ac).
- **^{19}F NMR** (471 MHz, $CDCl_3$) : δ -194.84 (dddd, *J* = 50.2, 10.2, 3.4, 1.2 Hz, F_α).

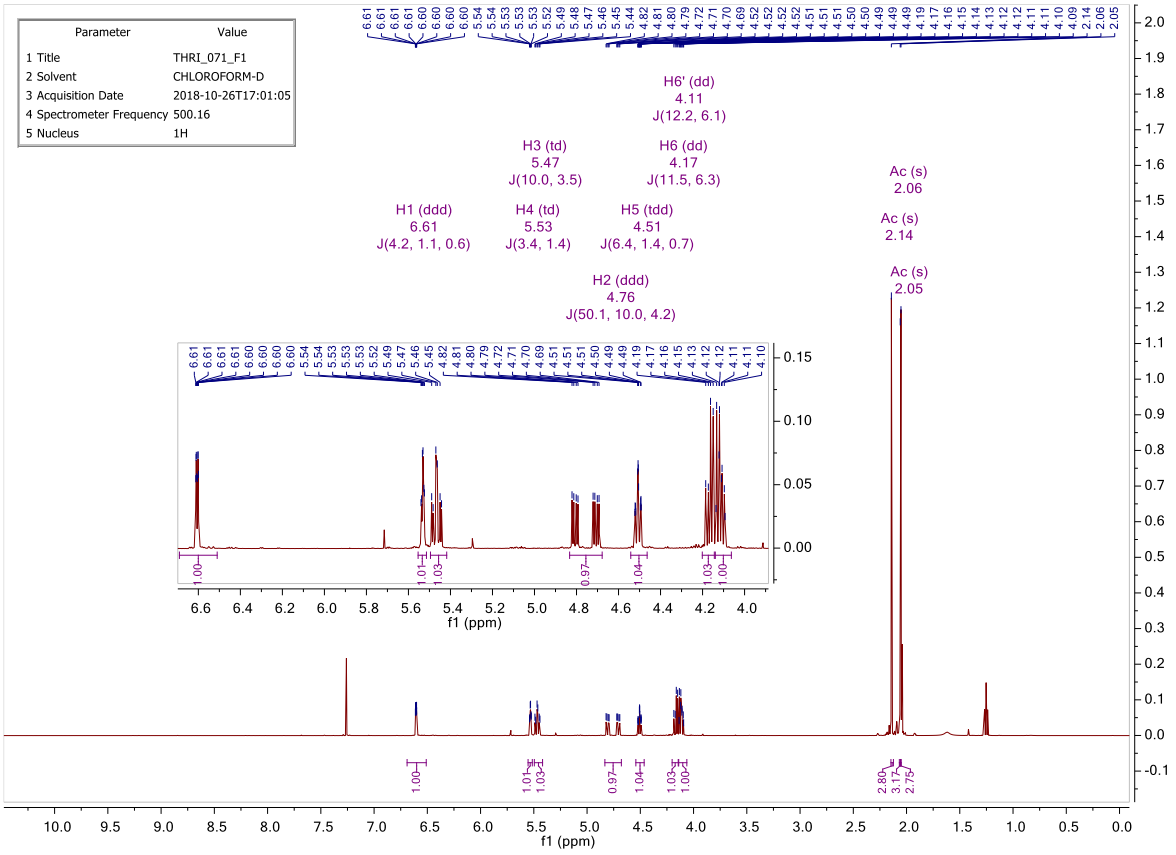
Parameter Value
1 Title THRI_071_F1
2 Solvent CHLOROFORM-D
3 Acquisition Date 2018-10-26T17:01:05
4 Spectrometer Frequency 500.16
5 Nucleus 1H
H6' (dd)
4.11
J(12.2, 6.1)
H3 (td)
5.47
J(10.0, 3.5)
H6 (dd)
4.17
J(11.5, 6.3)
Ac (s)
2.06
Ac (s)
2.14
H1 (ddd)
6.61
J(4.2, 1.1, 0.6)
H4 (td)
5.53
J(3.4, 1.4)
H5 (tdd)
4.51
J(6.4, 1.4, 0.7)
Ac (s)
2.05
H2 (ddd)
4.76
J(50.1, 10.0, 4.2)
f1 (ppm)

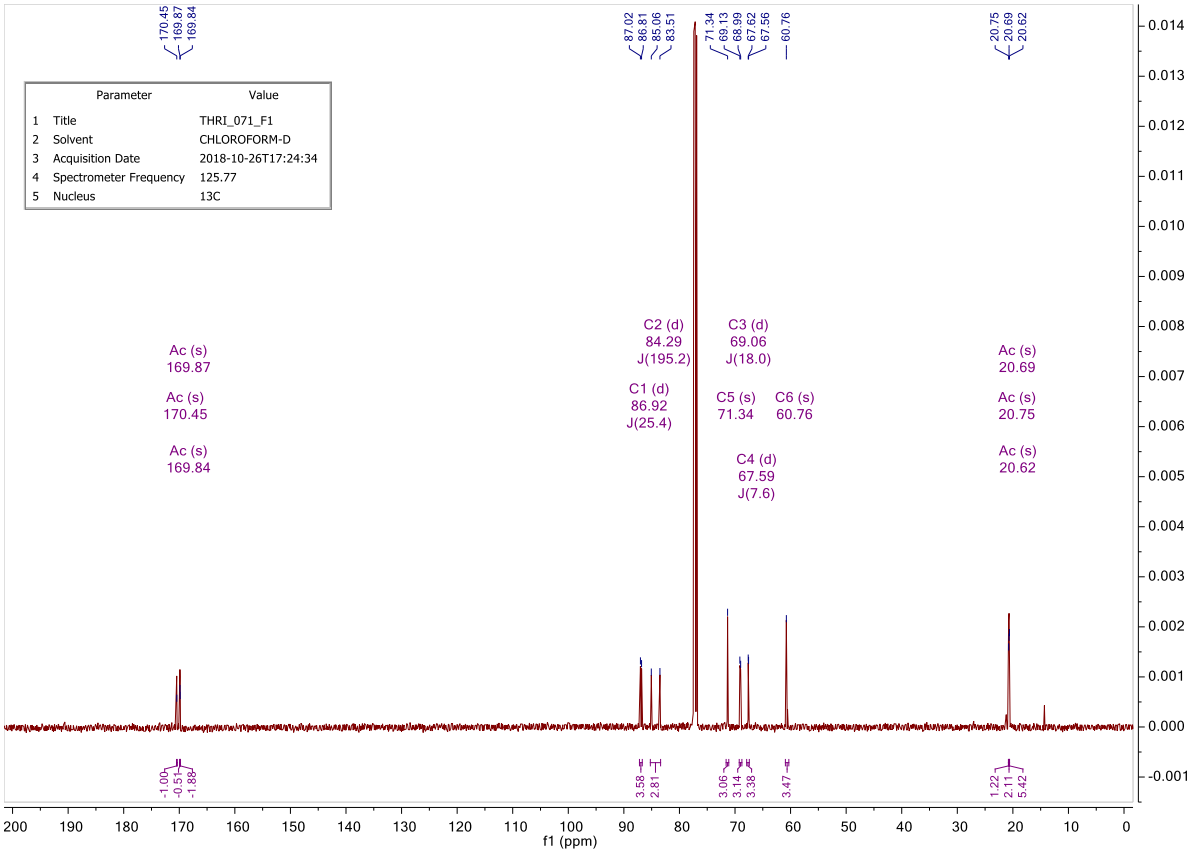
Parameter Value
1 Title THRI_071_F1
2 Solvent CHLOROFORM-D
3 Acquisition Date 2018-10-26T17:24:34
4 Spectrometer Frequency 125.77
5 Nucleus 13C
Ac (s)
169.87
Ac (s)
170.45
Ac (s)
169.84
C2 (d)
84.29
J(195.2)
C3 (d)
69.06
J(18.0)
C1 (d)
86.92
J(25.4)
C5 (s)
71.34
C6 (s)
60.76
C4 (d)
67.59
J(7.6)
Ac (s)
20.69
Ac (s)
20.75
Ac (s)
20.62
f1 (ppm)

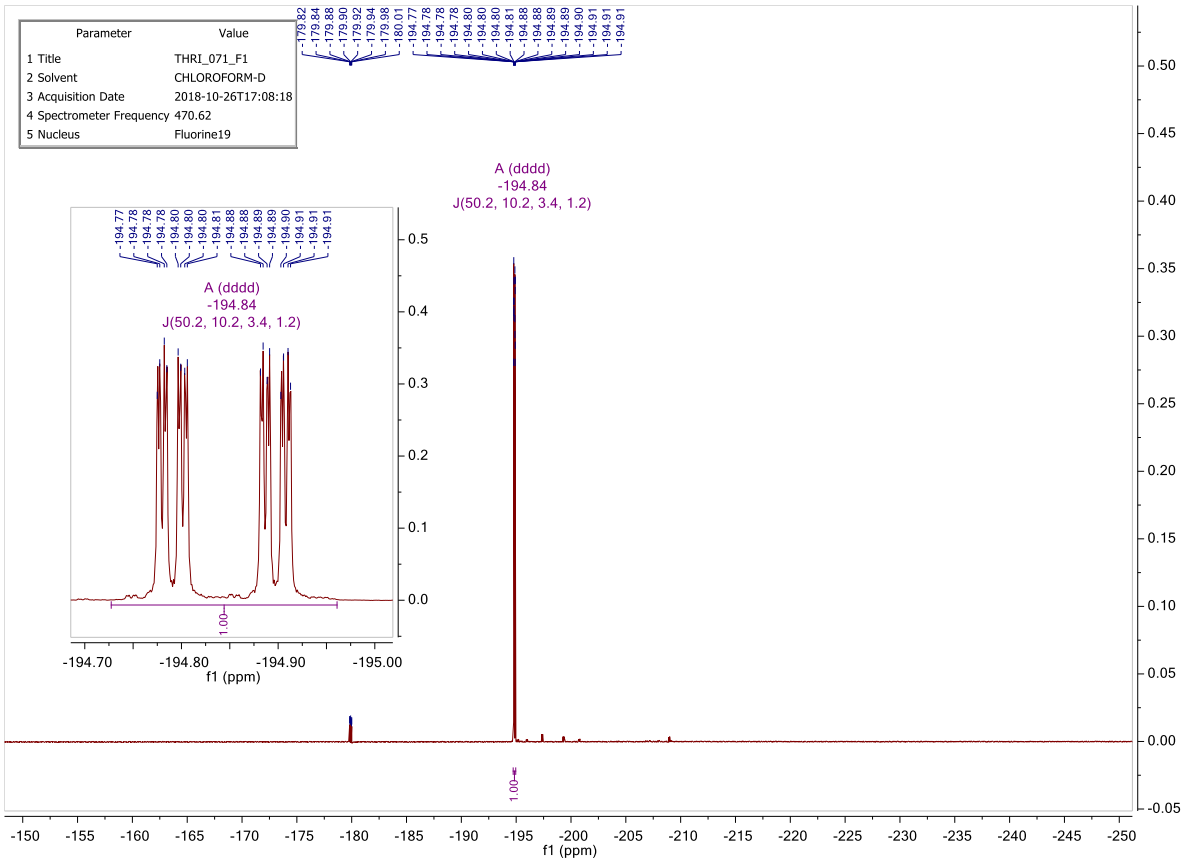
Parameter Value
1 Title THRI_071_F1
2 Solvent CHLOROFORM-D
3 Acquisition Date 2018-10-26T17:08:18
4 Spectrometer Frequency 470.62
5 Nucleus Fluorine19
A (dddd)
-194.84
J(50.2, 10.2, 3.4, 1.2)
1.00
f1 (ppm)

VI.2.12 3,4,6-tri-*O*-acetyl-2-deoxy-2-fluoro-D-galactal

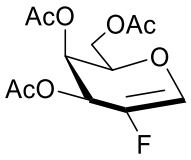

In a dried flask, 3,4,6-tri-*O*-acetyl-2-deoxy-2-fluoro-α-D-galactopyranosyl bromide (6.190 g, 16.68 mmol, 1 eq.) was dissolved in dry acetonitrile (56 mL) under argon atmosphere. Distilled Et_3N (6.97 mL, 50.03 mmol, 3.0 eq.) was added dropwise to the solution under stirring at room temperature. Then the temperature of the reaction was adjusted to reflux for 2 hours. The reaction was quenched by careful addition of HCl 1M (50 mL) at 0°C. Then the mixture was diluted with EtOAc (50 mL) and the aqueous phase was extracted with EtOAc (50 mL). The organic phases were combined, dried over $MgSO_4$, filtrated and concentrated *in vacuo*. Purification was done with silica gel chromatography (Cyclohexane/EtOAc (6:4)) to obtain a yellow syrup (68 % yield). Analytical data collaborated with those described in the literature.[53]

- **Formula :** $C_{12}H_{15}FO_7$
- **Molecular weight :** 290.24 g/mol
- **R_f :** 0.69 (EtOAc/Cyclohexane 1:1)
- **Aspect :** Yellow syrup
- **^{1}H NMR** (500 MHz, $CDCl_3$) : δ 6.75 (dd, *J* = 4.7, 1.2 Hz, 1H, H-1), 5.87 (dq, *J* = 5.0, 1.1 Hz, 1H, H-3), 5.44 (ddd, *J* = 5.0, 3.6, 2.4 Hz, 1H, H-4), 4.32 (dd, *J* = 11.3, 7.6 Hz, 1H, H-6), 4.27 – 4.23 (m, 1H, H-5), 4.19 (dd, *J* = 11.3, 4.5 Hz, 1H, H6'), 2.13 (s, 3H, Ac), 2.09 (s, 3H, Ac), 2.08 (s, 3H, Ac).
- **^{13}C NMR** (126 MHz, $CDCl_3$) : δ 170.68 (Ac), 170.20 (Ac), 169.95 (Ac), 142.78 (d, *J* = 244.2 Hz, C-2), 132.52 (d, *J* = 40.5 Hz, C-1), 76.91 (C-5), 64.28 (d, *J* = 6.8 Hz, C-4), 62.88 (d, *J* = 21.6 Hz, C-3), 61.16 (C-6), 20.88 (Ac), 20.68 (Ac), 20.66 (Ac).
- **^{19}F NMR** (471 MHz, $CDCl_3$) : δ -168.04 (s).

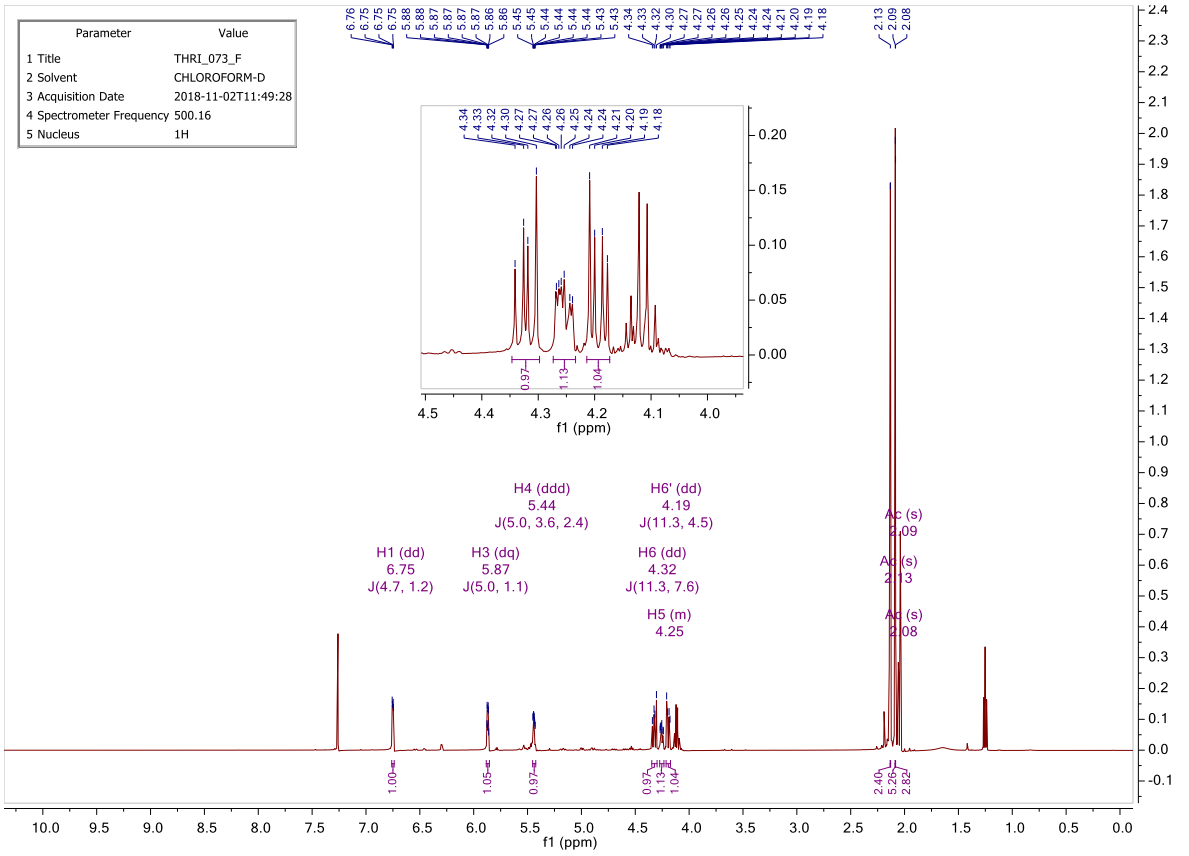
Parameter Value
1 Title THRI_073_F
2 Solvent CHLOROFORM-D
3 Acquisition Date 2018-11-02T11:49:28
4 Spectrometer Frequency 500.16
5 Nucleus 1H
H4 (ddd)
5.44
J(5.0, 3.6, 2.4)
H6' (dd)
4.19
J(11.3, 4.5)
H1 (dd)
6.75
J(4.7, 1.2)
H3 (dq)
5.87
J(5.0, 1.1)
H6 (dd)
4.32
J(11.3, 7.6)
H5 (m)
4.25
Ac (s)
2.09
Ac (s)
2.13
Ac (s)
2.08
f1 (ppm)

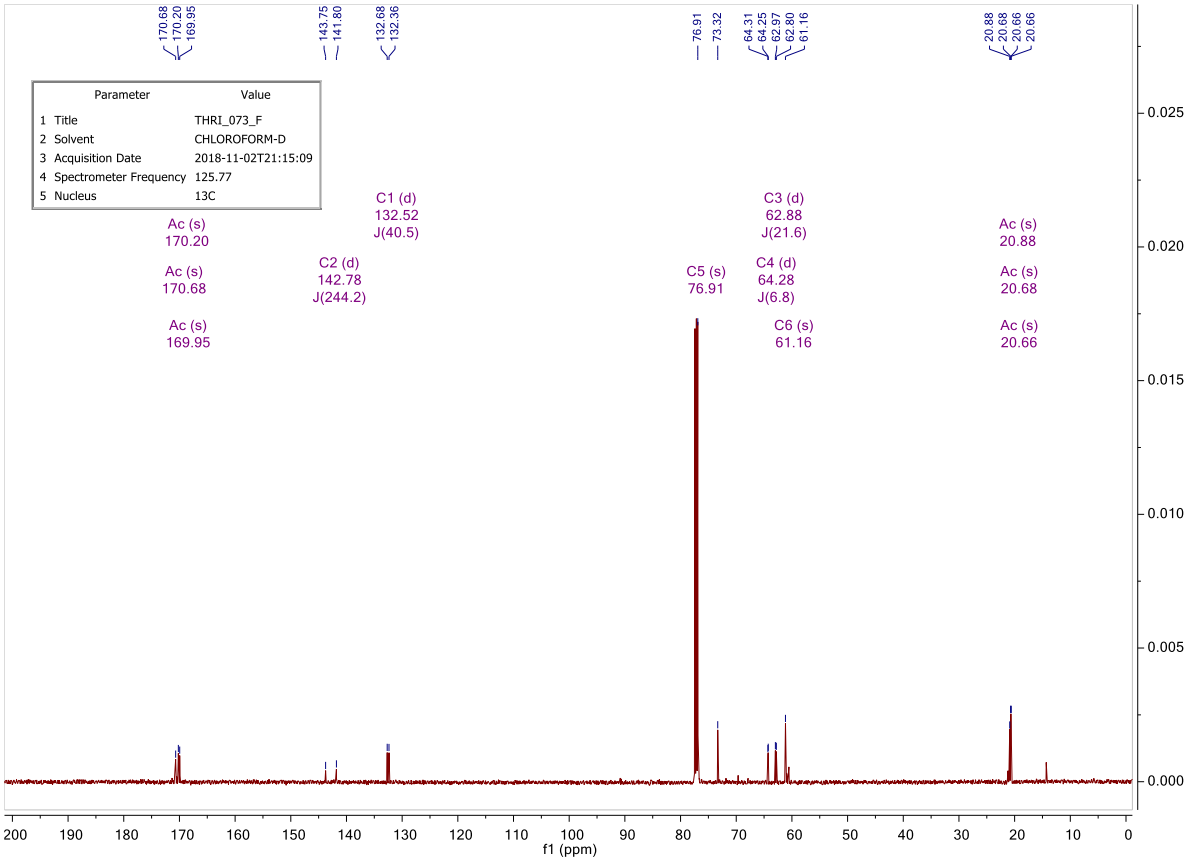
Parameter Value
1 Title THRI_073_F
2 Solvent CHLOROFORM-D
3 Acquisition Date 2018-11-02T21:15:09
4 Spectrometer Frequency 125.77
5 Nucleus 13C
Ac (s)
170.20
Ac (s)
170.68
Ac (s)
169.95
C1 (d)
132.52
J(40.5)
C2 (d)
142.78
J(244.2)
C5 (s)
76.91
C3 (d)
62.88
J(21.6)
C4 (d)
64.28
J(6.8)
C6 (s)
61.16
Ac (s)
20.88
Ac (s)
20.68
Ac (s)
20.66
f1 (ppm)

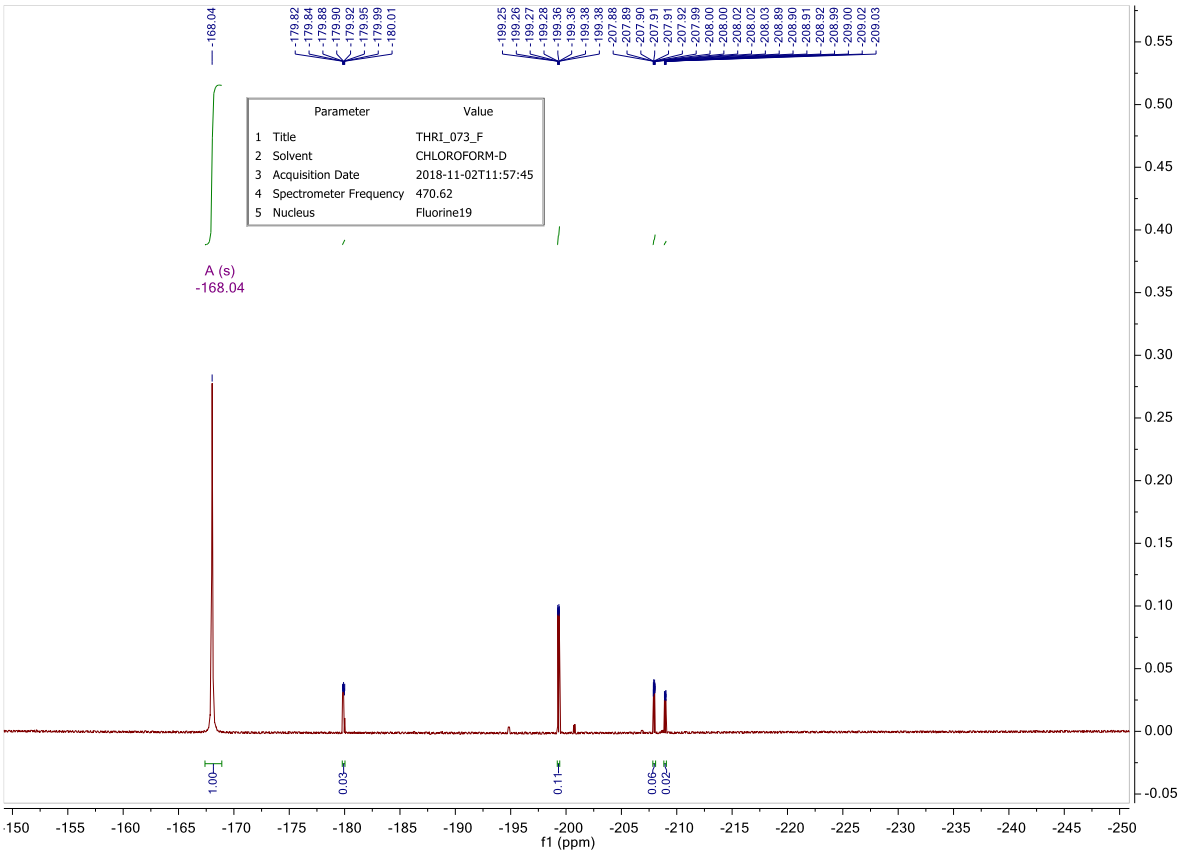
-168.04
-179.82
-179.84
-179.88
-179.90
-179.92
-179.95
-179.99
-180.01
-199.25
-199.26
-199.27
-199.28
-199.36
-199.36
-199.38
-199.38
-207.88
-207.89
-207.90
-207.91
-207.91
-207.92
-207.99
-208.00
-208.00
-208.02
-208.02
-208.03
-208.89
-208.90
-208.91
-208.92
-208.99
-209.00
-209.02
-209.03
Parameter Value
1 Title THRI_073_F
2 Solvent CHLOROFORM-D
3 Acquisition Date 2018-11-02T11:57:45
4 Spectrometer Frequency 470.62
5 Nucleus Fluorine19
A (s)
-168.04
1.00
0.03
0.11
0.06
0.02
f1 (ppm)

VI.2.13 3,4,6-tri-*O*-acetyl-2-deoxy-2-fluoro-α-D-galactopyranose

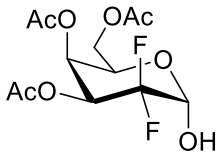

In a dried flask, 3,4,6-tri-*O*-acetyl-2-deoxy-2-fluoro-D-galactal (3.280 g, 11,3 mmol, 1 eq.) was dissolved in a 4:1 (v:v) mixture of nitromethane in water (214 mL) under argon atmosphere. Under stirring, Selectfluor® (6.005 g, 17.0 mmol, 1.5 eq.) was added to the solution which was left overnight at room temperature. The following day, the mixture was heated to reflux for 30 minutes. Once it had cooled down to room temperature, the crude was poured into brine (400 mL) and the aqueous phase was extracted with EtOAc (2 x 400 mL). The organic phases were combined, dried over $MgSO_4$, filtrated and concentrated *in vacuo*. Purification was performed by silica gel chromatography (EtOAc/Cyclohexane 1:1) to obtain a colorless syrup (33 % yield). Analytical data collaborated with those described in the literature.[53]

- **Formula :** $C_{12}H_{16}F_2O_8$
- **Molecular weight :** 326.25 g/mol
- **R_f :** 0.61 (EtOAc/Cyclohexane 1:1)
- **Aspect :** Colorless syrup
- **^{1}H NMR** (500 MHz, $CDCl_3$) : δ 5.51 – 5.43 (m, 2H, H-3 + H-4), 5.30 (dd, *J* = 5.0, 1.8 Hz, 1H, H-1), 4.57 (td, *J* = 6.6, 1.0 Hz, 1H, H-5), 4.17 (d, *J* = 1.4 Hz, 1H, H-6), 4.16 (d, *J* = 1.7 Hz, 1H, H-6'), 2.15 (s, 3H, Ac), 2.10 (s, 3H, Ac), 2.06 (s, 3H, Ac).
- **^{13}C NMR** (126 MHz, $CDCl_3$) : δ 170.79 (Ac), 170.64 (Ac), 169.82 (Ac), 114.32 (t, J = 252.4 Hz, C-2), 92.05 (t, J = 31.4 Hz, C-1), 67.44 (d, J = 3.8 Hz, C-4), 66.54 (C-5), 65.77 (t, J = 19.1 Hz, C-3), 61.56 (C-6), 20.80 (Ac), 20.68 (Ac), 20.53 (Ac).
- **^{19}F NMR** (471 MHz, $CDCl_3$) : δ -119.71 (dddd, *J* = 252.0, 19.6, 4.8, 1.3 Hz), -119.77 (dddt, *J* = 253.5, 41.3, 9.7, 4.0, 1.9 Hz).
- **HRMS (ESI) :** *m/*z Calculated for $C_{12}H_{16}F_2O_8$ $[M+Na]^+$: 349.0705; found : 349.0707; δ = 0.3 ppm

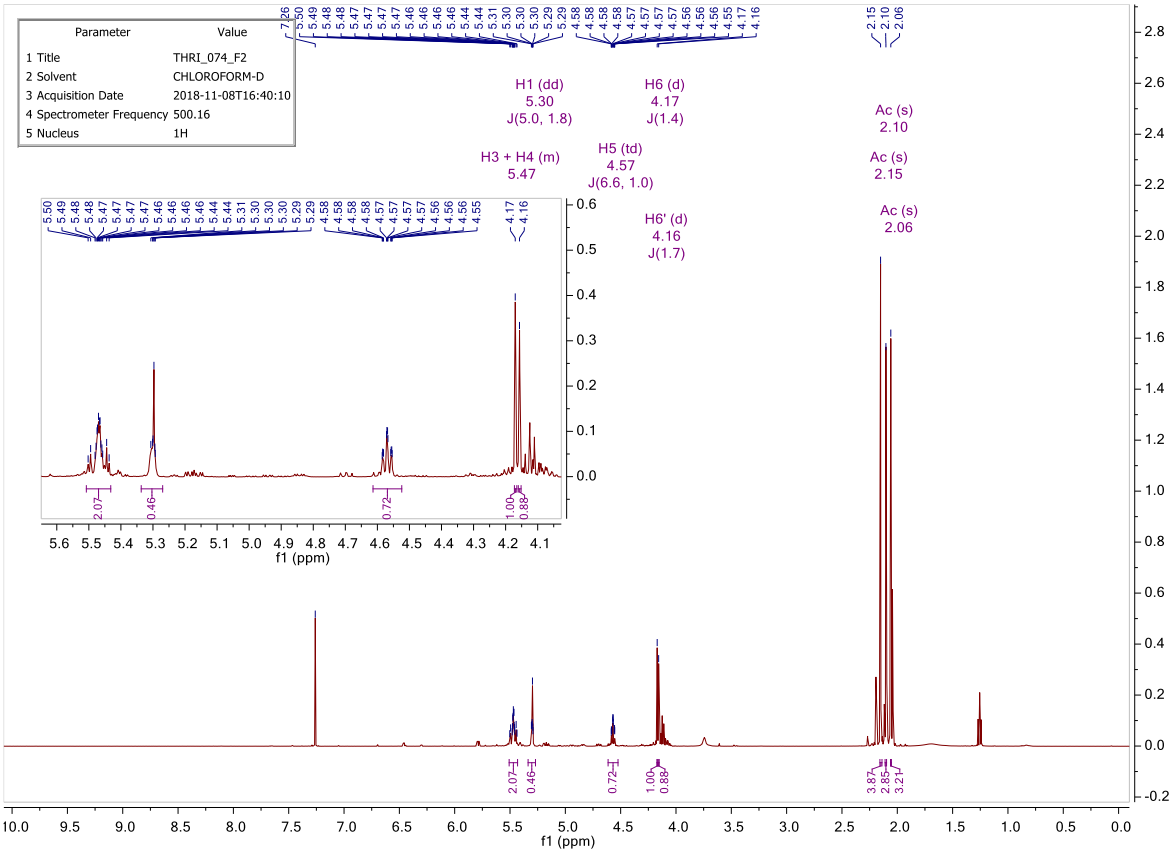
Parameter Value
1 Title THRI_074_F2
2 Solvent CHLOROFORM-D
3 Acquisition Date 2018-11-08T16:40:10
4 Spectrometer Frequency 500.16
5 Nucleus 1H
H1 (dd)
5.30
J(5.0, 1.8)
H6 (d)
4.17
J(1.4)
H3 + H4 (m)
5.47
H5 (td)
4.57
J(6.6, 1.0)
H6' (d)
4.16
J(1.7)
Ac (s)
2.10
Ac (s)
2.15
Ac (s)
2.06
f1 (ppm)

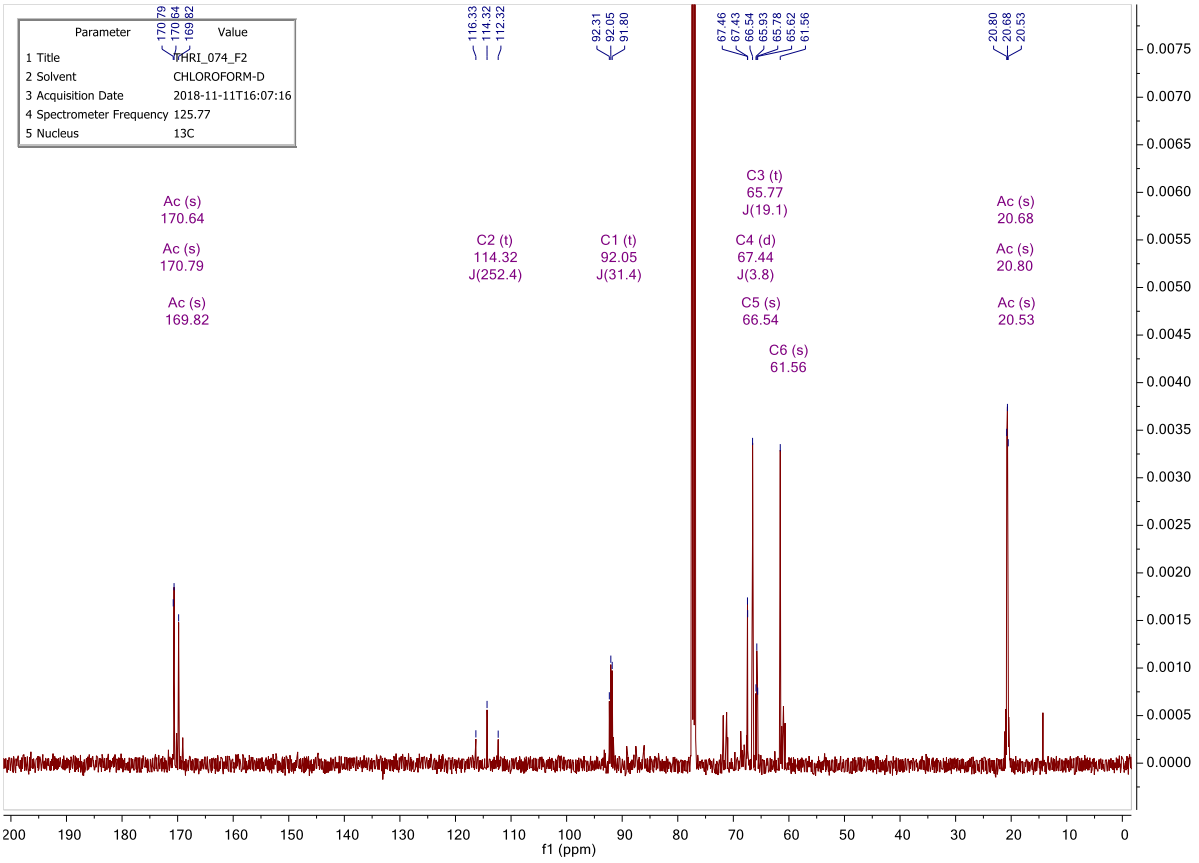
Parameter Value
1 Title THRI_074_F2
2 Solvent CHLOROFORM-D
3 Acquisition Date 2018-11-11T16:07:16
4 Spectrometer Frequency 125.77
5 Nucleus 13C
Ac (s)
170.64
Ac (s)
170.79
Ac (s)
169.82
C2 (t)
114.32
J(252.4)
C1 (t)
92.05
J(31.4)
C3 (t)
65.77
J(19.1)
C4 (d)
67.44
J(3.8)
C5 (s)
66.54
C6 (s)
61.56
Ac (s)
20.68
Ac (s)
20.80
Ac (s)
20.53
f1 (ppm)

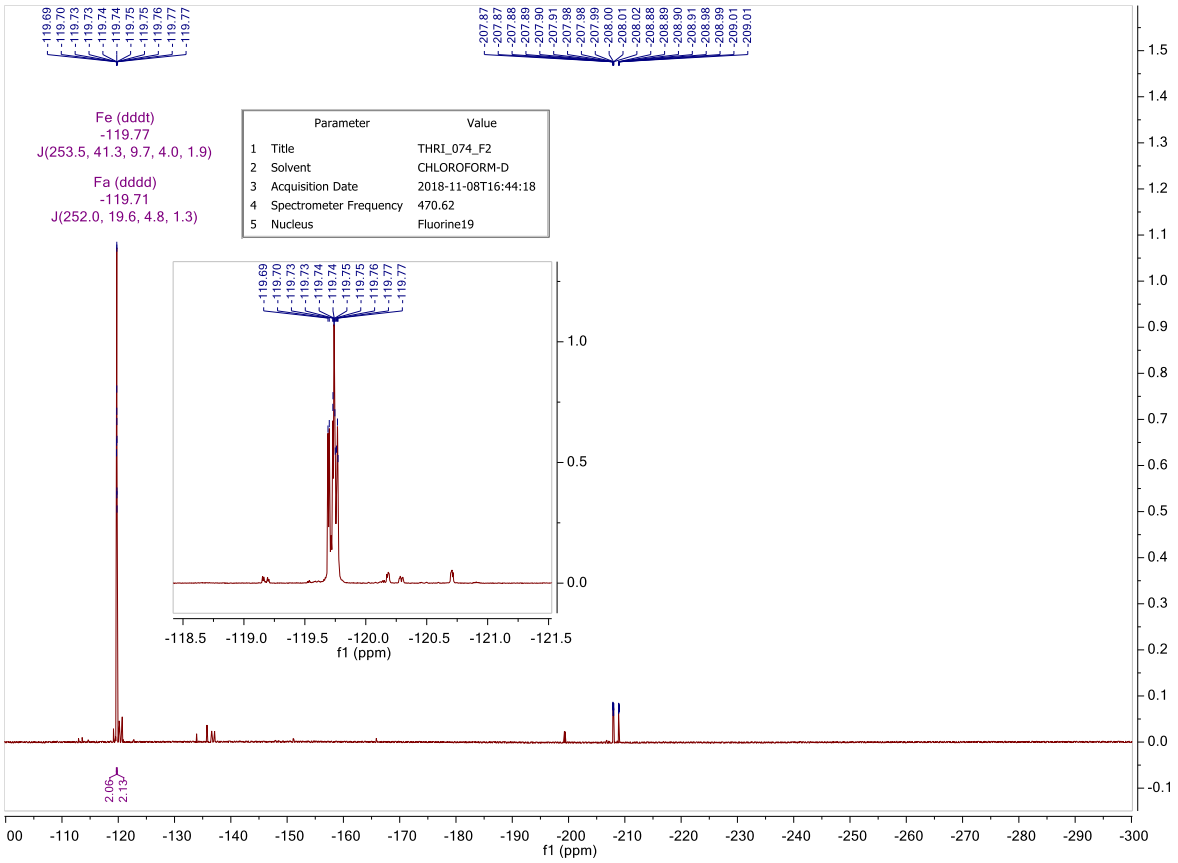
-119.69
-119.70
-119.73
-119.73
-119.74
-119.74
-119.75
-119.75
-119.76
-119.77
-119.77
-207.87
-207.87
-207.88
-207.89
-207.90
-207.91
-207.98
-207.98
-207.99
-208.00
-208.01
-208.02
-208.88
-208.89
-208.90
-208.91
-208.98
-208.99
-209.01
-209.01
Fe (dddt)
-119.77
J(253.5, 41.3, 9.7, 4.0, 1.9)
Fa (dddd)
-119.71
J(252.0, 19.6, 4.8, 1.3)
Parameter
Value
1 Title
THRI_074_F2
2 Solvent
CHLOROFORM-D
3 Acquisition Date
2018-11-08T16:44:18
4 Spectrometer Frequency
470.62
5 Nucleus
Fluorine19
f1 (ppm)
2.06
2.13
f1 (ppm)

VII. Bibliography

(1) Chiu, L. C.; Christoph, L.; Ying, Z. *Respirology* **2013**, *18* (7), 1047–1055.

(2) WHO. *Global Tuberculosis Report*; **2018**.

(3) Sandhu, G. K. *J. Glob. Infect. Dis.* **2011**, *3* (2), 143–150.

(4) Plyffer, G. E. In *Mycobacterium: General characteristics, Laboratory Detection, and staining procedures.*; Murray, P. R., Ed.; ASM Press: Washington, DC, **2007**; p 543.

(5) Ernst, J. D. *Nat. Rev. Immunol.* **2012**, *12*, 581.

(6) Nunes-Alves, C.; Booty, M. G. et al. *Nat. Rev. Microbiol.* **2014**, *12* (4), 289–299.

(7) Pieters, J. *Cell Host Microbe* **2008**, *3* (6), 399–407.

(8) Akira, S.; Uematsu, S.; Takeuchi, O. *Cell* **2006**, *124* (4), 783–801.

(9) Daffé, M. *Tuberculosis* **2015**, *95*, S155–S158.

(10) Shen, L. *Caractérisation de La Galactofuranohydrolase Rv3096 de Mycobacterium Tuberculosis*. Master thesis, Université de Lille, **2016**.

(11) Alderwick, L. J.; Harrison, J. et al. *Cold Spring Harb. Perspect. Med.* **2015**, *5* (8), 1–16.

(12) Payne, K. M.; Hatfull, G. F. *PLoS One* **2012**, *7* (3), 1–14.

(13) Brennan, P. J. *Tuberculosis* **2003**, *83* (1), 91–97.

(14) Kieser, K. J.; Rubin, E. J. *Nat. Rev. Microbiol.* **2014**, *12*, 550.

(15) Bhamidi, S.; Scherman, M. S. et al. *J. Biol. Chem.* **2011**, *286* (26), 23168–23177.

(16) Koshland, D. E. *Biol. Rev.* **1953**, *28* (4), 416–436.

(17) McCarter, J. D.; Withers, S. G. *Curr. Opin. Struct. Biol.* **1994**, *4* (6), 885–892.

(18) Ndeh, D.; Rogowski, A. et al. *Nature* **2017**, *544*, 65.

(19) Terwisscha van Scheltinga, A. C.; Armand, S. et al. *Biochemistry* **1995**, *34* (48), 15619–15623.

(20) Yip, V. L. Y.; Varrot, A. et al. *J. Am. Chem. Soc.* **2004**, *126* (27), 8354–8355.

(21) Purich, D. L. In *Enzyme Kinetics and Mechanism, Part F: Detection and Characterization of Enzyme Reaction Intermediates*; Purich, D. L., Ed.; Academic Press: Cambridge, MA, **2002**; p 501.

(22) Delbrouck, J. A.; Chêne, L. P.; Vincent, S. P. In *Fluorine in Life Sciences: Pharmaceuticals, Medicinal Diagnostics, and Agrochemicals*; Haufe, G., Leroux, F., Eds.; Academic Press: Cambridge, MA, **2018**; p 500.

(23) Collins, P. M. In *Dictionary of Carbohydrates*; CRC Press: Boca Raton, FL, **2005**; p 1282.

(24) Nyffeler, P. T.; Durón, S. G. et al. *Angew. Chemie Int. Ed.* **2004**, *44* (2), 192–212.

(25) Priebe, W.; Fokt, I.; Grynkiewicz, G. In *Glycoscience: Chemistry and Chemical Biology*;

Fraser-Reid, B. O., Tatsuta, K., Thiem, J., Eds.; Springer Berlin Heidelberg: Berlin, **2008**; p 699.

(26) Kozikowski, A. P.; Lee, J. *J. Org. Chem.* **1990**, *55* (3), 863–870.

(27) Chen, H.; Xian, T. et al. *Carbohydr. Res.* **2016**, *431*, 42–46.

(28) Vincent, S. P.; Burkart, M. D. et al. *J. Org. Chem.* **1999**, *64* (14), 5264–5279.

(29) Albert, M.; Dax, K.; Ortner, J. *Tetrahedron* **1998**, *54* (19), 4839–4848.

(30) Wang, Z. In *Comprehensive Organic Name Reactions and Reagents*; Wang, Z., Ed.; Wiley Online Library: Hoboken, NJ, **2010**; p 3123.

(31) Peltier, P.; Euzen, R. et al. *Carbohydr. Res.* **2008**, *343* (12), 1897–1923.

(32) Kashiwagi, G. A.; Mendoza, V. M. et al. *Org. Biomol. Chem.* **2012**, *10* (31), 6322–6332.

(33) Cattiaux, L.; Sendid, B. et al. *Bioorg. Med. Chem.* **2011**, *19* (1), 547–555.

(34) Baldoni, L.; Marino, C. *J. Org. Chem.* **2009**, *74* (5), 1994–2003.

(35) Zhang, Q.; Liu, H. *J. Am. Chem. Soc.* **2001**, *123* (28), 6756–6766.

(36) Bordoni, A.; de Lederkremer, R. M.; Marino, C. *Bioorg. Med. Chem.* **2010**, *18* (14), 5339–5345.

(37) Marino, C.; Caridea, S. P. et al. In *Carbohydrate Chemistry : Proven Synthetic Methods*; Vogel, C., Murphy, P., Eds.; CRC Press: Boca Raton, FL, **2018**; Vol. 4, p 91.

(38) Gallo-Rodriguez, C.; Kashiwagi, G. A. In *Selective Glycosylations: Synthetic Methods and Catalysts*; Bennet, C. S., Ed.; Wiley-VCH: Weinheim, **2017**; p 378.

(39) Lide, D. R. In *CRC Handbook of Chemistry*; Lide, D. R., Ed.; CRC Press: Boca Raton, FL, **2005**; p 2712.

(40) Danalev, D.; Legentil, L. et al. *Tetrahedron Lett.* **2011**, *52*, 1121–1123.

(41) Andersen, S. M.; Heuckendorff, M.; Jensen, H. H. *Org. Lett.* **2015**, *17* (4), 944–947.

(42) Stick, R. V; Watts, A. G. *Monatsh. Chem.* **2002**, *133* (4), 541–554.

(43) Koeners, H. J.; de Kok, A. J. et al. *Recl. Trav. Chim. Pays-Bas* **1980**, *99* (11), 355–362.

(44) Massinon, O. *Synthèse de Dinitrophénylglycosides En Vue de l'étude Des Propriétés Catalytiques de Polymères Imprimés*. Master thesis, Facultés Universitaires Notre-Dame de la Paix: Namur, **2011**.

(45) Clayden, J.; Greeves, N.; Warren, S. In *Organic Chemistry*; Oxford University Press: New York, NY, **2012**; p 1234.

(46) Kwan, E. E.; Zeng, Y. et al. *Nat. Chem.* **2018**, *10* (9), 917–923.

(47) Bubb, W. A. *Concepts in Magnetic Resonance* **2003**, *19A* (1), 1–19.

(48) Taha, H. A.; Richards, M. R.; Lowary, T. L. *Chem. Rev.* **2013**, *113* (3), 1851–1876.

(49) Chen, H.-M.; Withers, S. G. *ChemBioChem* **2007**, *8* (7), 719–722.

(50) Ly, H. D.; Howard, S. et al. *Carbohydr. Res.* **2000**, *329* (3), 539–547.

(51) Withers, S. G.; Rupitz, K.; Street, I. P. *J. Biol. Chem.* **1988**, *263* (17), 7929–7932.

(52) Rempel, B. P.; Withers, S. G. *Glycobiology* **2008**, *18* (8), 570–586.

(53) Francisco, C. G.; González, C. C. et al. *Chem. Eur. J.* **2008**, *14* (35), 10871.

(54) N'Go, I.; Golten, S. et al. *Chem. Eur. J.* **2014**, *20* (1), 106–112.

(55) van Straaten, K. E.; Kuttiyatveetil, J. R. A. et al. *J. Am. Chem. Soc.* **2015**, *137* (3), 1230–1244.

(56) Zhao, J.; Wei, S. et al. *Carbohydr. Res.* **2010**, *345* (1), 168–171.

(57) Allman, S. A.; Jensen, H. H. et al. *ChemBioChem* **2009**, *10* (15), 2522–2529.

(58) Hayashi, T.; Murray, B. W. et al. *Bioorg. Med. Chem.* **1997**, *5* (3), 497–500.

(59) Rempel, B. P.; Withers, S. G. *Org. Biomol. Chem.* **2014**, *12* (16), 2592–2595.

(60) Salvadó, M.; Amgarten, B. et al. *Org. Lett.* **2015**, *17* (11), 2836–2839.